

**UNIVERSIDADE FEDERAL DA PARAÍBA
CENTRO DE CIÊNCIAS EXATAS E DA NATUREZA
PROGRAMA DE PÓS-GRADUAÇÃO EM CIÊNCIAS BIOLÓGICAS (ZOOLOGIA)**

JONAS DE ANDRADE SANTOS

**REVISÃO DO COMPLEXO *OPHIOSCION PUNCTATISSIMUS* MEEK &
HILDEBRAND, 1925 (ACTINOPTERYGII: SCIAENIDAE)**

JOÃO PESSOA, 2022

**REVISÃO DO COMPLEXO *OPHIOSCION PUNCTATISSIMUS* MEEK &
HILDEBRAND, 1925 (ACTINOPTERYGII: SCIAENIDAE)**

Dissertação apresentada ao Programa de Pós-Graduação em Ciências Biológicas (Zoologia) da Universidade Federal da Paraíba, como requisito parcial para a obtenção do título de Mestre em Ciências Biológicas.

Orientador: Prof. Dr. Telton Pedro Anselmo Ramos
Coorientador: Prof. Dr. Ricardo de Souza Rosa

JOÃO PESSOA, 2022

Catálogo na publicação
Seção de Catalogação e Classificação

S237r Santos, Jonas de Andrade.

Revisão do complexo *Ophioscion punctatissimus* Meek & Hildebrand, 1925 (Actinopterygii: Sciaenidae) / Jonas de Andrade Santos. - João Pessoa, 2022.

127 f. : il.

Orientação: Telton Pedro Anselmo Ramos.

Coorientação: Ricardo de Souza Rosa.

Dissertação (Mestrado) - UFPB/CCEN.

1. Zoologia. 2. Alometria. 3. Especiação. 4. Morfologia do otólito. 5. *Stellifer*. 6. Taxonomia. I. Ramos, Telton Pedro Anselmo. II. Rosa, Ricardo de Souza. III. Título.

UFPB/BC

CDU 59(043)

JONAS DE ANDRADE SANTOS

**REVISÃO DO COMPLEXO *OPHIOSCION PUNCTATISSIMUS* MEEK & HILDEBRAND,
1925 (ACTINOPTERYGII: SCIAENIDAE)**

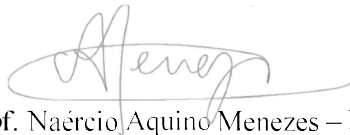
Esta dissertação foi julgada e aprovada para obtenção do Grau de Mestre em Ciências Biológicas, área de concentração Zoologia no Programa de Pós-Graduação em Ciências Biológicas da Universidade Federal da Paraíba.

João Pessoa, 27 de 01 de 2022.

BANCA EXAMINADORA



Prof. Telton Pedro Anselmo Ramos – Dr. - (UFPB) - Orientador



Prof. Naércio Aquino Menezes – Dr. - (USP)



Prof. Lilian Casatti – Dr. - (UNESP)

AGRADECIMENTOS

Primeiramente agradeço aos meus orientadores, Prof. Telton Ramos e Prof. Ricardo Rosa, pelo aceite de orientação, pela paciência e orientação nesse período fora do normal. Aos colegas do LABICT (Antônio, Érika, Rafael, Vivi) e aos que passaram pelo Café.com Peixe, pelas sugestões em análises, gráficos e também pelas conversas menos sérias nesse período. Aos professores e colegas do mestrado pelas discussões e sugestões no trabalho.

Aos amigos e colegas pelas ajudas em análise e sugestões no trabalho, e especialmente pelo auxílio em coletas e trabalhos em coleção agradeço: Elizabete Sampaio, Hemile Marianne, Klleyza Santos, Leonardo Moraes, Marcelo Carvalho-Júnior, Natália Souza, Rafael Oliveira, Sílvio Marques, Verônica Costa.

E pela disponibilidade no envio de material das coleções e auxílio nas visitas, agradeço a Paulo Roberto, Jailza Oliveira, Klleyza Santos, Jean Joyeux, Kathiani Bastos, Wolmar Wosiacki, Ângelo Dourado, Mariangeles Arce, Mark Sabaj, Karsten Hartel, Andrew Williston, Alfredo Carvalho-Filho e Ning Chao. Também agradeço a Pedro Romano e Gabriela Figueiredo pelas sugestões em análises. Pela revisão do português agradeço à Jaciene Andrade.

RESUMO

Sciaenidae é uma família de peixes rica no ambiente marinho, cujas espécies são conhecidas pela produção de som e outras especializações morfológicas no sistema sensorial, como os otólitos (i.e., estrutura inerte do ouvido interno) relativamente grandes, e hipertrofia dos canais cefálicos da linha lateral. Em Stelliferinae, a baixa disparidade fenotípica levou às incertezas taxonômicas. Os gêneros *Stellifer* e *Ophioscion* são reconhecidos como não monofiléticos – aqui reconhecemos que *Ophioscion* Gill, 1863 é sinônimo júnior de *Stellifer* Oken, 1817. O gênero passa então a ser distinguido dos demais pela contagem de vértebras (10 + 15) e pelo par de *lapillus* aproximadamente do mesmo tamanho do *sagitta* (oval). O complexo *Stellifer punctatissimus* é um dos exemplos de incerteza dentro de Stelliferinae, inicialmente reconhecido numa base morfológica como tendo mais duas espécies. No entanto essa hipótese não era confirmada por dados moleculares, que sugeriram apenas duas linhagens evolutivas nesse complexo. Assim, testamos a hipótese morfológica de três espécies utilizando morfometria linear e geométrica no formato do corpo, além de abordagens como índices de forma, Fourier e morfometria geométrica no formato (geral e no *sulcus acusticus*) e contorno dos otólitos. Foi encontrado um padrão de sobreposição no morfoespaço, com uma leve distinção entre *S. punctatissimus* e as demais espécies. As taxas de crescimento de algumas estruturas (e.g., diâmetro do olho, altura do pedúnculo caudal) mostraram padrões alométricos distintos entre as espécies. O mesmo foi visto para o otólito, com diferentes padrões de crescimento em um dos índices de forma (i.e., retangularidade). A análise do contorno do otólito indicou que as espécies são grupos distintos (ANOVA, $F= 4.75$, $p < 0.001$) e bastante segregados, com mais de 94% de reclassificação desses grupos utilizando a Análise Discriminante Linear (LDA). A morfometria geométrica também recuperou distinções na forma do *sulcus acusticus*. A descrição dos otólitos mostrou leves distinções entre as espécies. Esses caracteres também podem ser comparados com espécies irmãs presentes apenas no Oceano Pacífico. Assim sendo, foi possível confirmar a hipótese morfológica, por usar métodos complementares; e a similaridade morfológica externa (reproduzida no morfoespaço) deve ter resultado de um processo recente de especiação ecológica. Apesar da aparente alta similaridade no formato das espécies, as diferenças em alometria podem sugerir um uso de hábitat distinto entre as espécies, o que concorda com a hipótese de especiação ecológica, além de alertar para a possibilidade de essas espécies estarem sob níveis de ameaça diferenciados.

Palavras-chave: alometria, especiação, morfologia do otólito, *Stellifer*, taxonomia

ABSTRACT

Sciaenidae are a speciose fish family in the marine environment, its members are well-known by their sound production and morphological specializations in the sensory system such as their relatively big otoliths (i.e., inert structure of the inner ear), and cephalic lateral line system. In Stelliferinae, the lower phenotypic disparity has led to taxonomic uncertainties. The genus *Stellifer* and *Ophioscion* are recognized as non-monophyletic; herein, we recognize that *Ophioscion* Gill, 1863 is a junior synonym of *Stellifer* Oken, 1817. The genus is distinguished from the other genera in Stelliferinae by their vertebral counts (10 + 15) and the enlarged lapillus; which is almost the same size of the oval shaped sagittal otoliths. The complex *Stellifer punctatissimus* is one of these examples of uncertainties; it was initially recognized on a morphological basis as presenting putatively two other species. However, this morphological hypothesis was not confirmed by molecular data, that suggested that occurs only two evolutionary lineages in this species complex. Thus, we tested herein the morphological hypothesis of three species on the complex by using linear and geometric morphometrics in the body shape. In addition, shape indices, Fourier descriptors and geometric morphometrics in the shape and outline of the otoliths were used. An overlapped pattern was found in the morphospace, but it also showed a slight distinction between *O. punctatissimus* and the other species. The growth rate patterns for some structures (e.g., eye diameter, peduncle height) showed distinct allometry among the species. The same occurred for the otoliths, with distinct growth patterns in one of the shape indices (i.e., rectangularity). The otolith's outline analysis indicated that the species are distinct groups (ANOVA, $F= 4.75$, $p < 0.001$) and highly segregated; Linear Discriminant Analysis (LDA) showed more than 94% in re-classification accuracy in such groups. Geometric morphometrics also recovered some distinction in the *sulcus acusticus*' shape. Also, otoliths' description showed slight distinctions among the species, some of these distinctions can be traced back to sister species – present only in the Pacific Ocean. Therefore, it was possible to confirm the morphological hypothesis by using complementary approaches. The likely external similarity in shape (mirrored in the morphospace) might have resulted from a recent ecological speciation process. Despite the appearing high similarity in species' shape, differences in allometry may suggest a distinct use of habitat among those species; which agrees with the hypothesis of ecological speciation. Additionally, it brings light to the likelihood that each one of those species are under specific threat levels.

Keywords: allometry, otolith morphology, speciation, *Stellifer*, taxonomy

1 INTRODUÇÃO GERAL

A família Sciaenidae, que inclui as “corvinas” e “pescadas”, é uma das famílias de peixes com a maior riqueza no ambiente marinho Neotropical, incluindo quase 300 espécies válidas (Chao 1978; Fricke et al. 2021). A diversidade morfológica nessa família permitiu a adaptação de suas espécies a uma variedade de habitats, como estuários e praias marinhas, sendo poucas delas estritamente de água doce ou associadas a recifes (Chao 1978). Apesar de evidências morfológicas e moleculares recentes suportarem o monofiletismo da família, as relações evolutivas em níveis taxonômicos menos inclusivos permanecem incertos (Chao 1978; Sasaki 1989; Lo et al. 2015; Hughes et al. 2018).

A falta de caracteres informativos tem levado a mudanças no posicionamento genérico de espécies morfológicamente similares, como as originalmente descritas como *Stellifer* Oken 1817 e que depois foram relocadas em *Ophioscion* Gill 1863, e vice-versa (Chao et al., 2021). Importante notar que apesar de ser um grupo bem estudado, recentemente ainda foram descritas espécies de Sciaenidae “escondidas” ou em potes de coleções de peixes (e.g., Chao et al., 2021 – *Stellifer musicki*) ou no ambiente (e.g., Marceniuk et al., 2019; Guimarães-Costa et al., 2020 – *Bairdiella ronchus* e *Isopisthus* sp.). Ultimamente, várias abordagens têm sido utilizadas na tentativa de catalogar essa diversidade (e.g., Lin et al., 2019; Marceniuk et al., 2019; Guimarães-Costa et al., 2020; Parenti, 2020; Chao et al., 2021).

O déficit Linneano, que deriva da falta de trabalhos básicos em taxonomia, é um dos principais fatores limitantes na otimização do conhecimento da biodiversidade e planos de conservação (Lomolino, 2004; Diniz-Filho et al., 2013). Isso tem um maior efeito nas espécies crípticas, pois a taxa do conhecimento taxonômico é bem mais rápida em táxons conspícuos (especialmente megafauna) do que em espécies crípticas e de pequeno tamanho (Riddle et al., 2011). De acordo com Wheeler et al. (2004), o déficit Linneano é mais uma questão de demora na descrição formal das espécies do que na descoberta destas. Essas espécies crípticas seriam as que teriam evoluído num contexto de baixa disparidade fenotípica, isto é, que pode ter resultado de processos como divergência recente, convergência, ou paralelismo e estase (Rabosky & Adams, 2012; Struck & Cerca, 2019).

Como os Sciaenidae são conhecidos por suas especializações no sistema sensorial (e.g., otólitos, linha lateral), é necessário avaliar a variação nesses sistemas, porque, por apresentarem tais especializações, pode-se reter um sinal filogenético da seleção natural (Trewavas, 1977; Chao, 1978; Schwarzhans, 1993). Caracteres internos, como otólitos e bexiga natatória, podem ser substitutos adicionais na discriminação de espécies de Sciaenidae proximamente relacionadas. Em particular, estudos utilizando otólitos e bexiga natatória têm conseguido resolver incongruências taxonômicas, especialmente separando gêneros ou grupos

supragenéricos (Casatti 2001; Chao et al. 2019).

Otólitos são estruturas calcificadas localizadas no ouvido interno de peixes ósseos (Teleostei) na forma de três canais semicirculares (utrículo, sáculo e lagena), nos quais estão inseridos os pares de *lapillus*, *sagitta* e *asteriscus* (Schulz-Mirbach et al. 2019). A forma do otólito é influenciada tanto por fatores extrínsecos, como salinidade e temperatura, quanto por fatores intrínsecos, como a fisiologia, mas também pela ontogenia. Por crescer ao longo do ciclo de vida dos peixes, otólitos parecem também responder a outros fatores como mudanças ontogenéticas, os quais são ligados aos gradientes ambientais (Volpedo and Fuchs 2010; Schulz-Mirbach et al. 2019). Da mesma forma, como eles carregam sinal dessas características, pesquisas que usam forma do otólito geram uma forma indireta e efetiva de investigar os hábitos de vida dessas espécies e de buscar caracteres diagnósticos em espécies crípticas. Tais análises contrastam com abordagens taxonômicas tradicionais, que geram maior sobreposição do que as análises de forma do otólito (Galley et al. 2006; Lombarte et al. 2006; Capoccioni et al. 2011).

Existem muitas técnicas para delimitação de contorno do otólito (e.g., índices de forma, wavelet, descritores de Fourier). Os índices de forma têm pouco poder de discriminação entre espécies crípticas, pois sua resolução é muito menor do que o necessário. No entanto essa técnica gera informações biológicas importantes, por elucidar a associação de padrões de forma com hábitos de vida, alimentação e uso da coluna d'água (Tuset et al. 2006; Wong et al. 2016; Assis et al. 2020; Ghanbarifardi et al. 2020). Os descritores de Fourier são mais eficientes em distinguir o nível de diferenças sutis em espécies crípticas, pois eles decompõem a borda do otólito em várias harmônicas, o que leva a quase uma completa cobertura da variação na borda do otólito (Rohlf and Archie 1984; Ferguson et al. 2011; Avigliano et al. 2018). A morfometria geométrica, assim como os descritores de Fourier, apresenta uma excelente resolução da variação em espécies crípticas ou em grupos ricos em espécies (Anjos et al., 2020; Argolo et al. 2020). Em contraste, impedimentos metodológicos prejudicam a aplicação dos métodos de morfometria geométrica, devido à falta de pontos homólogos, o seu uso fica restrito às descrições de borda através de *semilandmarks* (Ramírez-Pérez et al. 2010; Tuset et al. 2016), e, como tal, geralmente reduz a o poder estatístico do método (Wong et al. 2016). No entanto isso inclui dados adicionais quando aplicado a estruturas como o *sulcus acusticus* (i.e., *ostium* e *cauda*), e, como resultado, essas informações podem ser aplicadas para discussões taxonômicas, na capacidade auditiva e identificação de presa (Farré et al. 2016; Byrd et al. 2020; Granados-Amores et al. 2020).

A fim de avaliar tanto a variação intraespecífica quanto a variação interespecífica do complexo *Stellifer punctatissimus* (Meek & Hildebrand, 1925), foram realizadas análises de

morfometria linear e morfometria geométrica na forma do corpo, com o objetivo de descrever os padrões de forma do corpo, alometria e dimorfismo sexual. Além disso, diante da incerteza taxonômica trazida pelas hipóteses moleculares, foi testada a hipótese de três espécies distintas nesse complexo, através da análise de forma do otólito.

A presente dissertação encontra-se estruturada em dois capítulos e um apêndice. O Capítulo 1 trata da revisão taxonômica do complexo *Stellifer punctatissimus*, que inclui análises morfológicas lineares e geométricas no formato do corpo, a fim de avaliar efeitos de alometria e dimorfismo sexual nos padrões morfológicos encontrados nas espécies desse complexo. No Capítulo 2 é testada a hipótese morfológica de três espécies neste complexo e trata da diferenciação taxonômica entre elas, através da aplicação de diversos métodos em morfologia e forma do otólito. O apêndice (artigo publicado) dá base taxonômica para as mudanças tratadas no presente trabalho dissertativo, ao passo que, descreve e redescreve espécies inclusas no complexo estudado.

2 REFERENCIAL TEÓRICO

Na subfamília Stelliferinae ('*Stellifer*-group' sensu Chao 1978), o status taxonômico da maioria dos seus gêneros ainda não está bem resolvido devido à alta similaridade morfológica e mesmo à falta de caracteres diagnósticos para a distinção desses táxons (Chao et al. 2015; Silva et al. 2018). A subfamília é definida, entre outras características, pela presença de bexiga natatória com duas câmaras e *lapillus* largo, e apresenta aproximadamente 50 espécies válidas, classificadas nos gêneros *Odontoscion*, *Elattarchus*, *Corvula*, *Bairdiella* e *Ophioscion*/*Stellifer*.

O gênero *Ophioscion* Gill, 1863 foi descrito por Gill (1863), com descrição sucinta e subjetiva, para incluir a espécie *Ophioscion typicus* Gill, 1863. Esta apenas foi diferenciada de *Bairdiella armata* Gill, 1863. Posteriormente, a ausência de apêndices na câmara anterior da bexiga natatória e a distância interorbital maior que 3.5 (em relação ao tamanho da cabeça) passou a definir o gênero, de acordo com Chao (1978). Em revisão de Sciaenidae, Sasaki (1989) considerou apenas um caráter das placas faríngeas (60) como autapomorfia de *Ophioscion*, no entanto, como apontam Chao et al. (2021), esse caráter deveria ser considerado uma homoplasia. Assim sendo, o gênero seria faltante em autapomorfia, da mesma forma que outros gêneros com posição taxonômica incerta dentro da subfamília (i.e., *Elattarchus* e *Corvula*). Adicionalmente, filogenias mostram que não é possível o reconhecimento do gênero *Ophioscion* como monofilético, já que foi encontrado um relacionamento mais próximo entre algumas espécies desse gênero com *Stellifer* Oken, 1817 do que com suas congêneres (Santos et al. 2013; Barbosa et al. 2014; Lo et al. 2015; Silva et al. 2018).

Foi designado por Chao et al. (2021) que “*Ophioscion* Gill, 1863” seria sinônimo júnior de *Stellifer* Oken, 1817 e delinearão sinônimo júnior de *Stellifer punctatissimus* (Meek & Hildebrand, 1925) (i.e., “*Ophioscion panamensis*”). Assim, eles resolveram uma contínua incerteza na identidade taxonômica desses táxons, além de ratificar sinônimos em espécies proximamente relacionadas. Após a descrição por Meek & Hildebrand (1925), foi reconhecido por Chao (2002) que, na verdade, *Stellifer punctatissimus* se tratava de um complexo de espécies, com possivelmente mais duas espécies. No entanto, dados moleculares apontam para apenas duas linhagens evolutivas nesse complexo (Barbosa et al. 2014; Silva et al. 2018). Dessas, uma foi descrita para a costa da Venezuela (*Stellifer gomezi* – Cervigón, 2011) – sendo recentemente redescrita, a fim de incluir variação na costa brasileira –; a outra foi também recentemente descrita para o Nordeste e Sudeste da costa brasileira (*Stellifer menezesi* – Chao et al., 2021).

REFERÊNCIAS

- Anjos MS, Bitencourt JA, Nunes LA, Sarmento-Soares LM, Carvalho DC, Armbruster JW, et al. Species delimitation based on integrative approach suggests reallocation of genus in Hypostomini catfish (Siluriformes, Loricariidae). *Hydrobiologia*. 2020; 847:563–78. <https://doi.org/10.1007/s10750-019-04121-z>
- Argolo LA, López-Fernández HL, Batalha-Filho H, Affonso PRAM. Unraveling the systematics and evolution of the '*Geophagus*' *brasiliensis* (Cichliformes: Cichlidae) species complex. *Mol Phylogenet Evol*. 2020; 150:e106855. <https://doi.org/10.1016/j.ympev.2020.106855>
- Assis IO, Silva VEL, Souto-Vieira D, Lozano AP, Volpedo AV, Fabr e NN. Ecomorphological patterns in otoliths of tropical fishes: Assessing trophic groups and depth strata preference by shape. *Environ Biol Fishes*. 2020; 103(4):349–61. <https://doi.org/10.1007/s10641-020-00961-0>
- Avigliano E, Rol n ME, Rosso JJ, Mabragna E, Volpedo AV. Using otolith morphometry for the identification of three sympatric and morphologically similar species of *Astyanax* from the Atlantic Rain Forest (Argentina). *Environ Biol Fish*. 2018; 101:1319–28. <https://doi.org/10.1007/s10641-018-0779-2>
- Barbosa AJB, Sampaio I, Schneider H, Santos S. Molecular phylogeny of weakfish species of the *Stellifer* group (Sciaenidae, Perciformes) of the Western South Atlantic based on mitochondrial and nuclear data. *PLoS ONE*, 2014; 9 (7), e102250.
- Byrd BL, Hohn AA, Krause JR. Using the otolith sulcus to aid in prey identification and improve estimates of prey size in diet studies of a piscivorous predator. *Ecol Evol*. 2020; 10(8): 3584–3604. <https://doi.org/10.1002/ece3.6085>
- Cappocionni F, Costa C, Aguzzi J, Menesatti P, Lombarte A, Ciccotti E. Ontogenetic and environmental effects on otolith shape variability in three Mediterranean European eel (*Anguilla anguilla*, L.) local stocks. *J Exp Mar Biol Ecol*. 2011; 397(1):1–7. <https://doi.org/10.1016/j.jembe.2010.11.011>
- Casatti L. *Petilipinnis*, a new genus for *Corvina grunniens* Schomburgk, 1843 (Perciformes, Sciaenidae) from the Amazon and Essequibo river basins and redescription of *Petilipinnis*

- grunniens*. Pap Avulsos Zool. 2001; 42(7):169–81. <https://doi.org/10.1590/S0031-10492002000700001>
- Cervigón F. Los Peces de Venezuela. Vol. VI. Edit. Ex Libris, Caracas. 2011. p. 96–98.
- Chao LN, Chang CW, Chen MH, Guo CC, Lin BA, Liou YY, et al. *Johnius taiwanensis*, a new species of Sciaenidae from the Taiwan Strait, with a key to *Johnius* species from Chinese waters. Zootaxa. 2019; 4651(2):259–70. <https://doi.org/10.11646/zootaxa.4651.2.3>
- Chao LN. A basis for classifying western Atlantic Sciaenidae (Pisces: Perciformes). NOAA (National Oceanic and Atmospheric Administration) Technical Report NMFS (National Marine Fisheries Service). 1978; Circular No. 415, p. 1–64.
- Chao NL, Carvalho-Filho A, Santos JA. Five new species of Western Atlantic stardrums, *Stellifer* (Perciformes: Sciaenidae) with a key to Atlantic *Stellifer* species. Zootaxa 2021; 4991(3): 434–66. <https://doi.org/10.11646/zootaxa.4991.3.2>
- Chao NL, Frédoú FL, Haimovici M, Peres MB, Polidoro B, Raseira M, et al. A popular and potentially sustainable fishery resource under pressure – extinction risk and conservation of Brazilian Sciaenidae (Teleostei: Perciformes). Global Ecology and Conservation 2015; 4: 117–126. <https://doi.org/10.1016/j.gecco.2015.06.002>
- Chao NL. Sciaenidae. In: Carpenter KE, editor. The living marine resources of the Western Central Atlantic. FAO Species Identification Guide for Fishery Purposes and American Society of Ichthyologists and Herpetologists. 2002; Special Publication No. 5. Rome: FAO. p. 1583–1653.
- Diniz-Filho JA, Loyola RD, Raia P, Mooers AO, Bini LM. Darwinian shortfalls in biodiversity conservation. Trends in Ecology & Evolution 2013; 28: 689–695. <https://doi.org/10.1016/j.tree.2013.09.003>
- Farré M, Tuset VM, Maynou F, Recasens L, Lombarte A. Selection of landmarks and semilandmarks in fishes for geometric morphometric analyses: a comparative study based on analytical methods. Sci Mar. 2016; 80(2):175–86. <https://doi.org/10.3989/scimar.04280.15A>
- Ferguson GJ, Ward TM, Gillanders BM. Otolith shape and elemental composition: complementary tools for stock discrimination of mullet (*Argyrosomus japonicus*) in southern Australia. Fish Res. 2011; 110(1):75–83. <https://doi.org/10.1016/j.fishres.2011.03.014>
- Fricke R, Eschmeyer WN, Van der Laan R. Eschmeyer's catalog of fishes: genera/species by family/subfamily [Internet]. San Francisco: California Academy of Science; 2021. Available from: <http://researcharchive.calacademy.org/research/ichthyology/catalog/fishcatmain.asp>
- Galley EA, Wright PJ, Gibb FM. Combined methods of otolith shape analysis improve identification of spawning areas of Atlantic cod. ICES J Mar Sci. 2006; (63)9:1710–17. <https://doi.org/10.1016/j.icesjms.2006.06.014>
- Ghanbarifardi M, Gut C, Gholami Z, Esmaili HR, Gierl C, Reichenbacher B. Possible link between the structure of otoliths and amphibious mode of life of three mudskipper species (Teleostei: Gobioidae) from the Persian Gulf. Zool Middle East. 2020; 66(4):311–20. <https://doi.org/10.1080/09397140.2020.1805140>
- Gill, T.N. Descriptive enumeration of a collection of fishes from the western coast of Central America, presented to the Smithsonian Institution by Captain John M. Dow. Proceedings of the Academy of Natural Sciences of Philadelphia, 1863; 15, 162–174.
- Granados-Amores E, Granados-Amores J, Zavala-Leal OI, Flores-Ortega JR. Geometric morphometrics in the sulcus acusticus of the sagittae otolith as tool to discriminate species of the genus *Centropomus* (Centropomidae: Perciformes) from the southeastern Gulf of

- California. *Mar Biodivers.* 2020; 50:e10. <https://doi.org/10.1007/s12526-019-01030-1>
- Guimarães-Costa A, Machado FS, Reis-Filho JA, Andrade MC, Araújo RG, Miranda E, et al. DNA Barcoding for the assessment of the taxonomy and conservation status of the fish bycatch of the northern Brazilian shrimp trawl fishery. *Frontiers in Marine Science* 2020; 7: 566021. <https://doi.org/10.3389/fmars.2020.566021>
- Hughes LC, Ortí G, Huang Y, Sun Y, Baldwin CC, Thompson AW, et al. Comprehensive phylogeny of ray-finned fishes (Actinopterygii) based on transcriptomic and genomic data. *Proc Natl Acad Sci U S A.* 2018; 115(24):6249–54. <https://doi.org/10.1073/pnas.1719358115>
- Lin YJ, Qurban MA, Shen KN, Chao NL. Delimitation of tigertooth croaker *Otolithes* species (Teleostei: Sciaenidae) from the western Arabian Gulf using an integrative approach, with a description of *Otolithes arabicus* sp. nov. *Zoological Studies* 2019; 58: 10. <https://doi.org/10.6620/ZS.2019.58-10>.
- Lo PC, Liu SH, Chao NL, Nunoo FKE, Mok HK, Chen WJ. A multi-gene dataset reveals a New World origin and Oligocene diversification of croakers (Perciformes: Sciaenidae). *Molecular Phylogenetics and Evolution* 2015; 88: 132–43. <https://doi.org/10.1016/j.ympev.2015.03.025>
- Lombarte A, Chic Ò, Parisi-Baradad V, Olivella R, Piera J, García-Ladona E. A web-based environment for shape analysis of fish otoliths. The AFORO database. *Sci Mar.* 2006; 70:147–52. <https://doi.org/10.3989/scimar.2006.70n1147>
- Lomolino MV. Conservation biogeography. In: Lomolino L, Heaney LR, eds. *Frontiers of biogeography: new directions in the geography of nature.* Sunderland: Sinauer, 2004; 293–296.
- Marceniuk AP, Molina EG, Caires RA, Rotundo MM, Wosiacki WB, Oliveira C. Revision of *Bairdiella* (Sciaenidae: Perciformes) from the western South Atlantic, with insights into its diversity and biogeography. *Neotropical Ichthyology* 2019; 17(1): 1–18. <https://doi.org/10.1590/1982-0224-20180024>
- Meek SE, Hildebrand SF. The marine fishes of Panama. Part II. Field Museum of Natural History Publications 226. Zoological Series 15. 1925; Chicago: Field Museum of Natural History.
- Parenti P. An annotated checklist of fishes of the family Sciaenidae. *Journal of Animal Diversity* 2020; 2(1): 1–92. <https://doi.org/10.29252/JAD.2020.2.1.1>
- Rabosky DL, Adams DC. Rates of morphological evolution are correlated with species richness in salamanders. *Evolution* 2012; 66: 1807–1818. <https://doi.org/10.1111/j.1558-5646.2011.01557.x>
- Ramirez-Perez JS, Quinonez-Velazquez C, Garcia-Rodriguez FJ, Felix-Uraga R, Melo-Barrera FN. Using the shape of sagitta otoliths in the discrimination of phenotypic stocks in *Scomberomorus sierra* (Jordan and Starks, 1895). *J Fish Aquat Sci.* 2010; 5(2):82–93. <https://doi.org/10.3923/jfas.2010.82.93>
- Riddle BR, Ladle RJ, Lourie SA, Whittaker RJ. Basic biogeography: estimating biodiversity and mapping nature. In: Ladle RJ, Whittaker RJ, eds. *Conservation Biogeography.* 2011; Oxford: Wiley, 45–92. <https://doi.org/10.1002/9781444390001.ch4>
- Rohlf FJ, Archie JW. A comparison of Fourier methods for the description of wing shape in mosquitoes (Diptera: Culicidae). *Syst Biol.* 1984; 33(3):302–17. <https://doi.org/10.2307/2413076>
- Santos, S., Gomes, M.F., Ferreira, A.R.S., Sampaio, I. & Schneider, H. Molecular phylogeny of the western South Atlantic Sciaenidae based on mitochondrial and nuclear data. *Molecular Phylogenetics and Evolution* 2013; 66, 423–428. <https://doi.org/10.1016/j.ympev.2012.09.020>

- Sasaki K. Phylogeny of the family Sciaenidae, with notes on its zoogeography (Teleostei, Perciformes). *Memoirs of the Faculty of Fisheries Sciences* 1989; 36(1/2): 1–137. <https://doi.org/10.1007/BF02905681>
- Schulz-Mirbach T, Ladich F, Plath M, Heß M. Enigmatic ear stones: What we know about the functional role and evolution of fish otoliths. *Biol Rev.* 2019; 94:457–82. <https://doi.org/10.1111/brv.12463>
- Schwarzahns W. A comparative morphological treatise of recent and fossil otoliths of the family Sciaenidae (Perciformes). *Piscium Catalogus, Otolithi Piscium*, 1993; 1:1-245.
- Silva TF, Schneider H, Sampaio I, Angulo A, Brito MFG, Santos ACA, et al. 2018. Phylogeny of the subfamily Stelliferinae suggests speciation in *Ophioscion* Gill, 1863 (Sciaenidae: Perciformes) in the western South Atlantic. *Molecular Phylogenetics and Evolution* 125: 51–61. <https://doi.org/10.1016/j.ympev.2018.03.025>
- Struck TH, Cerca J. Cryptic species and their evolutionary significance. In: eLS. John Wiley & Sons, Ltd: 2019; Chichester. <https://doi.org/10.1002/9780470015902.a0028292>
- Trewavas E. The sciaenid fishes (croakers or drums) of the Indo-West-Pacific. *Trans Zool Soc London.* 1977; 33:253–541. <https://doi.org/10.1111/j.1096-3642.1977.tb00052.x>
- Tuset VM, Farré M, Otero-Ferrer JL, Vilar A, Morales-Nin B, Lombarte A. Testing otolith morphology for measuring marine fish biodiversity. *Mar Freshw Res.* 2016; 67:1037–48. <https://doi.org/10.1071/MF15052>
- Tuset VM, Rosin PL, Lombarte A. Sagittal otolith shape used in the identification of fishes of the genus *Serranus*. *Fish Res.* 2006; 81:316–25. <https://doi.org/10.1016/j.fishres.2006.06.020>
- Volpedo AV, Fuchs DV. Ecomorphological patterns of the lapilli of Paranoplatense Siluriforms (South America). *Fish Res.* 2010; 102(1-2):160–65. <https://doi.org/10.1016/j.fishres.2009.11.007>
- Wheeler QD, Raven PH, Wilson EO. *Science* 2004; 303, 285. <https://doi.org/10.1126/science.303.5656.285>
- Wong JY, Chu C, Chong VC, Dhillon SK, Loh KH. Automated otolith image classification with multiple views: an evaluation on Sciaenidae. *J Fish Biol.* 2016; 89(2):1324–44. <https://doi.org/10.1111/jfb.13039>

CAPÍTULO 1 – A reappraisal of *Stellifer punctatissimus* reveal trends on the species complex misidentification

JONAS DE ANDRADE SANTOS¹, TELTON PEDRO ANSELMO RAMOS², RICARDO DE SOUZA ROSA²

1. Programa de Pós-Graduação em Ciências Biológicas (Zoologia), Centro de Ciências Exatas e da Natureza, Universidade Federal da Paraíba, 58051-900, João Pessoa, PB, Brazil. <https://orcid.org/0000-0001-9245-1121>
2. Departamento de Sistemática e Ecologia, Centro de Ciências Exatas e da Natureza, Universidade Federal da Paraíba, 58051-900, João Pessoa, PB, Brazil.

Abstract

Even with modern taxonomic techniques being more common nowadays, there is still a likely high number of unknown biological diversity. Of those species that are already described, only part is well-studied, falling into the Linnean shortfall, that is, an unsuitable level of basic taxonomic knowledge. This is a major concern in the case of cryptic species, which mostly of cases requires an integration of approaches in order to better evaluate their diversity. It is also a constraint for species conservation, once we fail to address that hidden diversity. Herein, we carried out analyses of linear morphometrics and geometric morphometric methods (GMM) using an allometric and sexual dimorphism perspective. Our results retrieve the current morphological hypothesis of the presence of three species in this complex, however, as cryptic species, they show large overlap on its external morphology especially in groups such as males and juveniles. *Stellifer punctatissimus* stands out due to the deep body and rather smaller eye, while *S. gomezi* and *S. menezesi* overlap in many characters, being distinguished only by differences in eye size, nostrils, and pectoral-fin. Some important trends found in allometry likely explain past taxonomic errors on this group. Also, distinct growth patterns among these species may suggest a distinct habitat use by them. As a result of differential habitat use, it could be suggested that such species are under different threats, highlighting the need for that kind of studies that aim to fill taxonomic gaps in other groups.

Introduction

The Linnean shortfall is one of the major caveats to the improvement of biodiversity knowledge and conservation planning, as it means the lack of basic taxonomic work that masks an actual richness (Lomolino, 2004; Diniz-Filho et al., 2013). Despite the need for taxonomic work, there are several factors that hamper filling that knowledge gap. From one side there is the depreciation of taxonomic publications, shortage of taxonomists, and in other side the

taxonomic research suffers from governmental budget cut-offs (Engel et al., 2021; Santos & Carbayo, 2021). A major concern on this refers to the cryptic species, once the rate of taxonomical knowledge is faster in conspicuous (especially bigger ones) than it is in cryptic and smaller species (Riddle et al., 2011). Species that had evolved in a context of low phenotypic disparity would be named cryptic species, those ones are included in clades with narrow adaptive range, as a result of processes such as recent divergence, convergence, or parallelism and stasis (Rabosky & Adams, 2012; see review in Struck & Cerca, 2019). Additionally, another cause for this Linnean shortfall is that many “old/initial” works did not cover well those shortfalls (i.e., Linnean, Darwinian, Wallacean), because they were either locally restricted, too vague, and/or with few material examined (Nori et al., 2021). On top of that, the “catch-all-names” practice in taxonomy might have led to the non-completely reliability of online repositories, because adding records to one species might mask actual biodiversity, that is, species needing to be formally described or yet to be sampled (Hortal et al., 2015; Freitas et al., 2020, 2021). It could also be favored by the revisionary studies in such groups (Freitas et al., 2021). According to Wheeler et al. (2004), this Linnean shortfall is more a matter of delay of formal species’ description than in discovering them. In terms of descriptions, it could be facilitated by looking into natural history museum collections – which still holds a considerable part of the unknown biodiversity – and focusing on cryptic species, in doing so, addressing the Linnean shortfall in the facing of biodiversity crisis (Pinheiro et al., 2019; Engel et al., 2021; Frainer et al., 2021; Walters et al., 2021).

In recent years, a variety of approaches have attempted to account for the Sciaenidae biodiversity; reaching almost 300 valid species in this family (Lin et al., 2019; Marceniuk et al., 2019b; Guimarães-Costa et al., 2020; Parenti, 2020; Chao et al., 2021). It is noteworthy that despite being a rather well-studied fish family, yet “hidden” species are found either in fish collections’ jars (*Stellifer musicki* – see Chao et al., 2021) or in the environment (*Bairdiella ronchus* and *Isopisthus* sp. – see Marceniuk et al., 2019b; Guimarães-Costa et al., 2020). Chao (2002) recognized that *Stellifer punctatissimus* (Meek & Hildebrand, 1925) is a species complex with other two putative species. Of these, one was described to the Venezuelan coast (*Stellifer gomezi* – see Cervigón, 2011), and recently redescribed in order to cover variation from the Brazilian coast; the other one was recently described from Northeast to Southeastern Brazilian coast (*Stellifer menezesi* – see Chao et al., 2021). In a recent article, Chao et al. (2021) have indicated the junior synonym of *Stellifer punctatissimus* (Meek & Hildebrand, 1925), thus solving taxonomic uncertainties of this species complex.

It should be noted that factors such as allometry and sexual dimorphism might drive body shape variation across species or at the macroevolutionary level (Gould, 1966; Adams et

al., 2020). For instance, is evident the differentiation of feeding apparatus, sensory system, and proportions of structures throughout fish's life cycle (Chao & Musick, 1977; Deary & Hilton, 2016; Deary et al., 2016). As Sciaenidae members are known by the specializations in sensory system (i.e., otoliths, lateral line), is necessary to evaluate variation on those systems, because by presenting such specializations it should retain phylogenetic signal of natural selection (Trewavas, 1977; Chao, 1978; Schwarzhans, 1993).

In order to address both intraspecific and interspecific variation of *Stellifer punctatissimus* (Meek & Hildebrand, 1925), were carried out linear morphometric analyses and geometric morphometric methods; aiming to describe patterns in body shape, allometry, and sexual dimorphism. Additionally, taxonomic and conservation implications are discussed.

Materials and methods

Linear morphometrics

Were used point to point measures with a digital caliper (nearest 0.01 mm) following Hubbs & Laegler (2004) and Chao et al. (2021), except as follows, and some specific terms for morphological structures of sciaenids are based in Chao (1978) and Sasaki (1989). The body angle (upper in head) was calculated using measures that form a triangle, as described in Equation 1. In order to reduce unwanted variance (i.e., expanded ventral region by gonads, drumming muscle, and/or stomach content), the body depth measure was corrected by taking it from pectoral fin-base to dorsal fin-base.

$$\frac{(Predorsal^2) + (Body\ depth^2) - (Prepelvic^2)}{(2 * Predorsal * Body\ depth)}$$

Equation 1 – Body angle using principles of triangle measure, where *acos* was calculated and transformed from radians to angle degrees.

A total of 274 specimens of *Stellifer punctatissimus*, *S. gomezi* and *S. menezesi* were examined (Fig. 1). Additionally, the specimens analyzed by Chao et al. (2021) were included in the analysis, as well as additional comparative specimens of *S. naso* (6) and *S. scierus* (3). The fish collections acronyms follow Sabaj (2020).

Geometric morphometrics

In order to attempt to cover their geographic distribution, size variation and sexual dimorphism, we studied 124 specimens of *Stellifer punctatissimus*, *S. gomezi* and *S. menezesi*. Herein, the full dataset means by all specimens and reduced dataset only for *S. punctatissimus*, expect when

stated otherwise. We selected 11 landmarks to explain the overall body shape as follows: 1- Anterior-most margin of snout; 2- Anterior nostril; 3- Posterior nostril; 4- Mid lower margin of eye; 5- Mid upper margin of eye; 6- Origin of second dorsal-fin; 7- End of second dorsal-fin base; 8- End of anal-fin base; 9- Origin of anal-fin; 10- Lower insertion of pectoral-fin; 11- Upper insertion of pectoral-fin. Also, five (5) equally spaced semilandmarks, from the posterior vertical of eye orbit to the dorsal-fin base, were added to the dataset (Fig. 2).

Statistical analysis

The linear morphometrics data set was explored to choose the variables which better explained the variation among species. Allometric effect was removed from all measurements following Pinheiro et al. (2005). After this we standardized all variables and verified covariation among them using VIF- Variance inflation factor > 5 as a threshold to remove highly correlated variables. Another step was verifying the KMO- Kaiser-Meyer-Olkin measure using the suggested 0.5 threshold. A PCA procedure was performed using the packages factoextra (Kassambara & Mundt, 2016) and FactoMineR (Lê et al., 2008) in R platform (R Core Team, 2020). We performed MANOVA and ANOSIM to verify the differences among groups (species, sexes, ages). In order to check for outliers, the Cook's distance was used, where four times Cook's distance represented a cutoff for outliers.

In regard to the geometric morphometric methods, the photographs of each specimen were made using a Nikon D90 + 50 mm 1.8. Yongnuo lense mounted in a tripod above 45 cm of a foam cardboard. Images were analyzed using the Tps series (Rohlf, 2017a,b; 2021). In order to account for the variation in the nape (predorsal area), a curve was drawn on its border, from the posterior vertical of the margin of eye towards dorsal origin, this ending was initially a landmark. This curve was resampled to 5 points (by length), which were posteriorly assigned as landmarks, with the function of append tps curves to landmarks. The landmark at the final point of the curve was deleted, the remaining 5 points (semilandmarks – sLM) were then subject to a sliding step. All data were initially subjected to a Generalized Procrustes Analysis (GPA). To describe the Procrustes' residuals Principal Component Analysis (PCA), Linear Discriminant Analysis (LDA), Discriminant Analysis (DFA), and Canonical Variate Analysis (CVA) were carried out. As CVA tends to maximize variance, and we did not achieve the analysis presumptions in pooled-groups, we preferred to use a conservative interpretation of such data. The shape for each axis was evaluated through a Thin-plate splines.

Results

Species accounts

Stellifer gomezi (Cervigón, 2011)

Figure 3

Ophioscion sp. Valdez & Aguilera (1987)

Ophioscion sp. Cervigón (1993)

Ophioscion gomezi Cervigón (2011): 96–98 (description)

Material examined: (59 specimens) **Brazil:** **Bahia:** MZFS 17664, 2: 93-118 mm SL, (without locality, probably from Bahia state. P.R.D., Lopes *personal communication*). **Ilhéus:** MZFS 17678, 1: 105 mm SL, Ilhéus. **Itacaré:** MZFS 17101, 1: 132 mm SL, Itacaré. **Vera Cruz:** MZFS 17526, 1: 106 mm SL, Itaparica Island; MZFS 17930, 1: 78 mm SL, Itaparica Island; MZFS 16785, 17: 69-103 mm SL, Itaparica Island; MZFS 18142, 9: 79-100 mm SL, Itaparica Island; MZFS 12238, 1: 119 mm SL, Itaparica Island. **Espírito Santo:** CIUFES 131523, 1: 96.8 mm SL, Praia do Suá, Vitória. **Paraíba:** **Cabedelo:** UFPB 1460, 1: 103 mm SL, Miramar Beach; UFPB 180, 1: 67 mm SL, Miramar Beach. **Lucena:** UFPB 3212, 2: 93-101 mm SL, Lucena Beach; UFPB 3157, 2: 81-107 mm SL, Lucena Beach; UFPB 3074, 1: 113 mm SL, Lucena Beach; UFPB 3104, 3: 74-93 mm SL, Lucena Beach; UFPB 3127, 1: 83 mm SL, Lucena Beach; UFPB 3056, 1: 74 mm SL, Lucena Beach; UFPB 3325, 2: 87-99 mm SL, Lucena Beach; UFPB 3076, 3: 85-99 mm SL, Lucena Beach; UFPB 3190, 3: 75-86 mm SL, Lucena Beach; **João Pessoa:** UFPB 6601, 1: 96 mm SL, Cabo Branco Beach; UFPB 6556, 3: 58-75 mm SL, Cabo Branco Beach; UFPB 6600, 1: 82 mm SL, Seixas Beach.

Diagnosis.

Stellifer gomezi can be differentiated from all other Atlantic species of *Stellifer* by the inferior mouth (*vs.* terminal or oblique), except for *S. microps*, *S. naso* and *S. venezuelae*; from which it differs by the absence of appendages on the posterior margin of anterior gas bladder chamber (*vs.* kidney-shaped or tube-like appendages). Large eyes (4.1-4.6 in HL) (*vs.* more than 5.0 in HL) distinguish it from *S. microps*. Second dorsal spine close to or over two-thirds of the 3rd (*vs.* 2nd spine less than half of 3rd spine) differentiates it from *S. naso*. Longer pelvic-fin (less than 5.1 in SL) (*vs.* more than 6.4 in SL) distinguish it from *S. venezuelae*. Snout length less than 4.0 in HL (*vs.* snout length less than 4.0 in HL) distinguish it from *S. menezesi*. Both nostrils rounded, almost same sized, and in same horizontal (*vs.* anterior nostril directed forward, posterior nostril oval, vertically oriented and slightly larger than anterior) distinguish it from *S. menezesi*. The rounded nostrils of almost same size (*vs.* anterior nostril smaller than posterior, which is elongated closer to eye) also distinguish it from *S. punctatissimus*.

Description.

Dorsal rays X+I, 22-24; pectoral rays 18-19; anal rays II, 7; gill rakers 7-8 + 10-12 = 17-20; lateral line scales 47-49; scales above lateral line: to 1st dorsal 5-6, to 2nd dorsal 5-6; scales from lateral line to anal 10-11; circumpeduncular scales 18-21. Preopercular spines thin, spines closer to angle stronger and slightly longer but not reaching more than 1/3 of pupil diameter. Length of 2nd dorsal-fin spine in general surpassing slightly 2/3 of 3rd (rarely lower than 2/3). In the second dorsal the spine reach almost half of the first ray.

Body moderately compressed, generally elongated (4.0-5.0 in SL) (see “Sexual dimorphism”). The body angle varies between 61-66°, sometimes more than 70°. Head broad, firm to touch dorsally, conic. Snout long (3.5-3.8 in HL), rarely close to 3.9 in head length, surpassing by almost half its length the upper jaw tip, usually rounded but rarely straight shaped not quite surpassing the upper jaw. Snout without barbel, three upper and five marginal pores on snout. Chin with six pores, the median pair in a common pit. Dorsal profile rounded except some convex/concave regions, as nape usually rounded to straight, interorbital region slightly convex, ventral profile from rounded to flattened.

Mouth horizontal, subterminal, moderate to small (2.8-3.2 in HL). Teeth on upper jaw in viliform bands, the external larger than internal rows, anterior ones slightly larger than posterior. Teeth on lower jaw homogeneous in size. A small area without teeth in the anterior middle (close to the mandibular symphysis) of lower and upper jaw. Maxillary ends on vertical of middle eye to posterior margin of the eye. Eye moderate (4.1-4.6 in HL), orbit rounded. Gill rakers short and thin, the longest fits 1.6-2.4 in filament length and less than 2/3 of eye diameter.

Nostrils usually in the same horizontal, above to lower margin of eye, sometimes the anterior nostril it is set slightly below the posterior. Distance between nostrils nearly equal to height of posterior nostril; flap of anterior nostril rarely equal to this distance. Nostrils usually about the same size but some specimens with anterior nostril slightly smaller than posterior (anterior never larger than posterior), anterior nostril oval-shaped to rounded. The right anterior nostril occasionally slightly elongated. Posterior nostril usually of same size of anterior, but can be slightly larger than anterior, rounded to oval and usually not reaching the adipose eyelid.

Pectoral-fin almost reaching pelvic-fin tip in juveniles, but reaching or extending beyond pelvic-fin tip in adults. Pelvic-fin not reaching the vent even with its filament. Pelvic-fin filament length usually less but never surpassing the pupil diameter. Anal-fin truncate, second spine long (5.0-5.7 in SL) and strong, reaching or surpassing the first ray end. Caudal double truncate, smaller head length. Caudal peduncle moderately deep (9.5-10% of SL). Lateral line with anterior arch smooth, height to the dorsal 3.7-4.0 in HL.

Body with ctenoid scales overall excepting some parts of head: lachrymal, nostrils, snout, operculum membrane close to isthmus. Pectoral-fin base, area between pelvic fins as well on intermembranes of dorsal, pectoral, pelvic and anal fins mostly with small scales. Lateral line arborescent with a few dorsal and ventral branches.

Sexual dimorphism.

Males possess drumming muscles (sonic muscles) attached more anteriorly on its gas bladder mid-ventral section; muscles thin in juveniles but thick in adults when reach at least two times the skin thickness. Females lack the drumming muscles. Males generally with an elongated body; females have a deeper body.

Color in life.

Dark grayish to brownish all over the body, at least until upper pectoral horizontal, fins darker or equal to body color. Xanthophores occurs with chromatophores, but not so conspicuous as the chromatophores. Pale area only on isthmus, branchiostegal rays, part of operculum membrane and between pelvic to anal origin (sprinkled with chromatophores and xanthophores). An almost pale area below horizontal of the pectoral-fin. Pelvic-fin filament pale. Snout yellowish to brownish, densely covered by xanthophores and small chromatophores. Larger chromatophores towards preopercle; xanthophores rare in this area. Area around orbit (except above) covered by xanthophores and small chromatophores, supraorbital area most densely covered by chromatophores instead of xanthophores. Iris reddish to orange. Anal, caudal, pectoral and pelvic fins dark; paired fins with a pale margin mostly in distal tip. Darker apex in first dorsal-fin generally brown to gray. Darker area in the second dorsal covers 2/3 of the fin. Some inconspicuous lines below lateral line, formed by chromatophores at the middle of scales, more evident in paler specimens. Mouth pale, lips densely sprinkled by chromatophores and less by xanthophores. Black area among upper part of gill arches, covering at least the four uppermost gill rakers. A densely pigmented area around the pseudobranchiae as well almost the entire inside of operculum. Peritoneum mostly covered by silvery iridophores, with few chromatophores.

Color of preserved specimens.

Body brownish, faded ventrally (below pectoral-fin horizontal). Head with a distinct dark area on operculum due to heavily internal coloration by chromatophores. Also, a mix of small and large chromatophores near the snout, below nostrils and eye, and on preopercle.

Mouth pale, even on the lips. Iris white to yellowish faded color, its upper half with a black color or only a small strip on it. Area between snout and preopercle less pigmented in juveniles due to loss of xantophores (present in live specimens). The lines below lateral line can be more evident due to the higher contrast with a paler background. In alcohol the pectoral, pelvic and anal get a faded dark color or pale in some specimens. First dorsal-fin with an equal dark pigmentation, slightly darker distally. Last third of second dorsal-fin contrasts with first third in a dark coloration, but not so dark as other fins.

Distribution and habitat

Found mostly in sandy beaches exposed to waves, but also occurs in sand- or mud-bottoms (~12 m), rarely inside estuaries. Generally, its occurrence is linked to beaches closer to a river mouth and/or close to a reef bank. Its occurrence it is correlated to macrophytes accumulations in sandy beaches. It occurs from Caribbean, Venezuela and southwards to Southeastern Brazil.

Size

Maximum length close to 160 mm SL, commonly found around 80 mm SL.

Stellifer menezesi Chao, Carvalho-Filho & Santos, 2020

Figure 4

Material examined: (66 specimens) *Brazil:* **Alagoas:** MPEG 34496, 1: 77 mm SL, Jatiúca Beach; **Bahia:** Porto Seguro: MZFS 18131, 1: 84 mm SL, Porto Seguro; MZUSP 125604, 1: 102 mm SL, Porto Seguro. Vera Cruz: MZFS 16961, 18: 62-90 mm SL, Itaparica Island; MZFS 17688, 7: 62-66 mm SL, Itaparica Island; MZFS 17734, 7: 61-83 mm SL, Itaparica Island; MZFS 18142, 2: 69-77 mm SL, Itaparica Island; MZFS 18141, 4: 69-77 mm SL, Itaparica Island; MZFS 18177, 3: 71-81 mm SL, Itaparica Island; MZFS 17650, 4: 64-73 mm SL, Itaparica Island; MZFS 2100, 1: 78 mm SL, Itaparica Island; MZFS 16785, 2: 67-72 mm SL, Itaparica Island; MZFS 17125, 1: 108 mm SL, Itaparica Island. **Espírito Santo:** CIUFES 131523, 1: 84.29 mm SL, Praia do Suá, Vitória. **Paraíba:** Cabedelo: UFPB 419, 1: 37 mm SL, Miramar Beach. João Pessoa: UFPB 6556, 4: 47-54 mm SL, Cabo Branco Beach. Lucena: UFPB 3228, 2: 40-87 mm SL, Lucena Beach; UFPB 3056, 1: 76 mm SL, Lucena Beach; UFPB 3325, 1: 69 mm SL, Lucena Beach; UFPB 3076, 1: 76 mm SL, Lucena Beach. **Rio de Janeiro:** MZFS 6622, 2: 66-75 mm SL, Angra dos Reis. *Venezuela:* ANSP 144671, 1: 51.05 mm SL.

Diagnosis.

Stellifer menezesi can be differentiated from all other Atlantic species of *Stellifer* by the inferior mouth (*vs.* terminal or oblique), except for *S. microps*, *S. naso* and *S. venezuelae*; from which it differs by the absence of appendages on the posterior margin of anterior gas bladder chamber (*vs.* kidney-shaped or tube-like appendages). Large eyes (less than 4.0 in HL) (*vs.* more than 5.0 in HL) distinguish it from *S. microps*. Second dorsal spine reaching over two-thirds of the 3rd (*vs.* 2nd spine less than half of 3rd spine) differentiates it from *S. naso*. Longer pelvic-fin (less than 5.0 in SL) (*vs.* more than 6.4 in SL) distinguishes it from *S. venezuelae*. *Stellifer menezesi* has a more elongate body (especially in male adults), body depth equal or shorter than HL, paler body and fins not completely dark (*vs.* deep body, body depth higher than HL, darker body and black fins). The elongate shape of its pectoral-fin (in juveniles and adults) (*vs.* pectoral rounded in juveniles) also distinguishes it from *S. punctatissimus*. Pelvic-fin lack distal filament, if present is less than pupil diameter (*vs.* filament greater than eye diameter, or larger than pupil) distinguishes it from *S. punctatissimus*. Distance between nostrils almost the height of posterior nostril (*vs.* distance greater than height of posterior nostril, which is closer to eye) differentiates from *S. punctatissimus*. The anterior nostril directed forward, posterior nostril oval, vertically oriented and slight larger than anterior (*vs.* both rounded and almost same size) differentiates it from *S. gomezi*. Snout length more than 4.0 in HL (*vs.* snout less than 4.0 in HL) also differentiates *S. menezesi* from *S. gomezi*.

Description.

Dorsal rays X+I, 22-24; pectoral rays 18-19; anal rays II, 7; gill rakers 6-8 + 11-13 = 17-21; lateral line scales 46-50; scales above lateral line: to 1st dorsal-fin 5-6, to 2nd dorsal-fin 5-6; scales from lateral line to anal 9-11; circumpeduncular scales 18-20. Preopercular spines thin, the spines closer to the angle stronger and slightly longest than upper ones but not reaching more than 1/3 of pupil diameter. Length of 2nd dorsal-fin spine in general surpassing slightly 2/3 of the 3rd (rarely lower than 2/3). Second dorsal-fin spine length almost half of the first ray.

Body moderately compressed and elongated in general (4.0-5.0 in SL) (see “Sexual dimorphism”). The body angle varies between 60-68°, sometimes more than 70°. Head broad, firm to touch dorsally, conic. Snout short (4.0-4.5 in HL) surpasses by much less than half its length the upper jaw tip, usually rounded but sometimes the snout forms an angle between the ventral and dorsal face. Snout without barbel; three upper and five marginal pores on tip of snout. Chin with six pores, the median pair in a common pit. Dorsal profile rounded except

some convex/concave regions, nape usually rounded to slightly convex, interorbital region slightly convex, ventral profile from rounded to flattened.

Mouth horizontal, subterminal, moderate to small (2.7-3.2 in HL). Teeth on upper jaw in villiform bands, the external larger than internal rows, anterior ones slightly larger than posterior. Teeth on lower jaw homogeneous in size. A small area without teeth in the anterior middle (close to the mandibular symphysis) of lower and upper jaws. Maxillary ends on vertical of end pupil or between end of pupil and posterior margin of eye. Eye large (3.7-4.0 in HL); orbit rounded. Gill rakers short and thin, the longest fits 1.3-2.4 in gill filament length and less than 2/3 of eye diameter.

Nostrils usually in the same horizontal, above lower margin of eye; sometimes the anterior nostril it is set below the posterior. Distance between nostrils close to height of posterior nostril, flap of anterior nostril usually equal to this distance. Anterior nostril slightly smaller than posterior (anterior never larger than posterior), oval-shaped to elongate and directed forward. Anterior nostril occasionally distinct in shape bilaterally. Posterior nostril larger than anterior, bean-shaped and usually not reaching the adipose eyelid.

Pectoral-fin close to or reaching pelvic-fin tip in juveniles, and surpassing pelvic tip in adults. Pelvic-fin not reaching the vent even with its filament, when present. Pelvic-fin filament length usually less and never surpassing the pupil diameter. Anal-fin truncate, second spine short (4.8-5.8 in SL) and strong, almost reaching the end of first ray. Caudal-fin double truncate, smaller than head length. Caudal peduncle moderately deep (9.7-10.5% of SL). Lateral line with anterior arch smooth, height to the dorsal 3.8-4.1 in HL.

Body with ctenoid scales overall, excepting parts of head: lachrymal, nostrils, snout, operculum membrane close to isthmus. Pectoral base, between pelvic fins, intermembranes of dorsal, pectoral, pelvic and anal fins mostly with small scales. Lateral line arborescent with a few dorsal and ventral branches.

Sexual dimorphism.

Males with drumming muscles (sonic muscles) attached more anteriorly on its gas bladder mid-ventral section; muscles thin in juveniles but thick in adults, reaching at least two times in skin thickness. Females lack the drumming muscles. Males generally with an elongated body; females have a deeper body.

Color in life.

Body dark grayish to brownish, fins slightly darker or equal to body color. Xanthophores occurs with chromatophores, but not so conspicuous as the chromatophores. Pale

area only on isthmus, branchiostegal rays, part of operculum membrane and between pelvic to anal origin (sprinkled with chromatophores and xanthophores). Pelvic-fin filament pale. A slightly dark area below horizontal of the pectoral-fin. Snout yellowish to brownish, densely covered by xanthophores and small chromatophores. Area around the orbit (except above) covered by xanthophores and small chromatophores, supraorbital area densely covered by chromatophores instead of xanthophores. Iris reddish to orange. Larger chromatophores towards preopercle; xanthophores rare in this area. Anal, caudal, pectoral and pelvic fins dark; paired fins with a pale margin mostly in distal tip. Darker apex in first dorsal-fin, generally brown to grayish. Darker area in the second dorsal covers 2/3 of the fin. Some inconspicuous lines below lateral line, formed by chromatophores at the middle of scales, more evident in paler specimens. Mouth pale, lips densely sprinkled by chromatophores and less by xanthophores. Black area among upper part of gill arches, covering at least the four uppermost gill rakers. A densely pigmented dark area around the pseudobranchiae as well almost the entirely inside of operculum. Peritoneum mostly covered by silvery iridophores, with few chromatophores.

Color of preserved specimens.

Body brownish, fading ventrally. Head with a distinct dark area on operculum due to heavily internal coloration by chromatophores. Also, a mix of small and large chromatophores near snout, below nostrils and eye, and on preopercle. Mouth pale, even on the lips. Iris white to yellowish faded color, its superior half black or only with a small strip on it. Area between snout and preopercle less pigmented in juveniles due to loss of xanthophores (present in live specimens). The lines below lateral line can be more evident due to the higher contrast with a paler background. First dorsal-fin with even dark pigmentation, slightly darker distally. On the second dorsal the last third contrasts with a first third in a dark coloration, but not so dark as other fins. In alcohol the pectoral, pelvic and anal fins with faded dark color or pale in some specimens.

Distribution and habitats

Found mostly in sandy beaches, exposed to waves, rarely inside estuaries. Generally, its occurrence is linked to beaches somewhat near to a river mouth and with proximity from reef bank. Its occurrence is linked to macrophytes accumulations. It occurs from Northeastern Brazil to Southeastern, more common between Paraíba and Bahia states. Further research possibly may extend its range further north to the Venezuela coast.

Size

Maximum length close to 120 mm SL, commonly found around 60 mm SL.

Stellifer punctatissimus Meek & Hildebrand, 1925

Figures 5, 6

Ophioscion panamensis Schultz (1945): 126, 134 –136, Fig. 8 (key; description; Fox Bay, Colon, Panama

Material examined: (149 specimens) **Brazil:** **Alagoas:** UFPB 3373, 4: 45-55 mm SL, Pajuçara Beach; MPEG 34370, 6: 77-115 mm SL, Jaraguá; MPEG 34397, 7: 70-107 mm SL, Jaraguá; MPEG 34500, 1: 80 mm SL, Jatiúca; **Bahia:** MZFS 7745, 1: 138 mm SL, (without locality, probably from Bahia state. P.R.D., Lopes *personal communication*); MZFS 17694, 1: 109 mm SL, Caravelas; **Ilhéus:** MZFS 17683, 2: 77-86 mm SL; MZFS 11718, 1: 59 mm SL; MZFS 9998, 2: 51-55 mm SL; MZFS 9213, 3: 82-92 mm SL, Malhado Beach; **Itacaré:** MZFS 5334, 1: 100 mm SL; **Mucuri:** MZFS 5735, 1: 140 mm SL, Mucuri River; **Porto Seguro:** MZFS 17525, 1: 61 mm SL; MZFS 18116, 1: 81 mm SL; **Valença:** MZFS 1690, 1: 115 mm SL; **Vera Cruz:** MZFS 11863, 3: 32-45 mm SL, Itaparica Island; MZFS 17551, 2: 63-76 mm SL, Itaparica Island; MZFS 17669, 1: 41 mm SL, Itaparica Island; MZFS 17665, 3: 57-82 mm SL, Itaparica Island; MZFS 822, 2: 51-61 mm SL, Itaparica Island; MZFS 811, 2: 42-52 mm SL, Itaparica Island. **Espírito Santo:** CIUFES 1834, 3: 61.08-62.38 mm SL, Ilha do Frade, Vitória; CIUFES 131692, 1: 98.93 mm SL; CIUFES 131756, 2: 81.97-95.89 mm SL. **Paraíba:** **Cabedelo:** UFPB 102, 1: 78 mm SL, Paraíba River; UFPB 413, 2: 55-87 mm SL, Miramar Beach; UFPB 180, 5: 54-68 mm SL, Cabedelo Beach; UFPB 1457, 1: 67 mm SL, Miramar Beach; UFPB 1923, 1: 72 mm SL, Miramar Beach; UFPB 1922, 1: 67 mm SL, Cabedelo Beach; UFPB 1460, 1: 76 mm SL, Miramar Beach; UFPB 6004, 1: 51 mm SL, Miramar Beach; UFPB 725, 2: 63-72 mm SL, Miramar Beach; UFPB 601, 1: 142 mm SL, Poço Beach; UFPB 412, 1: 73 mm SL, Miramar Beach; UFPB 419, 5: 36-71 mm SL, Miramar Beach; UFPB 421, 7: 63-70 mm SL, Miramar Beach; **João Pessoa:** UFPB 1967, 1: 95 mm SL, Tambaú Beach; UFPB 6556, 2: 64-70 mm SL, Cabo Branco Beach; UFPB 1915, 4: 43-50 mm SL, Cabo Branco Beach; UFPB 1933, 3: 49-55 mm SL, Bessa Beach; UFPB 829, 1: 55 mm SL, Cabo Branco Beach; UFPB 4560, 6: 50-81 mm SL, Cabo Branco Beach; UFPB 6558, 1: 92 mm SL, Cabo Branco Beach; UFPB 1330, 1: 66 mm SL, Barra de Gramame; UFPB 2124, 3: 53-58 mm SL, Cabo Branco Beach; UFPB 2000, 2: 56-77 mm SL, Tambaú Beach UFPB 4558, 2: 101-106 mm SL, Cabo Branco Beach; UFPB 6402, 1: 73 mm SL, Cabo Branco Beach; UFPB 1314, 4: 35-65 mm SL, Ponta do Seixas Beach; UFPB 1916, 1: 48 mm SL, Tambaú Beach; **Lucena:** UFPB 3228, 1: 59 mm SL, Lucena Beach; UFPB 3174, 1: 102 mm SL, Lucena Beach; UFPB 3206, 1: 113 mm SL, Lucena Beach;

UFPB 3212, 2: 88-96 mm SL, Lucena Beach. **Pernambuco:** MZFS 460, 5: 61-72 mm SL, Itamaracá Island; MZFS 475, 2: 69-73 mm SL, Itamaracá Island; MZFS 428, 1: 72 mm SL, Itamaracá Island; **Rio Grande do Norte:** UFPB 689, 1: 67 mm SL, Tibau Beach. **Rio de Janeiro:** ANSP 121373, 3: 131-158 mm SL, Atafona, Rio de Janeiro. *Puerto Rico:* ANSP 115620, 9: 54.57-107 mm SL, Puerto Yabucoa; ANSP 115655, 2: 79.28-87.61 mm SL. *Venezuela:* ANSP 114130, 1: 133 mm SL, Peninsula de Araya, Estado Sucre.

Diagnosis.

Stellifer punctatissimus can be differentiated from all other Atlantic species by the inferior mouth (*vs.* terminal or oblique), except by *S. microps*, *S. naso* and *S. venezuelae*; from which it differs by the absence of appendages on the posterior margin of anterior gas bladder chamber (*vs.* kidney-shaped or tube-like appendages). *Stellifer punctatissimus* has a strongly arched back (especially in male adults), body depth much greater than HL, darker body and with black fins (*vs.* elongate body, body depth equal or shorter than HL, paler body in *S. menezesi* and *S. gomezi*). The rounded shape of its pectoral-fin (in juveniles) (*vs.* somewhat elongate) also distinguish it from *S. menezesi* and *S. gomezi*. Distance between nostrils greater than height of posterior nostril and set closer to eye (*vs.* distance between nostrils equal to posterior, which is oval and vertically oriented, not entirely close to eye), differentiates it from *S. menezesi*. The anterior nostril small, rounded, and posterior nostril elongated (*vs.* both nostrils rounded and almost the same size) distinguish *S. punctatissimus* from *S. gomezi*. The length of filament of pelvic-fin equal to or greater than eye diameter (*vs.* lacking filament, or filament equal to or shorter than pupil diameter) distinguishes *S. punctatissimus* from *S. menezesi*.

Description.

Dorsal rays X+I or II, 22-24; pectoral rays 18-22; anal rays II, 7; gill rakers 7-8 + 11-13 = 18-21; lateral line scales 46-50; scales above lateral line: to 1st dorsal-fin 6-7, to 2nd dorsal-fin 5-7; scales from lateral line to anal-fin 10-12; circumpeduncular scales 19-24. Preopercular spines thin, the spines closer to the angle stronger and longer but not reaching more than 1/3 of pupil diameter. Length of 2nd dorsal-fin spine in general surpassing slightly 2/3 of the 3rd (rarely lower than 2/3). Second dorsal-fin spine reaching almost half of the first ray, or more than half in individuals with X + II configuration.

Body moderately compressed, generally deep (3.5-4.8 in SL) (see “Sexual dimorphism”). The body angle usually between 55-75°, sometimes more than 80°. Head broad, firm to touch dorsally. Snout long (3.8-4.2) surpassing the upper jaw by almost half of its length or vertically oriented, reaching only the tip of upper jaw. Snout without barbels, with three

upper and five marginal pores on its tip; rostral fold slightly indented below the marginal pores. Chin with six pores, the median pair in a common pit. Dorsal profile straight to convex or concave, nape convex, interorbital region slightly concave, slightly convex region between frontal and nasal bones, ventral profile from flattened to rounded.

Mouth horizontal, subterminal, moderate to small (2.6-3.2 in HL). Teeth on upper jaw in villiform bands, the external larger than internal rows, anterior ones slightly larger than posterior. Teeth on lower jaw homogeneous in size. A small area without teeth on the middle of lower and upper jaw, close to the mandibular symphysis. Maxillary ends on vertical from posterior margin of pupil to posterior margin of eye. Eye large to moderate (3.8-5.0 in HL), orbit round. Gill rakers short and thin, the longest fits 1.5-3 in filament length and less than 2/3 of eye diameter.

Anterior nostril generally below lower margin of eye and the posterior one at the same level or above lower margin of eye. The distance between nostrils about two times the height of posterior, flap of anterior nostril usually equal to half of this distance. Anterior nostril slightly smaller than posterior (anterior never larger than posterior), round to slightly elongate in sub-adults. Anterior nostrils occasionally distinct in shape bilaterally. Posterior nostrils larger than anterior, shape oval to elongate and set close to adipose eyelid. Posterior nostril directed backwards in juveniles, not so evidently in adults.

Pectoral-fin not reaching pelvic-fin tip in juveniles, but beyond pelvic tip in adults. Pelvic-fin not reaching the vent in adults, but pelvic-fin filament can reach the vent. Pelvic-fin reaches or surpasses the vent in juveniles. Pelvic-fin filament length generally equal to pupil diameter but may be as large as eye diameter. Anal-fin truncate, second spine short (5.1-6.5 in SL) and strong, not reaching the first ray end. Caudal-fin double truncate, its length less than head length. Caudal peduncle deep (10-11% of SL). Lateral line with anterior arch slightly deep, height to the dorsal 3.2-3.8 in head length.

Body generally with ctenoid scales exception to lachrymal, nostrils, snout, operculum membrane close to isthmus, pectoral base, between pelvic fins as well on intermembranes of dorsal, pectoral, pelvic and anal fins were mostly are present small cycloid scales. Lateral line arborescent with a few dorsal and ventral branches.

Sexual dimorphism.

Males with drumming muscles (sonic muscles) attached more anteriorly on its gas bladder mid-ventral section, thin in juveniles but thick in adults, reaching at least two times the skin thickness. Males generally with snout shorter than females and a deeper body. Females

lack the drumming muscles. Their body is more elongated, but sometimes equal in depth to males, the head and snout more conic than in males.

Color in life.

Dark brownish all over the body, fins even darker than body. Xanthophores occurs with chromatophores, but not so conspicuous as the chromatophores. Pale area only on isthmus, branchiostegal rays, part of operculum membrane and between pelvic to anal origin (sprinkled with chromatophores and xanthophores). A distinct pale filament on pelvic fin. Snout yellowish to brownish, densely covered by xanthophores and small chromatophores. Area around the orbit (except above) covered by xanthophores and small chromatophores, supraorbital area most densely covered by chromatophores instead of xanthophores. Iris reddish to orange. Larger chromatophores towards to preopercle; xanthophores rare in this area. Anal, caudal, pectoral and pelvic dark but the paired fins present a pale margin mostly in distal tip. Darker apex in first dorsal-fin, generally brown to dark. Darker area in the second dorsal covers 2/3 of the fin. Almost 7-8 black lines below lateral line, formed by chromatophores at the middle of scales, more evident in paler specimens. Mouth pale, lips densely sprinkled by chromatophores and less by xanthophores. Black area among upper part of gill arches, covering at least the four uppermost. A densely pigmented dark area around the pseudobranchiae as well almost the entirely inside of operculum. Peritoneum mostly covered by silvery iridophores, with few chromatophores.

Color of preserved specimens.

Body brownish. Head with a distinct dark area on operculum due to heavily internal coloration by chromatophores. Also, a mix of small and large chromatophores near snout, below nostrils and eye, and on preopercle. Mouth pale, even on lips. Iris white to yellowish faded color, its superior half with a black color or only a small strip on it. Area between snout and preopercle less pigmented in juveniles due to loss of xanthophores (present in live specimens). Conspicuous line pattern on the side of the body of juveniles, due to contrast with a more "pale" background. In adults this pattern can be hidden by a large amount of small chromatophores, fading the large ones (here called "central chromatophores"), in a few specimens a conspicuous pattern it is shown even in adults with dark coloration (Figure 5). First dorsal-fin with an even dark pigmentation, slightly darker distally. On the second dorsal the last third contrasts with a first third in a dark coloration, but not so dark as other fins. In alcohol the pectoral, pelvic and anal fins stay dark but in long preserved specimens this

coloration fades. The pectoral and pelvic fins may present a pale area on lower half or close to the base.

Distribution and habitat

Found in sandy beaches, rarely inside estuaries but generally its occurrence is linked to a mouth of river, proximity from reef bank and exposed sand beaches. Its occurrence in beaches is linked to macrophyte accumulations. Adults are more common over sandy/mud bottoms close to 10-20m depth. It occurs from the Caribbean, Panama, southward to Southeastern Brazil.

Size

Maximum length close to 150 mm SL, commonly found around 80 mm SL

Remarks

Although its etymology, we found several specimens of *Stellifer punctatissimus* (Meek & Hildebrand, 1925) – with no “micro eye” – as misidentification of *Stellifer microps* (Steindachner, 1864). *Stellifer punctatissimus* has a large to moderate eye (rarely exceeds 5.0 in HL), distinguishing it from *S. microps* that has a smaller eye (5.2-6.8 in HL) (Chao, 2002; our study). Also, a recurrent issue were specimens identified as *Micropogonias furnieri* (Desmarest, 1823), this had occurred in the past in former “*Ophioscion*” synonyms (see Chao et al., 2021 – pp. 438 – 440), it could be easily distinguished by the long second dorsal-fin (27-29 rays) and presence of 3-5 series of barbels on the chin (Chao, 2002).

Morphological traits

In regard to linear morphometrics, the PCA gave a rather overlapped distribution, with *Stellifer gomezi* (GOME) and *S. menezesi* (MENE) sharing almost the same morphospace while *S. punctatissimus* (PUNC) slightly separated from them. This distinction was more accentuated in PC2 axis, which accounted for variation on body depth and eye diameter. This configuration was a result of PUNC having, in comparison, a smaller eye and higher body depth, it set together the other two species by them sharing a more elongate body and larger eye (especially MENE) (Table 1,2). However, some distinction is found between those species. At some level, the snout length, interorbital width, and pectoral-fin aspect-ratio could distinguish those species in PC1 axis (Fig. 7). Although, in a more general view they occupy a similar morphospace, which is reinforced by the low reclassification rate (50% - GOME; 34.3% - MENE), according to the LDA (Table 3). It was also recovered by the PCA, using geometric morphometrics

methods (GMM); however, it showed more overlapping among the species, but with the same kind of within variation of PUNC (largest). In the PC1, this variation was most associated with a deeper body, as well as changes on snout and nostrils. In the PC2, the variation was linked to a less deep body, convex nape, and pectoral-fin posteriorly positioned (Fig. 7). In order to identify possible geographic variation, we analyzed the reduced dataset (not shown). A clear pattern on geographic variation was not found, either when more general zoogeographic regions or more accurate ones were applied.

Allometry and growth patterns

In order to identify the most suitable meristic characters, violin plots initially were conducted (not shown). Of these, six characters were then selected to be displayed in scatterplots as follows: eye diameter, snout length, interorbital width (in HL), aspect-ratio of pectoral-fin, caudal peduncle height, and predorsal length (in SL) (Fig. 8).

In general, the eye diameter showed a little steeper pattern, both *S. gomezi* (GOME) and *S. punctatissimus* (PUNC) presented a more even steep pattern, while a less steep slope was found for *S. menezesi* (MENE). In regard to the snout length, a near zero slope was found for PUNC, while both GOME and MENE showed a negative less steep slope; although each one with nearly opposing data. The caudal peduncle height showed distinctiveness between PUNC and GOME/MENE, with the former presenting a negative less steep slope, whereas the latter presented a not steep slope. Of those meristic characters only the interorbital width showed a non-linear growth. Although a slight difference in steepness (below 80 mm - SL); in general, all the species presented an even steeper slope until nearly 80 mm. The values were then distinct, with GOME presenting a not steep slope which was contrasting in relation to PUNC that presented a smoother negative curve; reaching values of juveniles. In regard to the aspect-ratio of pectoral-fin, PUNC displayed the lowest values (rounder shape) and GOME/MENE entire overlapped values, the latter group with a slight higher value (slender shape) than the former. The predorsal length presented nearly not steep slope for MENE and GOME (positive and negative, respectively); while PUNC showed a negative less steep slope.

As presented before, interorbital width, eye diameter, snout length, and body depth were the most significant traits in explaining ontogenetic variations. This is reinforced by Common Allometric Component (CAC), which recovered a pattern similar to the one found in PCA (i.e., GOME/MENE forming a group somewhat distinct from PUNC); however, differently from PCA's results, CAC showed a higher overlap between PUNC and the pair GOME/MENE. It was correlated with size ($R^2 = 0.499506$) and the Residuals of Shape Coordinates (RSC) have accounted for 51.5% in shape' variance. Most of this variance in allometry was related to

growth of fin-bases, followed by snout- and nape-length, and eye diameter. It is noteworthy that, in CAC, head shape variance was linked to a longer nape (predorsal length) in association with a more developed hump especially on its posterior end. Whereas, in RSC1, most of the variation was found in the form of a less deep body, slight convex region on frontal, vertical position of nostrils, eye, and snout; as well as position of the fins (Fig. 9).

Sexual dimorphism

The all-males PCA retrieved a more overlapped pattern than all-females dataset, that is, it presented lower overlapping between pair GOME/MENE with PUNC. It can be confirmed by the LDA reclassification rate (Table 3), which presented 92.98% of correctly classified specimens for males, while all-females have reached 96.82%. As displayed by centroids in the PCA, in the all-males dataset those centroids were placed near to the average point, while in the all-females it was more segregated (considering specially PC2 axis). In regard of body shape, although it was more evident in all-females dataset, either males or females of PUNC presented a deeper body than GOME and MENE. Similarly, the geometric morphometric methods (GMM) gave a more overlapped pattern for males, whereas in females fewer specimens were overlapping (Fig. 10). This is related to the most disparity being found within males than females. However, in general, only in the PUNC that males presented deeper bodies than females, in GOME and MENE the females showed slightly deeper bodies (Fig. 11).

Key to the species of *Stellifer* (Modified from Chao et al., 2021)

- 1a. Mouth moderate to small, subterminal to inferior; position of anterior tip of upper jaw ventral to lower eye margin 2
- 1b. Mouth large, terminal to strongly oblique; position of anterior tip of upper jaw horizontal to or dorsal to lower eye margin 11
- 2a. Scales on top of head cycloid, smooth to touch; underside of lower jaw with 6 mental pores 3
- 2b. Scales on top of head ctenoid, rough to touch; underside of lower jaw with 5 mental pores 6
- 3a. Spinous dorsal-fin with XII or XIII spines; roof of mouth and underside of gill cover jet black; total gill rakers 37–40 *S. cervigoni* Chao, Carvalho-Filho & Santos, 2021 (Dominican Republica, Colômbia, Venezuela to Pará, Brasil)
- 3b. Spinous dorsal-fin with X or XI spines (rarely XII); roof of mouth pale to dusky, never black; total gill rakers fewer than 32 4

- 4a. Dorsal profile strongly arched; top of head firm to touch; total gill rakers 27–32, longest raker longer than gill filament; second anal-fin spine stout, about equal length to first soft ray, 1.9–2.4 in HL; anterior gas bladder with a pair of small knob-like appendages *S. colonensis* Meek & Hildebrand, 1925 (Panama, Puerto Rico, Haiti and Venezuela)
- 4b. Dorsal profile smoothly arched; top of head cavernous soft to touch; gill rakers fewer than 24, longest raker shorter than gill filament; second anal-fin spine 2.2–3.0 in HL; anterior gas bladder with digital-like tubes or U-shaped appendages 5
- 5a. Second anal-fin spine strong, equal to length of the first ray, 2.2–2.5 times in HL; appendage on gas bladder in short digital-like tubes *S. microps* (Steindachner, 1864) (Caribbean coast from Colombia to Northeastern Brazil)
- 5b. Second anal-fin spine shorter than first ray, 2.4–3.0 times in HL; a pair of U-shaped tubular appendages on gas bladder *S. brasiliensis* (Schultz, 1945) (Endemic to Brazil from the Northeast region to the Southeast region)
- 6a. Pelvic-fin short, 5.8 times or more in SL, its tip well anterior to tip of pectoral-fin; anterior chamber of gas bladder with a pair of kidney-shaped appendages 7
- 6b. Pelvic-fin moderately long, 5.8 times or less in SL, its tip reaching posteriorly to that of pectoral-fin; anterior chamber of gas bladder with or without appendages, but never kidney-shaped 8
- 7a. Eye large, 3.5–4.2 in HL, equal to or slightly longer than snout length; pelvic-fin 5.8–6.8 times in SL; total gill rakers 21–25 *S. naso* (Jordan, 1889) (Venezuela to Northeastern Brazil)
- 7b. Eye moderate, 4.1–5.3 in HL, shorter than snout length; pelvic-fin very short, 6.4–8.1 times in SL; total gill rakers 25–30 *S. venezuelae* (Schultz, 1945) (Honduras, Colombia, Venezuela and Trinidad)
- 8a. Eye small, 6.3–6.4 in HL; a small fish, females mature at 60 mm SL; pelvic-fin short, 5.2 to 5.8 times in SL; total gill rakers 25–29 *S. magoi* Aguilera, 1983 (Known only from Gulf of Venezuela)
- 8b. Eye moderately large, 6.2 or less in HL; females mature greater than 80 mm SL; pelvic-fin less than 5.2 in SL; total gill rakers fewer than 23; no appendages on posterior margin of anterior chamber of gas bladder 9
- 9a. Back strongly arched; body depth 3.5–4.8 in SL; pectoral and pelvic fins black; rounded pectoral-fin in juveniles (Fig. 12) *S. punctatissimus* (Meek & Hildebrand, 1925) (From Panama and Porto Rico through Caribbean and Northern South America and along Atlantic coast to Southeastern Brazil, at least São Paulo)

- 9b. Body elongate; body depth 4.0-5.0 in SL; pectoral and pelvic fins pale or black only distally; pectoral-fin elongate in juveniles 10
- 10a. Body depth equal to or less than HL; eye 4.1–5.6 in HL, slightly shorter than snout length; snout length less than 4.0 in HL; nostrils rounded and almost the same height; tip of pectoral-fin posterior to tip of pelvic-fin; fins pale to dusky *S. gomezi* (Cervigón, 2011) (Caribbean coast from Colombia to Venezuela and along Atlantic coast to Southeastern Brazil, at least to São Paulo)
- 10b. Body depth slightly greater than HL; eye 3.6–4.6 in HL, equal to or slightly greater than snout length; snout length more than 4.0 in HL; anterior nostril slightly oval and forward-directed forming an angle with the bean-shaped posterior nostril; tip of pectoral-fin reaching to or posterior to tip of pelvic-fin; distal portion of pectoral, pelvic and anal fins blackish *S. menezesi* Chao, Carvalho-Filho & Santos, 2021 (From Paraíba to São Paulo state, uncommon south of Bahia, on the Brazilian coast)
- 11a. Preopercular margin with two or three prominent spines 12
- 11b. Preopercular margin with four or more prominent spines 14
- 12a. Preopercular margin with three prominent spines (occasionally four on one side); total gill rakers 33–39; dorsal-fin rays 18–20 *S. stellifer* (Bloch, 1790) (Venezuela to Southern Brazil, one record from Puerto Rico)
- 12b. Preopercular margin with two prominent spines; total gill rakers 36 or more; dorsal-fin rays 20–24 13
- 13a. Nape and pre-dorsal region with one to several median rows of ctenoid scales; total gill rakers 36–52; inside of gill cover jet black; anterior chamber of gas bladder with a pair of long tubular appendages *S. rastrifer* (Jordan, 1889) (Venezuela to Rio Grande do Sul, Brazil)
- 13b. Scales on nape and pre-dorsal region cycloid; total gill rakers 52–59; inside of gill cover dusted with melanophores; anterior chamber of gas bladder with a pair of small knob-like appendages *S. griseus* Cervigón, 1966 (Venezuela, Honduras, and Trinidad)
- 14a. Eye large, greater than snout length, 3.4–4.5 in HL; anal-fin rays 9 (rarely 8); total gill rakers 29–36 *S. musicki* Chao, Carvalho-Filho & Santos, 2021 (Found in Brazil, from Pará to Bahia)
- 14b. Eye moderate to small, shorter than snout, 4.4 times or more in HL; anal-fin rays 8 (rarely 9); total gill rakers 28–48 15
- 15a. Underside of lower jaw with four mental pores; eye small, 5.1–6.4 in HL 16
- 15b. Underside of lower jaw with six mental pores; eye moderately large, 4.4–5.5 in HL 17

- 16a. Head scales all cycloid, scales on body ctenoid; total gill rakers 41–48 *S. chaoi*
Aguilera, Solano & Valdez, 1983 (Colombia and Gulf of Venezuela)
- 16b. Head squamation cycloid only in interorbital region; total gill rakers 28–37..... *S. collettei* Chao, Carvalho-Filho & Santos, 2021 (Southeast Venezuela, Surinam, French Guyana to Southeastern Brazil)
- 17a. Top of head extremely cavernous, spongy to touch; total gill rakers 29–33, longest raker about equal to filament length at the angle; gas bladder appendage knob-like *S. lanceolatus* (Holbrook, 1855) (Chesapeake Bay to Gulf of Mexico)
- 17b. Head not spongy to touch; total gill rakers 28–31, longest raker longer than filament length at the angle; gas bladder without appendages *S. macallisteri* Chao, Carvalho-Filho & Santos, 2021 (Caribbean sea from Canal zone Panama, Colombia to Gulf of Venezuela, also in Dominican Republic)

Discussion

A deficient sampling is a major concern in taxonomy, as it could lead to nomenclatural instability (Reis et al., 2020) and work as basis to the Linnean shortfall (Lomolino, 2004; Nori et al., 2021). Herein, our results support this by showing a variation way bigger than formerly recognized by Meek & Hildebrand (1925), even if we disregard the species complex itself, it also points to poor sampling as a cause of further taxonomic issues. Perhaps, it falls also into other shortfalls such as Darwinian and Wallacean, due to their interdependence with the Linnean (Lomolino, 2004; Hortal et al., 2015).

In their *Stellifer punctatissimus* (Meek & Hildebrand, 1925) description, Meek & Hildebrand (1925) failed to address intraspecific variation, such as the supposed lack of dark streaks on its body and pelvic-fin filament. In doing so, they undermine the diagnose of such taxa, once both characters were used to distinguish from its former congeners, but later found to be variable in its population. The presence of dark streaks is a rather common trait in Stelliferinae members from Eastern Pacific, thus, the variable condition in Atlantic species may retrieve the evolutionary history of such group by sharing a “recent” common ancestor in the amphiamerican region (Lo et al., 2015; Aguilera et al., 2016; Silva et al., 2018). Among the species there is no clear pattern of this trait. Despite being more common in preserved juveniles of *Stellifer punctatissimus*, it is also found in adults even with a darker coloration, the same occurs in *S. gomezi* and *S. menezesi*. Finally, the presence/length of a pelvic-fin filament has generated doubt across time, once it was too often used in a subjective way. Meek & Hildebrand (1925) stated that it “projects well beyond the longest [pelvic-fin] rays”, while Schultz (1945) – on his “*Ophioscion panamensis*” description, says that the pelvic-fin ends in a short filament,

precluding comparisons. However, by comparing plate and description, it seems that the former definition was correct and Schultz' description was likely only subjective (not completely wrong). Additionally, Chao et al. (2021) describe *S. menezesi* as having a short filament, whereas as restated herein, it has indeed a short filament but with a length reference (i.e., usually less and never surpassing the pupil diameter).

Furthermore, even though Schultz (1945) did include specimens of *Stellifer punctatissimus* in his work, he relied on a few small individuals of a reduced geographic area – falling into the Wallacean shortfall (Hortal et al., 2015). As a result, such minute variations are explained as being at a species-level, disregarding allometry trends on intraspecific variation. Body shape can respond for environmental changes or distinctions (Bonini-Campos et al., 2019; Gilbert et al., 2020; Figueiredo et al., 2021), but it may also carry strong allometry signal, as such, it could hide differences associated with allometry and hampering phylogenetic inferences and history biology data (Castro et al., 2021; Lacerda et al., 2021). Allometry might have a main effect on modulate phenotypic disparity in animals (Castro et al., 2021), and a distinct integration pattern in body development, may lead to larger ontogenetic disparities (Evans et al., 2017). Our results reinforce this idea by showing ontogenetic distinction among species, it also indicates that initial Schultz' assumption was inadequate, once morphological variations should be considered as being affected by allometry (Voje et al., 2014; Klingenberg, 2016). For instance, although not considered as diagnostic character, the interorbital space (herein, interorbital width) is described as broad and a little convex, whereas, we show that it varies according to size and strongly by species. In respect to allometry, the trends presented herein recover patterns in size and position of fins at a macroevolutionary level within Actinopterygii (Larouche et al., 2018). Comparatively, other traits such as body depth may also be related to benthic-pelagic axis transitions at the macroevolutionary scale, it seems to indicate difference among species and by habit groups (Clabaut et al., 2007; Deary & Hilton, 2016; Deary & Hilton, 2017). In cichlids, Clabaut et al. (2007) points out that benthic prey feeders have a less deep body, however, it seems that in marine fishes this is rather a characteristic of pelagic species (Tavera et al., 2018; Friedman et al., 2020).

In sciaenids, traits such as eye diameter, which increases with size and towards pelagic species, are an example of other trends (Busserolles et al., 2013; Deary & Hilton, 2017). Likewise, this increasing in eye size means higher visual acuity, as a result, it might allow such species to prey upon smaller and mobile food items (Davis & Birdsong, 1973; Goatley & Bellwood, 2009; Caves et al., 2017; Liggins et al., 2021). It agrees with diet data for *Stellifer punctatissimus* species complex, which show that most of its prey are small and mobile (Santos et al., 2021), but it should be evaluated in further research whether such habit varies

significantly among those species. It could be suggested that *S. menezesi* has a diet more linked with such type of prey and not varying along its life cycle, while the other species may present a diet shift along their ontogeny. Moreover, a smaller interorbital width might promote a more accurate fishes' prey selection, it also indicates that those species are more linked to benthic habit (Gatz, 1979; Rüber & Adams, 2001; Pessanha et al., 2015); likely, by having a smaller interorbital width, adults of *S. gomezi* are the closest to benthic habitat, whereas, in the other extreme is *S. punctatissimus* with the largest values of this trait. However, in our case it is uncertain if those variations could retrieve such large difference in water column positioning, especially considering its occurrence in shallow waters.

Additionally, an inappropriate sampling also hampers identification of sexual dimorphism patterns. Because some females of *S. punctatissimus* presented a “male pattern” in body shape (the contrary it was rarer), there is no pronounced pattern in sexual dimorphism. However, there are a few aspects important to notice. Within the complex, it was more often found larger females (deep body), while in *S. punctatissimus* the contrary it was more common. In a recent article, Berendzen et al. (2021) identify a greater segregation in males-only analyses, indicating a faster morphological divergence in males than in the rest of the population. Interestingly, we found more disparity within males than females, thus, the former encompasses a slight larger morphospace and it gave a lower percentage of correctly classified specimens. Additionally, there are other factors that might have influence upon shape and disparity between sexes, such as latitudinal gradients, that seem to change the level of sexual dimorphism and to distinctively drive selection of traits in systems of female- and male-choice (Lima-Filho et al., 2017; Murray et al., 2021). As they present differences in growth rates and shape, is expected that in further analysis could show body size patterns (e.g., Bergmann's rule) varying by species, potentially with sexual dimorphism signal.

All points considered, identification of species complex needs to consider as many factors as possible and to apply different approaches in order to shed light on this shadow zone. Because the evolutionary origin itself might lead to constraints in phenotypic disparity, such as stasis and niche conservatism, it turns more difficult to identify cryptic species than “regular” ones (Struck & Cerca, 2015; Riddle et al., 2011). As shown for mullets (*Mugil* spp.) and snooks (*Centropomus* spp.), this conservatism may contribute to taxonomic uncertainty, because not always morphological and molecular approaches are congruent (Figueiredo-Filho et al., 2021; Neves et al., 2021). For instance, on the *Stellifer punctatissimus* complex there is an ongoing disagreement between morphological and molecular views, the former has described three species on its complex whereas the latter presented two lineages in this complex (Barbosa et al., 2014; Silva et al., 2018; Chao et al., 2021). Comparatively, their “lineage I” could be

tentatively identified as *S. punctatissimus*, while the “lineage II” may include together *S. gomezi* and *S. menezesi* (Silva et al., 2018; this study). It partially agrees with some of our results, such as PCA’s, that present two groups. However, as discussed herein, it may also result from an evolutionary history that has led to a low morphological distinction without clear genetic divergence, as recorded for marine catfishes and seabasses, where environmental distinctions might have acted as a driver of species’ divergence (Carvalho-Filho et al., 2009; Marceniuk et al., 2019a), although, those lineages or morphotypes were not in every case considered as distinct species. Therefore, such mismatch between ours and molecular propositions are likely to be caused by such methods not recovering a result of a recent process of ecological and/or incipient speciation, that seems to be more frequent than expected for the marine environment (Carvalho-Filho et al., 2009, 2010; Marceniuk et al., 2019a; Aderne et al., 2022). It shows that, especially in cryptic species, filling the taxonomic gap (i.e., Linnean shortfall) through a Linnaean renaissance is mandatory, in order to describe and expand this knowledge before we lose more species in this biodiversity crisis (Wilson, 2017; Walters et al., 2021).

Furthermore, such measures are extremely important in the context that we still discover new species, genera or even families (de Pinna et al., 2018; Frainer et al., 2021). This diversity is somewhat “hidden” in natural history museums, either by lack of specimens (de Pinna et al., 2018) or inaccessibility by DNA barcoding (Zhang, 2010), although, several works have attempt to recover DNA from formalin-fixed fish specimens (e.g., Chakraborty et al., 2006; Appleyard et al., 2021; Hahn et al., 2021). Additionally, that diversity could being hidden in plain sight in environments such as Amazonian headwaters (de Pinna et al., 2018) and at bycatch (Keledjian et al., 2014; Chao et al., 2015; Chao et al., 2021). In their review, Bickford et al. (2006) point out several issues in regard to cryptic species conservation, probably one of the most important are the implications in ecology studies, due to those complexes may mask distinct functional traits and growth rates, as presented here (Geller, 1999; Bickford et al., 2006). As a result, it could lead to species even more rarer than expected being under the umbrella of other endangered or threatened species, as such, it should be considered that different species require specific conservation strategies (Schönrogge et al., 2002). As each species may have distinct ecologies and shapes, they could also respond differently to threats (Caires et al., 2019), thus, in a context of cryptic species with distinct shape that could suggest distinct habitat use (e.g., water column, distance from coast), this should be carefully addressed through conservation assessment.

Acknowledgments

We are grateful to Paulo Roberto, Jailza Oliveira, Klleyza Santos, Jean Joyeux, Kathiani Bastos, Wolmar Wosiacki, Ângelo Dourado, Mariangeles Arce, Mark Sabaj, Karsten Hartel, Andrew Williston, Alfredo Carvalho-Filho, and Ning Chao, for their assistance in museum visits and loan of specimens. We thank Leonardo Moraes, Verônica Costa, Marcelo Carvalho-Júnior, Rafael Oliveira, Natália Souza and Hemille Mariane for their help in fieldwork. We are also grateful to Pedro Romano, Gabriela Figueiredo, João Capretz for their suggestions on data analysis. JAS received scholarship from the Coordenação de Aperfeiçoamento de Pessoal de Nível Superior, Brazil (CAPES – finance code 001).

Literature cited

- Adams DC, Glynne E, Kaliontzopoulou A. 2020. Interspecific allometry for sexual shape dimorphism: Macroevolution of multivariate sexual phenotypes with application to Rensch's rule. *Evolution* 74(9): 1908–1922. <https://doi.org/10.1111/evo.14049>
- Aderne AF, Bitencourt JA, Watanabe LA, Schneider H, Affonso PRM, Sampaio I. 2022. Allopatric divergence and secondary contact of two weak fish species (*Macrodon ancylodon* and *Macrodon atricauda*) from the South Atlantic. *Fish Res* 245: e106126. <https://doi.org/10.1016/j.fishres.2021.106126>
- Aguilera OA, Schwarzhans W, Béarez P. 2016. Otoliths of the Sciaenidae from the Neogene of tropical America. *Palaeo Ichthyologica* 14: 7–90.
- Appleyard SA, Maher S, Pogonoski JJ, Bent SJ, Chua X-Y, McGrath A. 2021. Assessing DNA for fish identifications from reference collections: the good, bad and ugly shed light on formalin fixation and sequencing approaches. *Journal of Fish Biology* 98: 1421–1432. <https://doi.org/10.1111/jfb.14687>
- Barbosa AJB, Sampaio I, Schneider H, Santos S. 2014. Molecular phylogeny of weakfish species of the *Stellifer* group (Sciaenidae, Perciformes) of the Western South Atlantic based on mitochondrial and nuclear data. *PLoS ONE* 9 (7): e102250.
- Berendzen PB, Holmes SR, Abels JR, Black CR. 2021. Morphological diversity within the Ozark minnow (*Notropis nubilus*: Leuciscidae). *Journal of Fish Biology*: 1–10. <https://doi.org/10.1111/jfb.14951>
- Bickford D, Lohman DJ, Sodhi NS, Ng PKL, Meier R, Winker K, et al. (2007). Cryptic species as a window on diversity and conservation. *Trends in Ecology & Evolution* 22(3): 148–155. <https://doi.org/10.1016/j.tree.2006.11.004>
- Bonini-Campos B, Lofeu L, Brandt R, Kohlsdorf T. 2019. Different developmental environments reveal multitrait plastic responses in South American Anostomidae fish. *JEZ-B Zool (Molecular and Developmental Evolution)* 332: 238–244. <https://doi.org/10.1002/jez.b.22905>
- Busserrolles F, Fitzpatrick JL, Paxton JR, Marshall NJ, Collin SP. 2013. Eye-size variability in deep-sea lanternfishes (Myctophidae): an ecological and phylogenetic study. *PLoS One* 8: e58519. <https://doi.org/10.1371/journal.pone.0058519>
- Caires RA, Santos WCR, Machado L, Oliveira C, Cerqueira NNCD, Rotundo MM, et al. 2019. The Tonkin weakfish, *Cynoscion similis* (Sciaenidae, Perciformes), an endemic species of the Amazonas-Orinoco Plume. *Acta Amazonica* 49: 197–207. <https://doi.org/10.1590/1809-4392201803481>
- Carvalho-Filho A, Ferreira CEL, Craig M. 2009. A shallow water population of

- Pronotogrammus martinicensis* (Guichenot, 1868) (Teleostei: Serranidae: Anthiinae) from South-western Atlantic, Brazil. *Zootaxa* 2228: 29–42. <https://doi.org/10.11646/zootaxa.2228.1.2>
- Carvalho-Filho A, Santos S, Sampaio I. 2010. *Macrodon atricauda* (Günther, 1880) (Perciformes: Sciaenidae), a valid species from the southwestern Atlantic, with comments on its conservation. *Zootaxa* 2519: 48–58. <https://doi.org/10.11646/zootaxa.2519.1.3>
- Castro KMSA, Amado TF, Olalla-Tárraga MÁ. et al. 2021. Water constraints drive allometric patterns in the body shape of tree frogs. *Scientific Reports* 11: 1218. <https://doi.org/10.1038/s41598-020-80456-1>
- Caves EM, Sutton TT, Johnsen S. 2017. Visual acuity in ray-finned fishes correlates with eye size and habitat. *Journal of Experimental Biology* 220: 1586–1596. <https://doi.org/10.1242/jeb.151183>
- Cervigón F. 2011. *Los Peces de Venezuela*. Vol. VI. Edit. Ex Libris, Caracas. p. 96–98.
- Chakraborty A, Sakai M, Iwatsuki Y. 2006. Museum fish specimens and molecular taxonomy: a comparative study on DNA extraction protocols and preservation techniques. *Journal of Applied Ichthyology* 22: 160–166. <https://doi.org/10.1111/j.1439-0426.2006.00718.x>
- Chao LN, Musick JA. 1977. Life history, feeding habits, and functional morphology of juvenile sciaenid fishes in the York river estuary. *Fishery Bulletin* 75: 657–702.
- Chao LN. 1978. A basis for classifying western Atlantic Sciaenidae (Pisces: Perciformes). NOAA (National Oceanic and Atmospheric Administration) Technical Report NMFS (National Marine Fisheries Service). Circular No. 415, p. 1–64.
- Chao NL, Carvalho-Filho A, Santos JA. 2021. Five new species of Western Atlantic stardrums, *Stellifer* (Perciformes: Sciaenidae) with a key to Atlantic *Stellifer* species. *Zootaxa* 4991(3): 434–66. <https://doi.org/10.11646/zootaxa.4991.3.2>
- Chao NL, Frédou FL, Haimovici M, Peres MB, Polidoro B, Raseira M, et al. 2015. A popular and potentially sustainable fishery resource under pressure – extinction risk and conservation of Brazilian Sciaenidae (Teleostei: Perciformes). *Global Ecology and Conservation* 4: 117–126. <https://doi.org/10.1016/j.gecco.2015.06.002>
- Chao NL. 2002. Sciaenidae. In: Carpenter KE, editor. *The living marine resources of the Western Central Atlantic*. FAO Species Identification Guide for Fishery Purposes and American Society of Ichthyologists and Herpetologists. Special Publication No. 5. Rome: FAO. p. 1583–1653.
- Clabaut C, Bunje PME, Salzburger W, Meyer A. 2007. Geometric morphometric analyses provide evidence for the adaptive character of the tanganyikan cichlid fish radiations. *Evolution* 61(3): 560–578. <https://doi.org/10.1111/j.1558-5646.2007.00045.x>
- Davis WP, Birdsong RS. 1973. Coral reef fishes which forage in the water column. *Helgoländer Wiss Meeresunters* 24: 292–306. <https://doi.org/10.1007/BF01609520>
- de Pinna M, Zuanon J, Rapp-Py-Daniel L, Petry P. 2018. A new family of neotropical freshwater fishes from deep fossorial Amazonian habitat, with a reappraisal of morphological characiform phylogeny (Teleostei: Ostariophysi). *Zoological Journal of the Linnean Society* 182(1): 76–106. <https://doi.org/10.1093/zoolinnean/zlx028>
- Deary AL, Hilton EJ. 2016. Comparative ontogeny of the feeding apparatus of sympatric drums (Perciformes: Sciaenidae) in the Chesapeake Bay. *Journal of Morphology* 277: 183–195. <https://doi.org/10.1002/jmor.20488>
- Deary AL, Hilton EJ. 2017. Influence of cladogenesis on feeding structures in drums (Teleostei: Sciaenidae). *Zoology* 120: 53–61. <https://doi.org/10.1016/j.zool.2016.08.004>

- Deary AL, Metscher B, Brill RW, Hilton EJ. 2016. Shifts of sensory modalities in early life history stage estuarine fishes (Sciaenidae) from the Chesapeake Bay using X-ray micro computed tomography. *Environmental Biology of Fishes* 99: 361–375. <https://doi.org/10.1007/s10641-016-0479-8>
- Diniz-Filho JA, Loyola RD, Raia P, Mooers AO, Bini LM. 2013. Darwinian shortfalls in biodiversity conservation. *Trends in Ecology & Evolution* 28: 689–695. <https://doi.org/10.1016/j.tree.2013.09.003>
- Engel MS, Ceriaco LMP, Daniel GM, Dellapé PM, Löbl I, Marinov M, et al. 2021. The taxonomic impediment: a shortage of taxonomists, not the lack of technical approaches. *Zoological Journal of the Linnean Society* 193(2): 381–387. <https://doi.org/10.1093/zoolinnea/zlab072>
- Evans KM, Waltz B, Tagliacollo V, Chakrabarty P, Albert JS. 2017. Why the short face? Developmental disintegration of the neurocranium drives convergent evolution in neotropical electric fishes. *Ecology and Evolution* 7(6): 1783–1801. <https://doi.org/10.1002/ece3.2704>
- Figueiredo PICC, Malabarba LR, Fagundes NJR. 2021. Hydrography rather than lip morphology better explains the evolutionary relationship between *Gymnogeophagus labiatus* and *G. lacustris* in Southern Brazil (Cichlidae: Geophagini). *Neotropical Ichthyology* 19(4): e210054. <https://doi.org/10.1590/1982-0224-2020-0154>
- Figueiredo-Filho JM, Marceniuk AP, Feijó A, Siccha-Ramirez R, Ribeiro GS, Oliveira C, et al. 2021. Taxonomy of *Centropomus* Lacépède, 1802 (Perciformes: Centropomidae), with focus on the Atlantic species of the genus. *Zootaxa* 4942(3): 301–338. <https://doi.org/10.11646/zootaxa.4942.3.1>
- Frainer G, Carvalho FR, Bertaco VA, Malabarba LR. 2021. Museum specimens reveal a rare new characid fish genus, helping to refine the interrelationships of the Probolodini (Characidae: Stethaproninae). *Systematics and Biodiversity* 19(8): 1135–1148. <https://doi.org/10.1080/14772000.2021.1986167>
- Freitas TMS, Stropp J, Calegari BB, Calatayud J, De Marco Jr P, Montag LFA, et al. 2021. Quantifying shortfalls in the knowledge on Neotropical Auchenipteridae fishes. *Fish and Fisheries* 22: 87–104. <https://doi.org/10.1111/faf.12507>
- Friedman ST, Price SA, Corn KA, Larouche O, Martinez CM, Wainwright PC. 2020. Body shape diversification along the benthic–pelagic axis in marine fishes. *Proceedings of the Royal Society B* 287: 20201053. <https://doi.org/10.1098/rspb.2020.1053>
- Gatz AJ. 1979. Ecological morphology of freshwater stream fishes. *Tulane Studies in Zoology and Botany* 21(2): 91–124.
- Geller JB. 1999. Decline of a native mussel masked by sibling species invasion. *Conservation Biology* 13(3): 661–664. <https://doi.org/10.1046/j.1523-1739.1999.97470.x>
- Gilbert MC, Akama A, Fernandes CC, Albertson RC. 2020. Rapid morphological change in multiple cichlid ecotypes following the damming of a major clearwater river in Brazil. *Evolutionary Applications* 13(10): 2754–2771. <https://doi.org/10.1111/eva.13080>
- Goatley CH, Bellwood DR. 2009. Morphological structure in a reef fish assemblage. *Coral Reefs* 28: 449–457. <https://doi.org/10.1007/s00338-009-0477-9>
- Gould SJ. 1966. Allometry and size in ontogeny and phylogeny. *Biological Reviews* 41(4): 587–638. <https://doi.org/10.1111/j.1469-185X.1966.tb01624.x>
- Guimarães-Costa A, Machado FS, Reis-Filho JA, Andrade MC, Araújo RG, Miranda E, et al. 2020. DNA Barcoding for the assessment of the taxonomy and conservation status of the fish bycatch of the northern Brazilian shrimp trawl fishery. *Frontiers in Marine Science* 7: 566021.

<https://doi.org/10.3389/fmars.2020.566021>

Hahn EE, Alexander MR, Grealy A, Stiller J, Gardiner DM, Holleley CE. 2021. Unlocking inaccessible historical genomes preserved in formalin. *Molecular Ecology Resources* 00: 1–18. <https://doi.org/10.1111/1755-0998.13505>

Hortal J, de Bello F, Diniz-Filho JAF, Lewinsohn TM, Lobo JM, Ladle RJ. 2015. Seven shortfalls that beset large-scale knowledge of biodiversity. *Annual Review of Ecology and Systematics* 46: 523–549. <https://doi.org/10.1146/annurev-ecolsys-112414-054400>

Hubbs CL, Lagler KF. 2004. Fishes of the Great Lakes region. Rev. Edition of 1964 by G.R. Smith. University of Michigan Press, Ann Arbor, Michigan, p. 332. <https://doi.org/10.3998/mpub.17658>

Kassambara A, Mundt F. 2016. factoextra: Extract and Visualize the Results of Multivariate Data Analyses. Available from: <https://CRAN.R-project.org/package=factoextra>, r package version 1.0.3, 2016.

Keledjian A, Lowell B, Warrenchuk J, Shester G, Hirshfield M, Cano-Stocco D. 2014. Wasted Catch: Unsolved Problems in U.S. Fisheries. *Oceana* (2014)

Klingenberg CP. 2016. Size, shape, and form: concepts of allometry in geometric morphometrics. *Development Genes and Evolution* 226: 113–137. <https://doi.org/10.1007/s00427-016-0539-2>

Lacerda MBS, Grillo ON, Romano PSR. 2021. Rostral morphology of Spinosauridae (Theropoda, Megalosauroidae): premaxilla shape variation and a new phylogenetic inference. *Historical Biology*. <https://doi.org/10.1080/08912963.2021.2000974>

Larouche O, Zelditch ML, Cloutier R. 2018. Modularity promotes morphological divergence in ray-finned fishes. *Scientific Reports* 8(1): 7278. <https://doi.org/10.1038/s41598-018-25715-y>

Lê S, Josse J, Husson F. 2008. FactoMineR: an R package for multivariate analysis. *Journal of statistical software* 25(1): 1–18. <https://doi.org/10.18637/jss.v025.i01>

Liggins L, Kilduff L, Trnski T, Delrieu-Trottin E, Carvajal JI, Arranz V, et al. 2021. Morphological and genetic divergence supports peripheral endemism and a recent evolutionary history of *Chrysiptera* demoiselles in the subtropical South Pacific. *Coral Reefs*. <https://doi.org/10.1007/s00338-021-02179-7>

Lima-Filho PA, Bidau CJ, Alencar CERD, Molina WF. 2017. Latitudinal influence on the sexual dimorphism of the marine fish *Bathygobius soporator* (Gobiidae: Teleostei). *Evolutionary Biology* 44, 374–385. <https://doi.org/10.1007/s11692-017-9416-9>

Lin YJ, Qurban MA, Shen KN, Chao NL. 2019. Delimitation of tigertooth croaker *Otolithes* species (Teleostei: Sciaenidae) from the western Arabian Gulf using an integrative approach, with a description of *Otolithes arabicus* sp. nov. *Zoological Studies* 58: 10. <https://doi.org/10.6620/ZS.2019.58-10>.

Lo PC, Liu SH, Chao NL, Nunoo FKE, Mok HK, Chen WJ. 2015. A multi-gene dataset reveals a New World origin and Oligocene diversification of croakers (Perciformes: Sciaenidae). *Molecular Phylogenetics and Evolution* 88: 132–43. <https://doi.org/10.1016/j.ympev.2015.03.025>

Lomolino MV. 2004. Conservation biogeography. In: Lomolino L, Heaney LR, eds. *Frontiers of biogeography: new directions in the geography of nature*. Sunderland: Sinauer, 293–296.

Marceniuk AP, Burlamaqui TCT, Oliveira C, Carneiro J, Eleres B, Sales JBL. 2019a. Incipient speciation, driven by distinct environmental conditions, in the marine catfishes of the genus *Aspistor* (Siluriformes, Ariidae), from the Atlantic coast of South America. *J Zool Syst Evol*

Res 57: 1–18. <https://doi.org/10.1111/jzs.12261>

Marceniuk AP, Molina EG, Caires RA, Rotundo MM, Wosiacki WB, Oliveira C. 2019b. Revision of *Bairdiella* (Sciaenidae: Perciformes) from the western South Atlantic, with insights into its diversity and biogeography. *Neotropical Ichthyology* 17(1): 1–18. <https://doi.org/10.1590/1982-0224-20180024>

Meek SE, Hildebrand SF. 1925. The marine fishes of Panama. Part II. Field Museum of Natural History Publications 226. Zoological Series 15. Chicago: Field Museum of Natural History.

Murray CM, McMahan CD, Litmer AR, Goessling JM, Siegel D. 2021. Latitudinal gradients in sexual dimorphism: Alternative hypotheses for variation in male traits. *Ecology and Evolution* 00: 1–8. <https://doi.org/10.1002/ece3.8386>

Neves JMDM, Perez A, Fabré NN, Pereira RJ, Mott T. 2021. Integrative taxonomy reveals extreme morphological conservatism in sympatric *Mugil* species from the Tropical Southwestern Atlantic. *Journal of Zoological Systematics And Evolutionary Research* 59(1): 163–178. <https://doi.org/10.1111/jzs.12421>

Nori J, Semhan R, Abdala CS, Rojas-Soto O. 2021. Filling Linnean shortfalls increases endemism patterns: conservation and biogeographical implications for the extreme case of *Liolaemus* (Liolaemidae, Squamata) species. *Zoological Journal of the Linnean Society* 2021; zlab012. <https://doi.org/10.1093/zoolinnea/zlab012>

Parenti P. 2020. An annotated checklist of fishes of the family Sciaenidae. *Journal of Animal Diversity* 2(1): 1–92. <https://doi.org/10.29252/JAD.2020.2.1.1>

Pessanha ALM, Araújo FG, Oliveira REM, Silva AF, Sales NS. 2015. Ecomorphology and resource use by dominant species of tropical estuarine juvenile fishes. *Neotropical Ichthyology* 13(2): 401–412. <https://doi.org/10.1590/1982-0224-20140080>

Pinheiro A, Teixeira CM, Rego AL, Marques JF, Cabral HN. 2005. Genetic and morphological variation of *Solea lascaris* (Risso, 1810) along the Portuguese coast. *Fisheries Research* 73(1-2): 67–78. <https://doi.org/10.1016/j.fishres.2005.01.004>

Pinheiro HT, Moreau CS, Daly M, Rocha LA. 2019. Will DNA barcoding meet taxonomic needs? *Science* 365(6456): 873–874. <https://doi.org/10.1126/science.aay7174>

R Core Team. 2020. R: A language and environment for statistical computing. [internet] R Foundation for Statistical Computing. Available from: <https://www.R-project.org/>

Rabosky DL, Adams DC. 2012. Rates of morphological evolution are correlated with species richness in salamanders. *Evolution* 66: 1807–1818. <https://doi.org/10.1111/j.1558-5646.2011.01557.x>

Reis RE, Britski HA, Britto MR, Buckup PA, Calegari BB, Camelier P, et al. 2019. Poor taxonomic sampling undermines nomenclatural stability: A reply to Roxo et al. (2019). *Zootaxa* 4701(5): 497–500. <https://doi.org/10.11646/zootaxa.4701.5.10>

Riddle BR, Ladle RJ, Lourie SA, Whittaker RJ. 2011. Basic biogeography: estimating biodiversity and mapping nature. In: Ladle RJ, Whittaker RJ, eds. *Conservation Biogeography*. Oxford: Wiley, 45–92. <https://doi.org/10.1002/9781444390001.ch4>

Rohlf FJ. 2017a. tpsDig2 v.2.27. State University of New York at Stony Brook.

Rohlf FJ. 2017b. tpsRelw, v. 1.69. State University of New York at Stony Brook.

Rohlf FJ. 2021. tpsUtil v.1.69. State University of New York at Stony Brook.

Rüber L, Adams DC. 2001. Evolutionary convergence of body shape and trophic morphology in cichlids from Lake Tanganyika. *Journal of Evolutionary Biology* 14(2): 325–332. <https://doi.org/10.1046/j.1420-9101.2001.00269.x>

- Sabaj MH. 2020. Codes for natural history collections in ichthyology and herpetology. *Copeia* 108(3): 593–669. <https://doi.org/10.1643/ASIHCODONS2020>
- Santos CMD, Carbayo F. 2021. Taxonomy as a political statement: the Brazilian case. *Zootaxa* 5047(1): 92–94. <https://doi.org/10.11646/zootaxa.5047.1.8>
- Santos JA, Oliveira RL, Guedes APP, Santos ACA, Moraes LE. 2021. Do macrophytes act as restaurants for fishes in a tropical beach? An approach using stomach content and prey availability analyses. *Regional Studies of Marine Science* 47: e101920. <https://doi.org/10.1016/j.rsma.2021.101920>
- Sasaki K. 1989. Phylogeny of the family Sciaenidae, with notes on its zoogeography (Teleostei, Perciformes). *Memoirs of the Faculty of Fisheries Sciences* 36(1/2): 1–137. <https://doi.org/10.1007/BF02905681>
- Schönrogge K, Barr B, Wardlaw JC, Napper E, Gardner MG, Breen J, et al. 2002. When rare species become endangered: cryptic speciation in myrmecophilous hoverflies. *Biological Journal of the Linnean Society* 75(3): 291–300. <https://doi.org/10.1046/j.1095-8312.2002.00019.x>
- Schultz LP. 1945. Three new sciaenid fishes of the genus *Ophioscion* from the Atlantic coasts of Central and South America. *Proceedings of the United States National Museum* 96(3192): 123–137. <https://doi.org/10.5479/si.00963801.96-3192.123>
- Schwarzahns W. 1993. A comparative morphological treatise of recent and fossil otoliths of the family Sciaenidae (Perciformes). *Piscium Catalogus, Otolithi Piscium* 1: 1–245.
- Silva TF, Schneider H, Sampaio I, Angulo A, Brito MFG, Santos ACA, et al. 2018. Phylogeny of the subfamily Stelliferinae suggests speciation in *Ophioscion* Gill, 1863 (Sciaenidae: Perciformes) in the western South Atlantic. *Molecular Phylogenetics and Evolution* 125: 51–61. <https://doi.org/10.1016/j.ympev.2018.03.025>
- Struck TH, Cerca J. 2019. Cryptic species and their evolutionary significance. In: eLS. John Wiley & Sons, Ltd: Chichester. <https://doi.org/10.1002/9780470015902.a0028292>
- Tavera J, Acero P. A, Wainwright PC. 2018. Multilocus phylogeny, divergence times, and a major role for the benthic-to-pelagic axis in the diversification of grunts (Haemulidae). *Molecular Phylogenetics and Evolution* 121: 212–223. <https://doi.org/10.1016/j.ympev.2017.12.032>
- Trewavas E. 1977. The sciaenid fishes (croakers or drums) of the Indo-West-Pacific. *Transactions Zoological Society of London* 33: 253–541. <https://doi.org/10.1111/j.1096-3642.1977.tb00052.x>
- Voje KL, Hansen TF, Egset CK, Bolstad GH, Pelabon C. 2014. Allometric constraints and the evolution of allometry. *Evolution* 68(3): 866–885. <https://doi.org/10.1111/evo.12312>
- Walters AD, Cannizzaro AG, Trujillo DA, Berg DJ. 2021. Addressing the Linnean shortfall in a cryptic species complex. *Zoological Journal of the Linnean Society* 192(2): 277–305. <https://doi.org/10.1093/zoolinnean/zlaa099>
- Wheeler QD, Raven PH, Wilson EO. 2004. *Science* 303, 285. <https://doi.org/10.1126/science.303.5656.285>
- Wilson EO. Biodiversity research requires more boots on the ground. *Nature Ecology & Evolution*, 1: 1590–1591. <https://doi.org/10.1038/s41559-017-0360-y>
- Zhang J. Exploiting formalin-preserved fish specimens for resources of DNA barcoding. 2010. *Molecular Ecology Resources* 10(6): 935–941. <https://doi.org/10.1111/j.1755-0998.2010.2838.x>

Table legends

Table 1. Eigenvector of PCA's (Principal Component Analysis). SN: Snout length; ED: Eye diameter; IW: Interorbital width; BD: Body depth; P1: Pectoral-fin aspect-ratio.

Table 2. Eigenvalue and cumulative percentage of PCA's components (Principal Component Analysis). SN: Snout length; ED: Eye diameter; IW: Interorbital width; BD: Body depth; P1: Pectoral-fin aspect-ratio.

Table 3. Percentage of correctly classified specimens (Jackknifed) using PCs scores as shape proxy in the Linear Discriminant Analysis (LDA). GOME: *Stellifer gomezi*; MENE: *Stellifer menezesi*; PUNC: *Stellifer punctatissimus*.

Table 1

	PC1	PC2	PC3	r2
SN	-0.90576	0.0372	-0.42216	0.8751
ED	-0.45286	0.71793	0.52867	0.954
IW	-0.92212	-0.18624	0.33914	0.8704
BD	-0.10175	0.90957	-0.40291	0.9543
P1	-0.8986	-0.3993	-0.18187	0.7761

Table 2

Component	Eigenvalue	% variance	% cumulative variance
PC1	2.290342	45.81	45.81
PC2	1.436362	28.73	74.53
PC3	0.703297	14.07	88.60
PC4	0.372276	7.45	96.05
PC5	0.197723	3.95	100

Table 3

Category	Species		
	GOME	MENE	PUNC
All-males	85.71%	93.18%	97.62%
All-females	87.10%	95.45%	100%
Full dataset	50%	34.29%	73.77%

Figure legends

Figure 1. Map of specimens examined: *Stellifer gomezi* (green dots); *S. menezesi* (blue dots); *S. punctatissimus* (red dots).

Figure 2. Specimen of *Stellifer punctatissimus* (Meek & Hildebrand, 1925) showing semilandmarks (filled grey circles) and landmarks (white dots); description accordingly to “Material and methods”.

Figure 3. *Stellifer gomezi* (Cervigón, 2011). A. MZFS 16785, 75.54 mm SL (male), Bahia state – Brazil. B. MZFS 17664, 116 mm SL (female), Bahia State – Brazil. C. MCZ 157273, 115 mm SL, Dominican Republic.

Figure 4. *Stellifer menezesi* Chao, Carvalho-Filho & Santos, 2021. A. UFPB 3228, 87.67 mm SL (male), Paraíba State – Brazil. B. MZFS 17650, 73.47 mm SL (male), Bahia State – Brazil. C. Holotype MZUSP 123409, 102 mm SL (female), Bahia State – Brazil.

Figure 5. *Stellifer punctatissimus* (Meek & Hildebrand, 1925). A. UFPB 3174, 102 mm SL (female), Paraíba State – Brazil. B. UFPB 601, 142 mm SL (male), Paraíba State – Brazil. C. UFPB 4558, 106 mm SL (male), Paraíba State – Brazil.

Figure 6. Coloration pattern in *Stellifer punctatissimus* complex. A. Juvenile of *S. punctatissimus* with chromatophores lines (MZFS 460, 72 mm SL, female, Pernambuco State – Brazil). B. Adult of *S. punctatissimus* with larger darker streaks (UFRPE 040, 91 mm SL, male, Pernambuco State – Brazil). C. Up-close in pattern of isolate chromatophores. D. Up-close in pattern of mixed size chromatophores. E. Up-close in pattern of densely punctuated chromatophores. Arrows indicates either lines or the so-called central chromatophores.

Figure 7. Principal Component Analysis (PCA) of linear morphometrics (top) and PCA of geometric morphometrics (bottom). GOME: *Stellifer gomezi*; MENE: *Stellifer menezesi*; PUNC: *Stellifer punctatissimus*.

Figure 8. Scatterplot of meristic characters: eye diameter (top-left); snout length (top-right); caudal peduncle height (middle-left); interorbital width (middle-right); aspect ratio of pectoral-fin (bottom-left); predorsal length (bottom-right). GOME: *Stellifer gomezi*; MENE: *Stellifer menezesi*; PUNC: *Stellifer punctatissimus*.

Figure 9. Common Allometric Component (CAC) of geometric morphometrics. Thin-plate splines at the right: CAC (+0.1) – top; RSC 1 (+0.1) – bottom. GOME: *Stellifer gomezi*; MENE: *Stellifer menezesi*; PUNC: *Stellifer punctatissimus*.

Figure 10. Biplot resulting from Principal Component Analysis (PCA) of all-males (top) and all-females (middle) dataset using linear morphometrics and Canonical Variate Analysis (CVA) of geometric morphometrics (bottom). GOME: *Stellifer gomezi*; MENE: *Stellifer menezesi*; PUNC: *Stellifer punctatissimus*.

Figure 11. Violin plots of body depth (in Standard length – SL) by species and sex. GOME: *Stellifer gomezi*; MENE: *Stellifer menezesi*; PUNC: *Stellifer punctatissimus*. M: Male; F: Female.

Figure 12. Pectoral-fin of *Stellifer punctatissimus*. Top – Recently fixed specimen (MZFS 17525, 61.81 mm SL, male, Bahia State – Brazil); Bottom – Live specimen in side and front view (66 mm SL, not preserved).

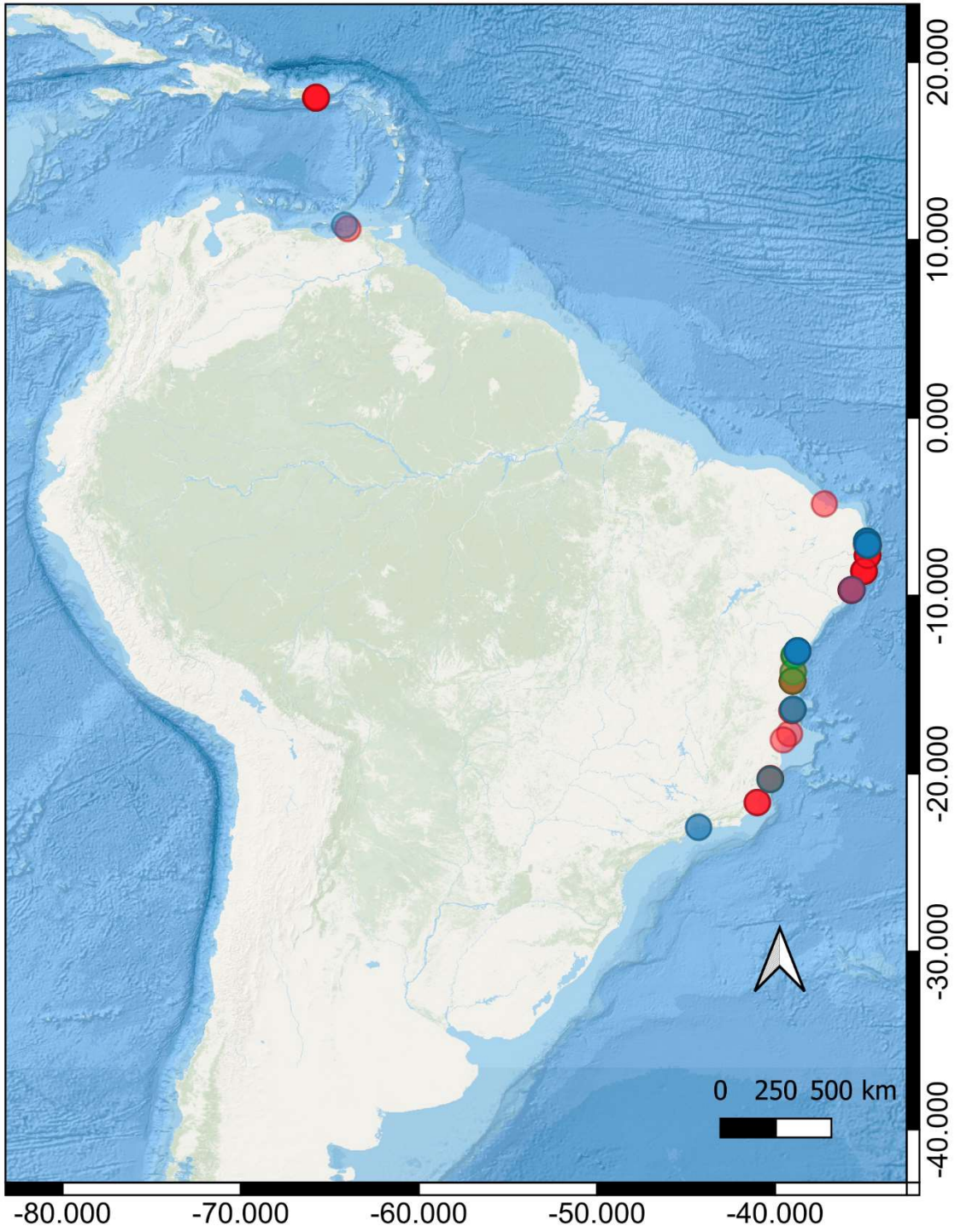


Fig. 1

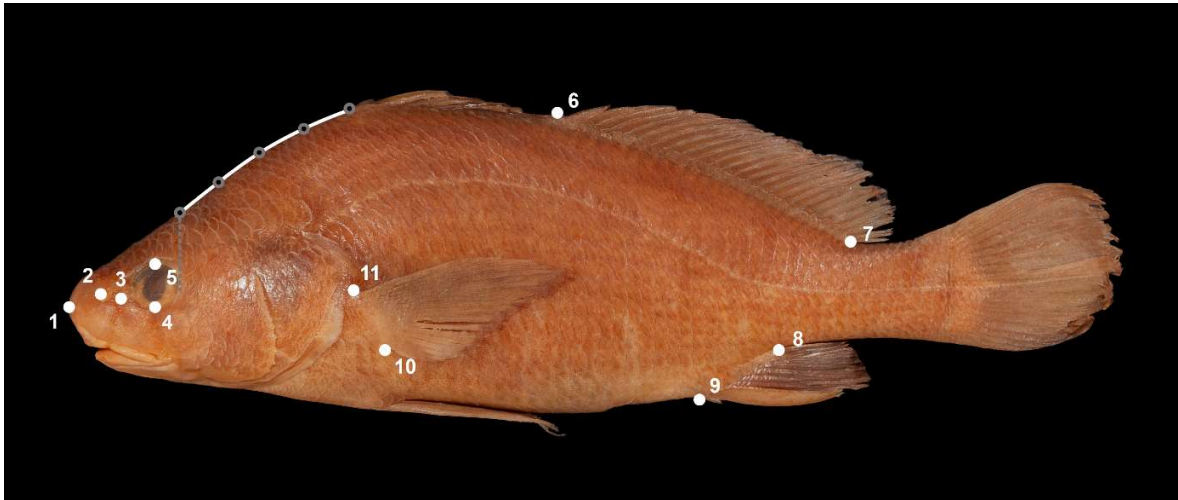


Fig. 2

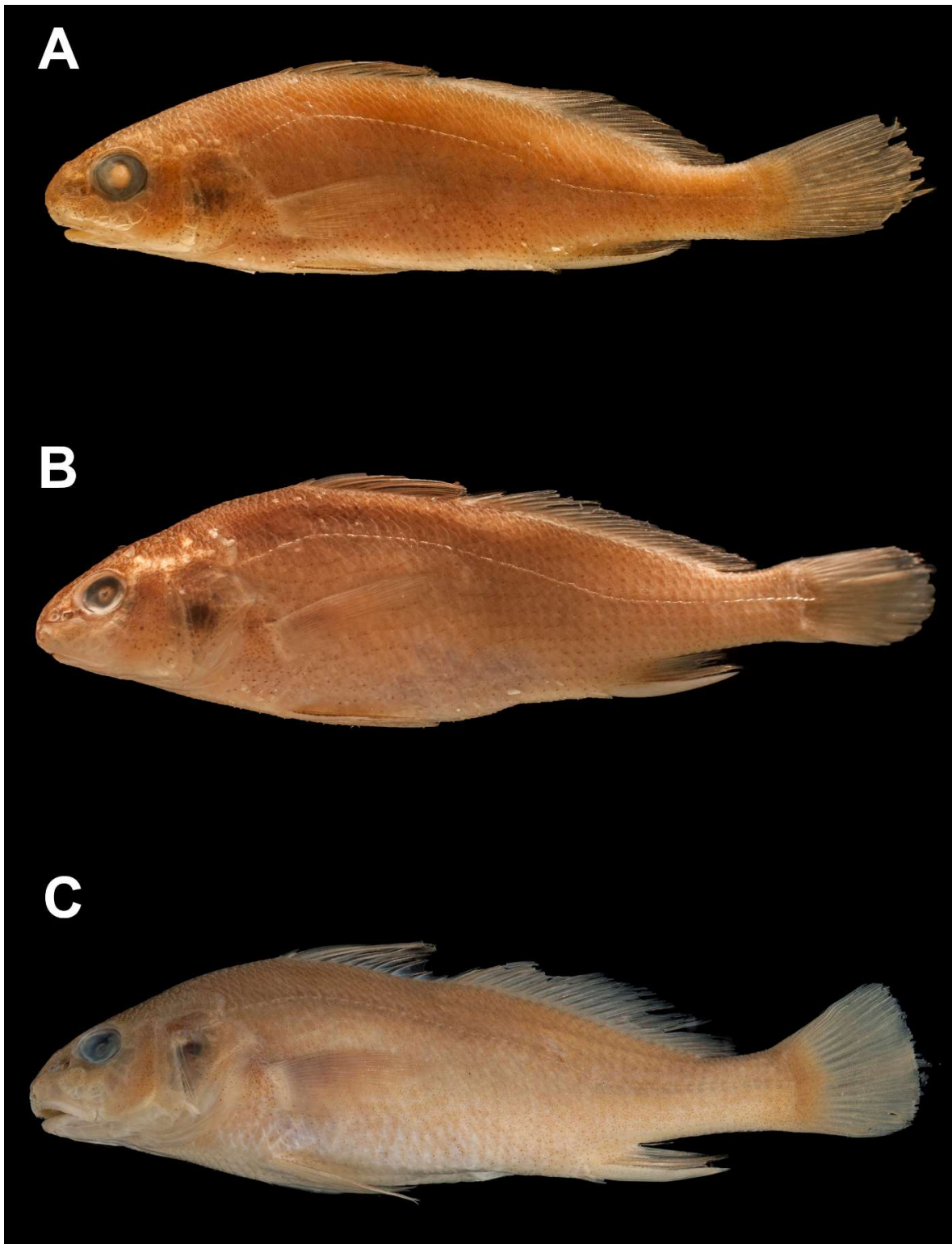


Fig. 3

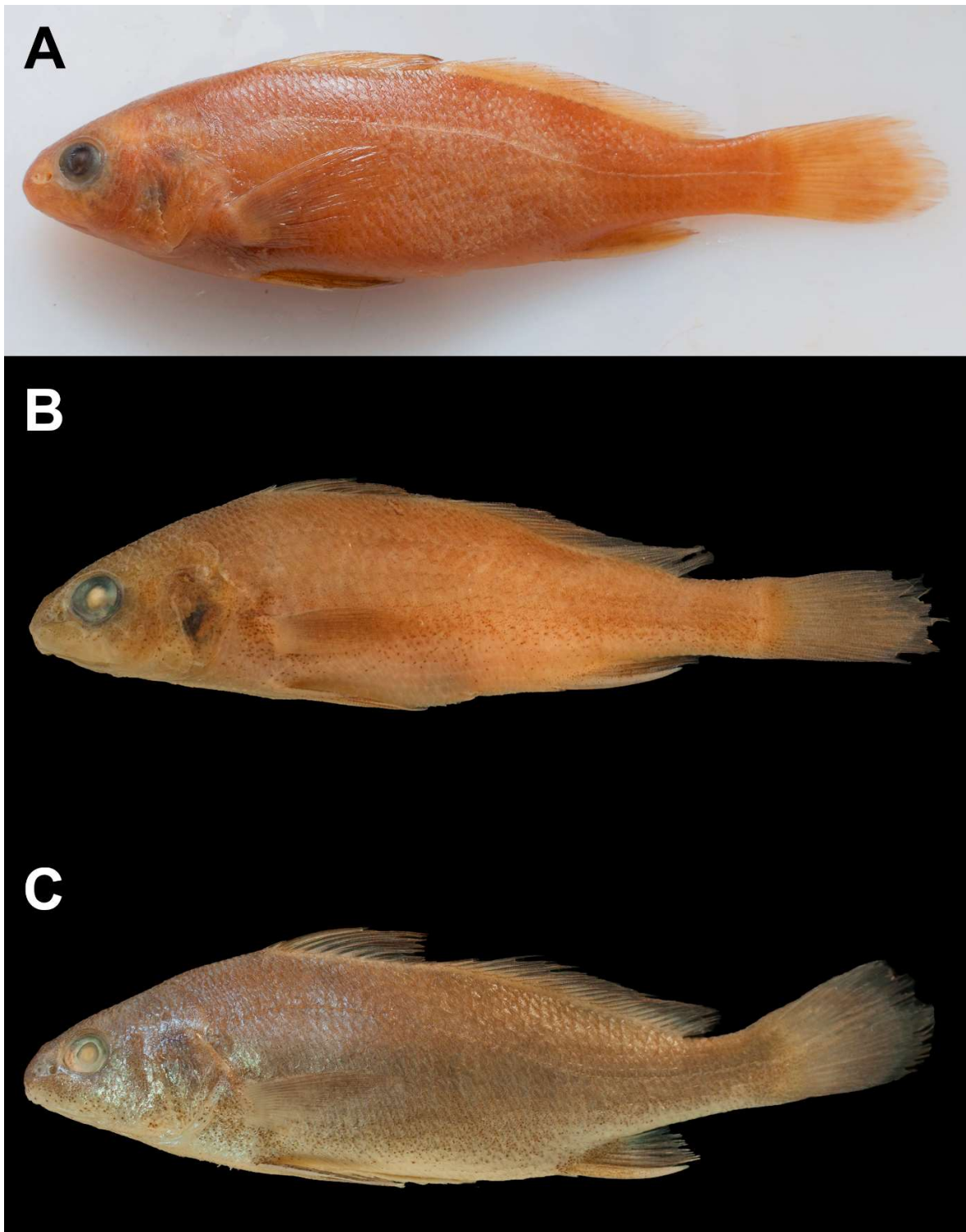


Fig. 4

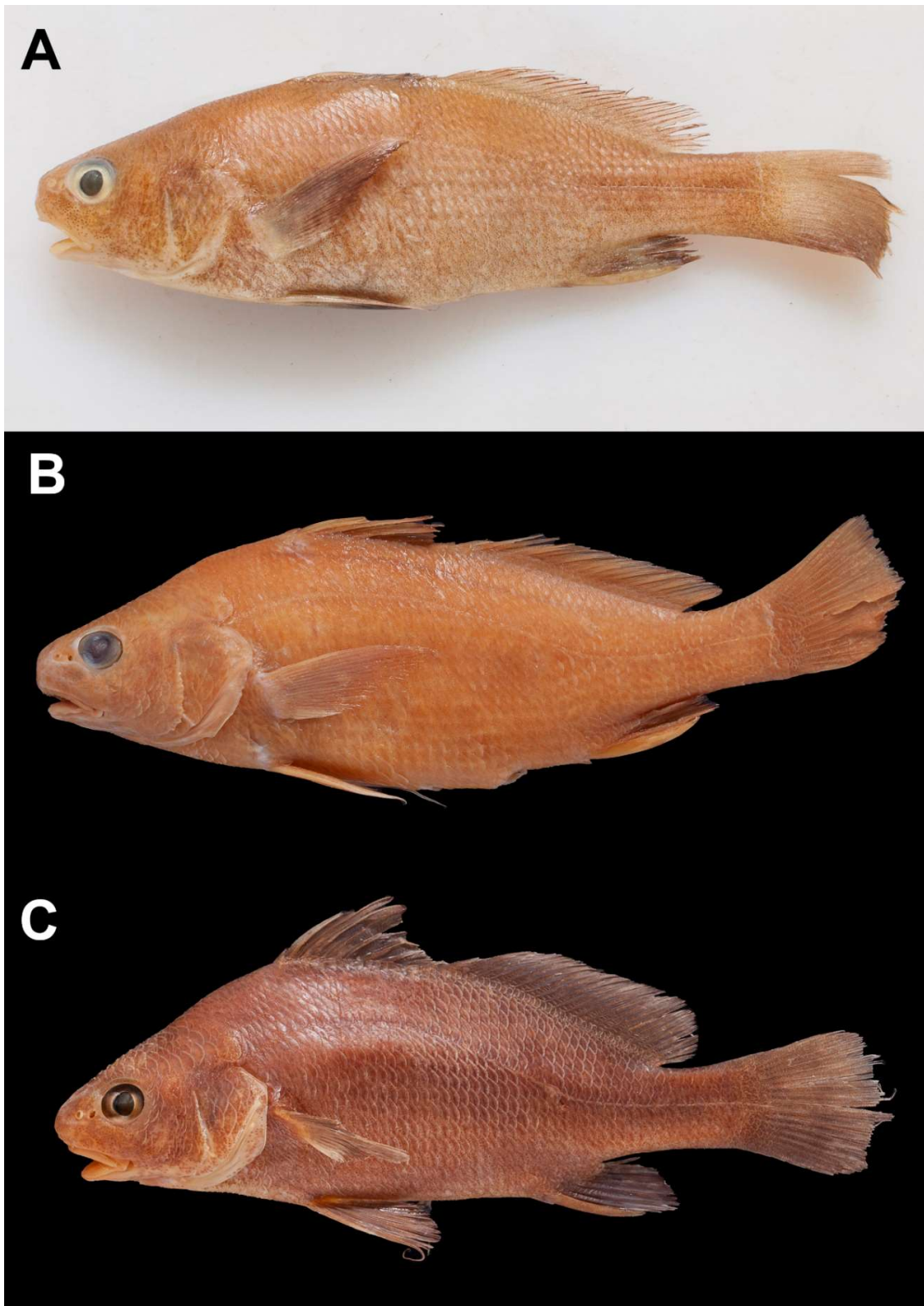


Fig. 5

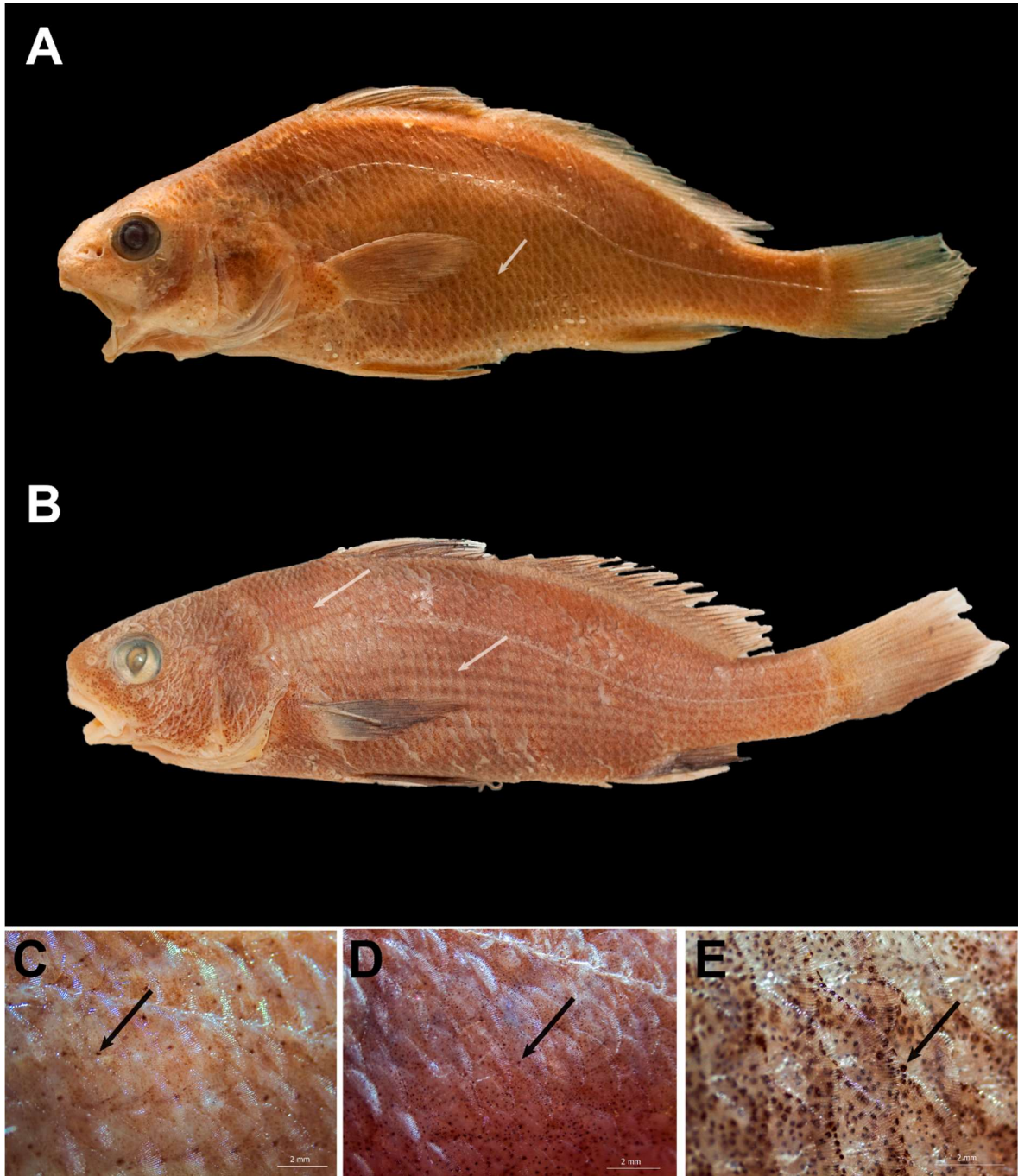


Fig. 6

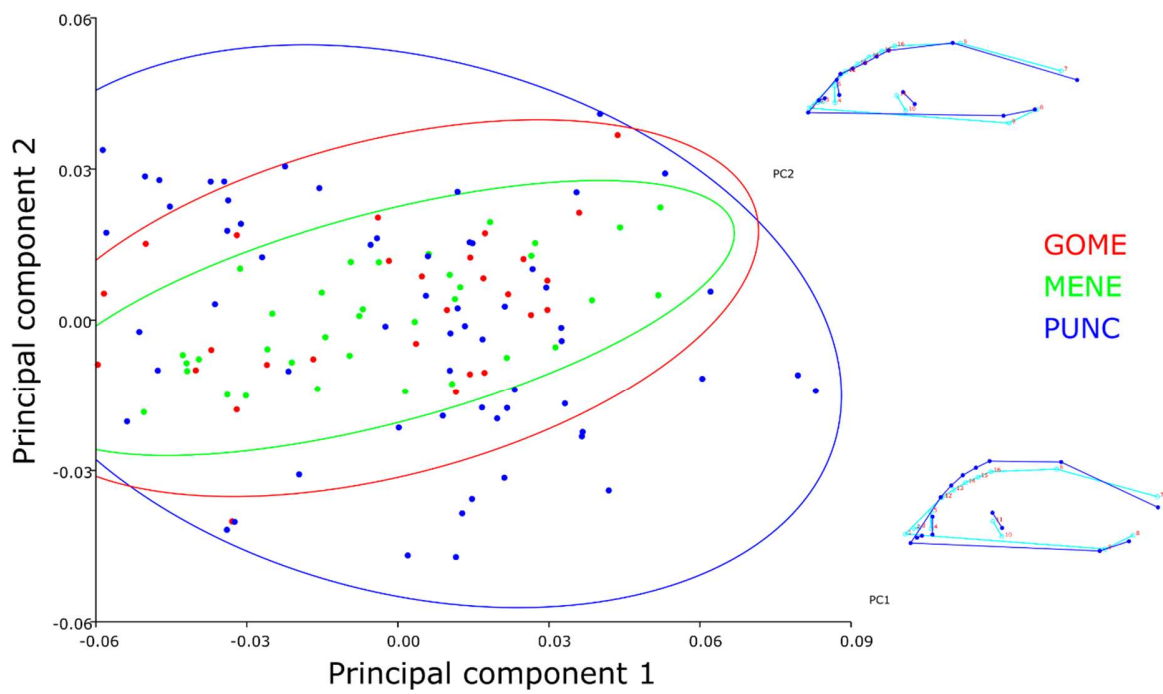
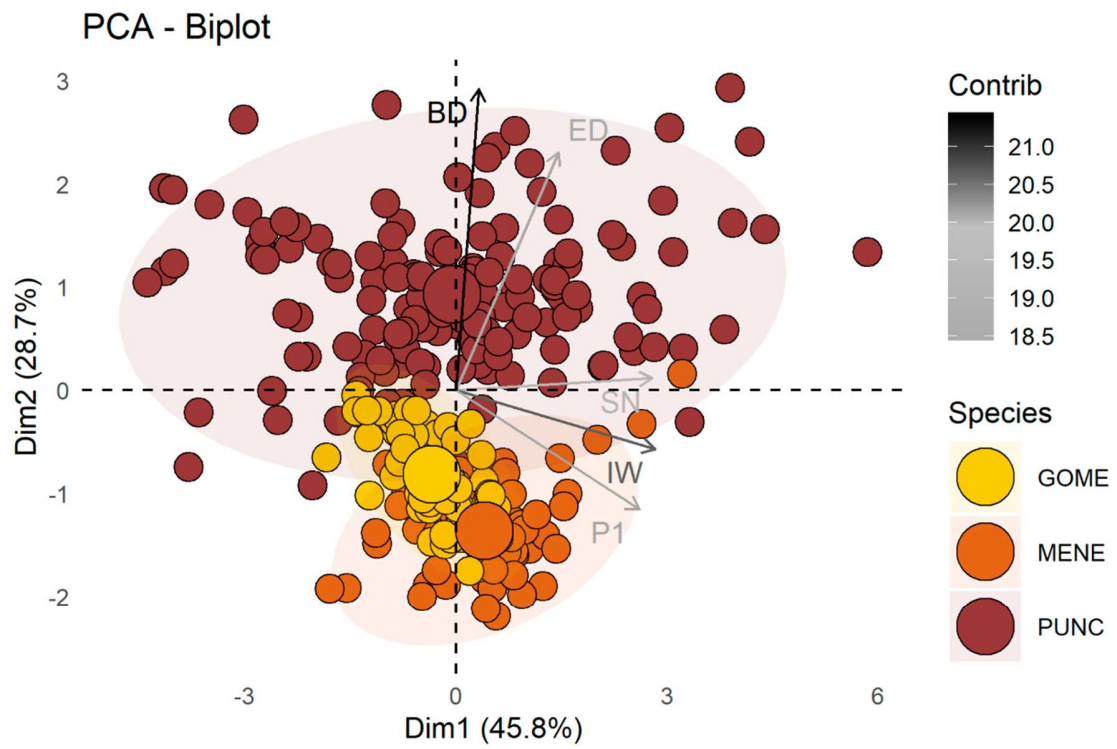


Fig. 7

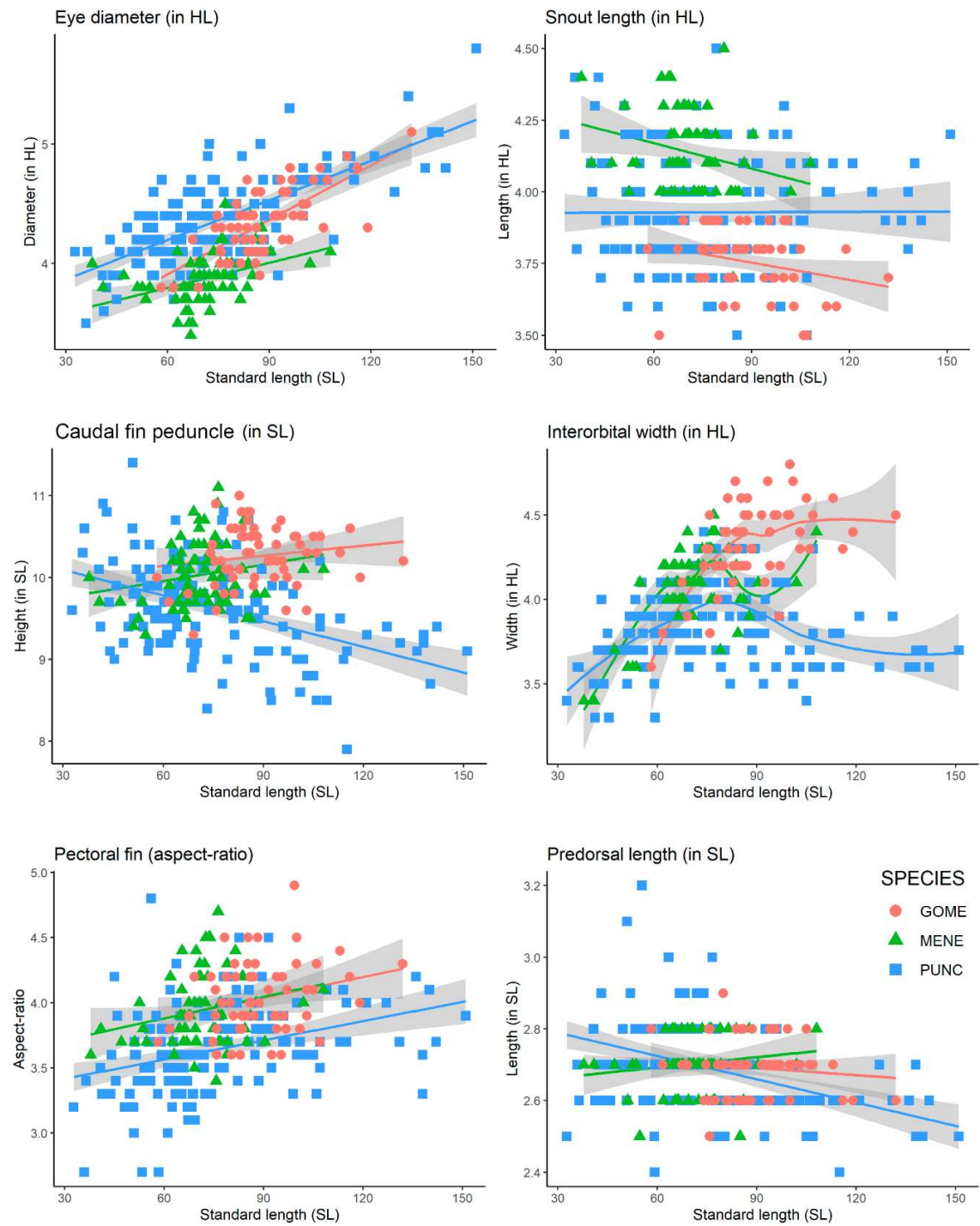


Fig. 8

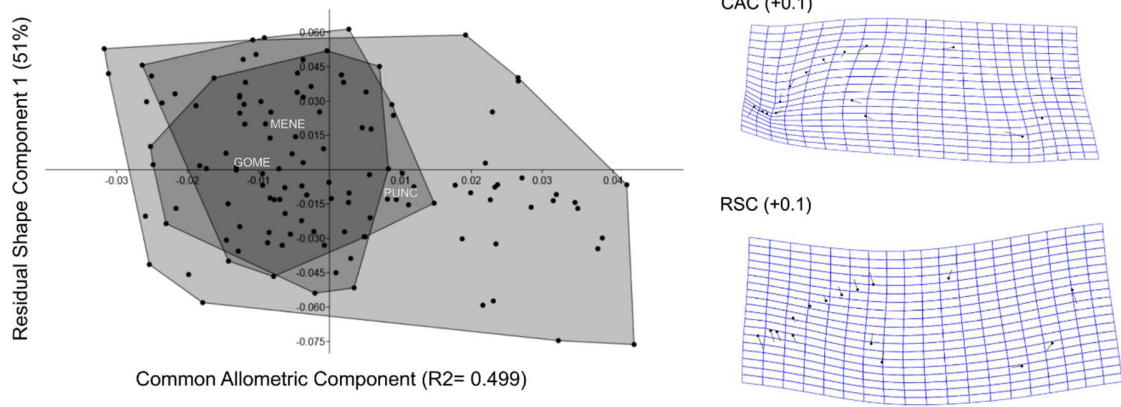


Fig. 9

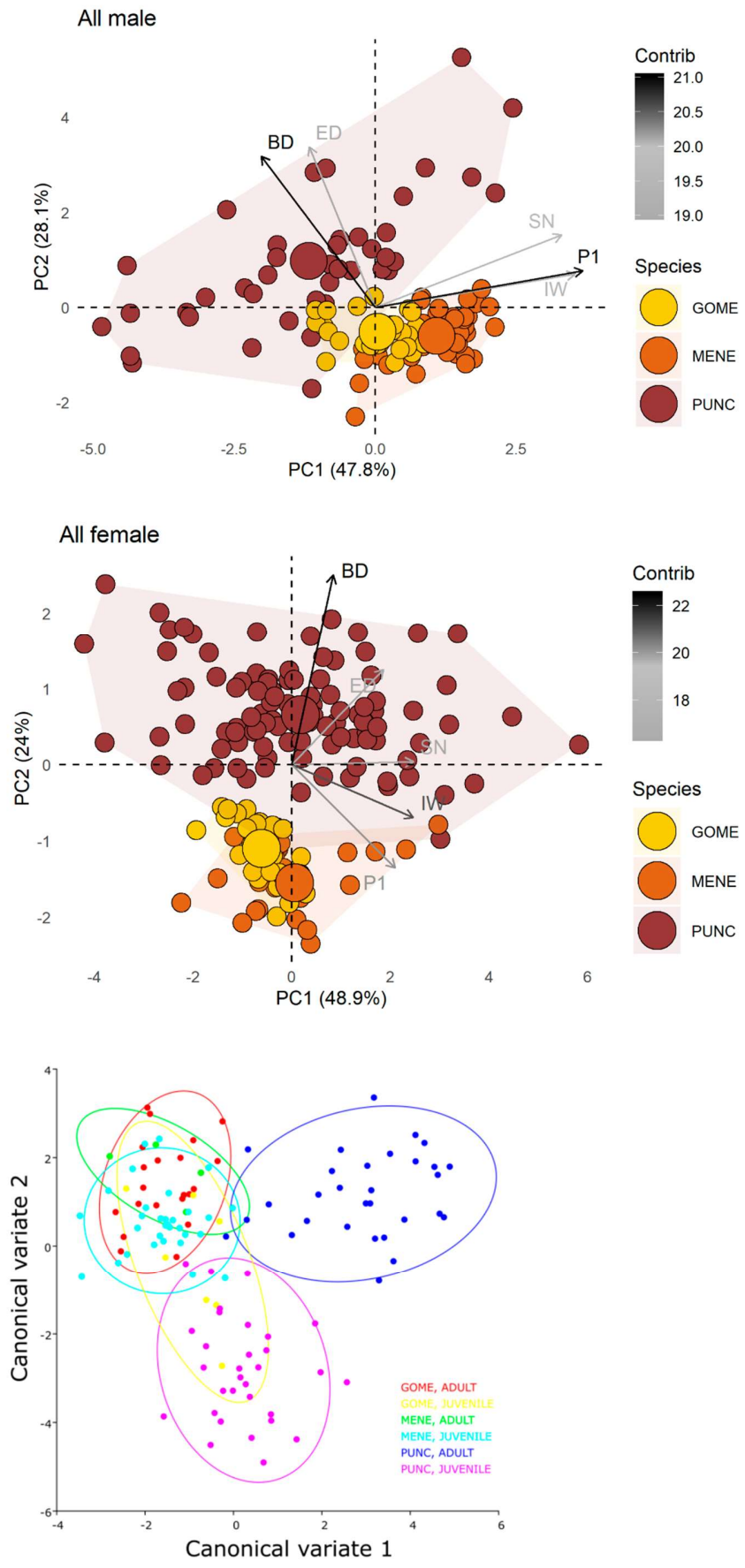


Fig. 10

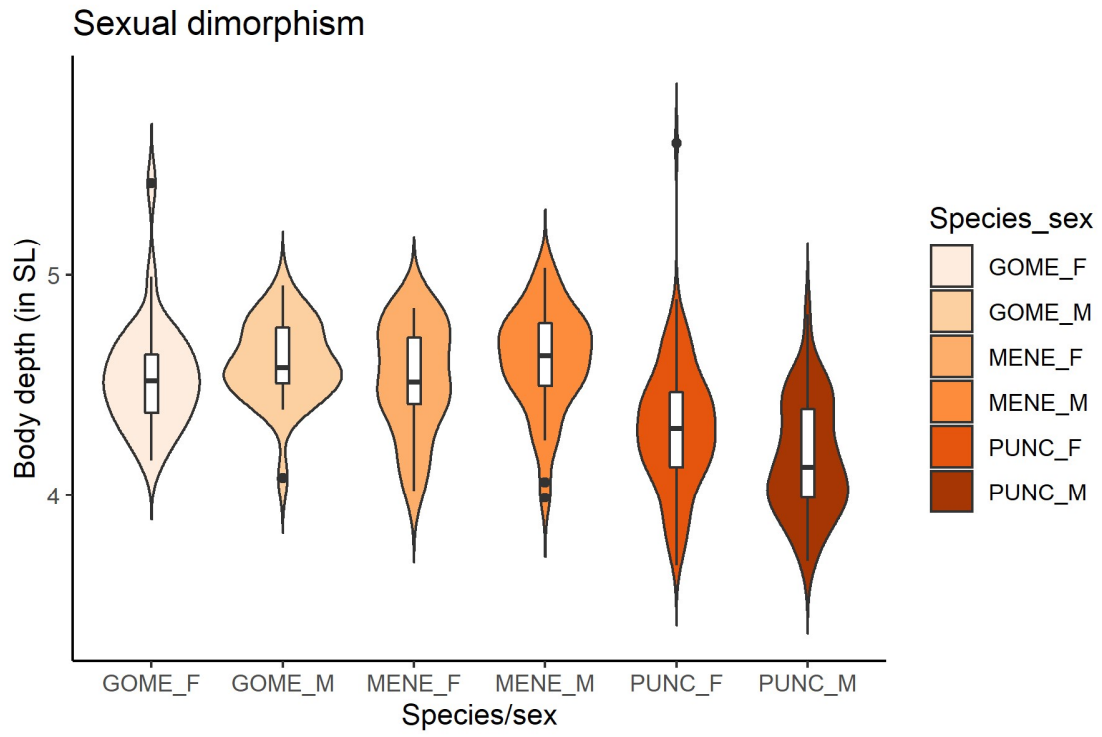


Fig. 11



Fig. 12

Capítulo 2 – Disentangling the croaker basket: Use of otolith shape analysis to distinguish three cryptic species

Jonas de Andrade Santos¹, Rafael Menezes¹, Telton Pedro Anselmo Ramos², Ricardo de Souza Rosa²

¹Programa de Pós-Graduação em Ciências Biológicas (Zoologia), Centro de Ciências Exatas e da Natureza, Universidade Federal da Paraíba, 58051-900, João Pessoa, PB, Brazil

²Departamento de Sistemática e Ecologia, Centro de Ciências Exatas e da Natureza, Universidade Federal da Paraíba, 58051-900, João Pessoa, PB, Brazil

Abstract

Sciaenidae (croakers) is known for specializations in the sensory systems such as lateral line and otoliths. Within this family, some members of the Stelliferinae remain taxonomically unresolved due to their cryptic aspects and low phenotypic disparities. The spotted croaker *Stellifer punctatissimus* putatively comprises a species complex formed by three species (the “croaker basket”), but molecular data have indicated only two evolutionary lineages. Herein, we test the hypothesis that this basket is composed by *Stellifer gomezi* (GM), *S. menezesi* (MN), and *S. punctatissimus* (PC), using the otolith shape and morphology to differentiate them. Seventy-seven sagittal otoliths (GM= 30, MN= 30, PC= 17) were photographed to detect the otolith contour by Elliptical Fourier descriptors (EFDs). Ten otoliths were used to detect shape variation in the *sulcus acusticus* through semilandmarks. Differences in otolith shape were recorded among the species by PerANOVA ($F= 4.75$, $p < 0.001$) and by the LDA, demonstrating three highly segregated groups (re-classification accuracy over 94%). Also, were recorded small variations on the *sulcus acusticus*, otolith gross morphology, and in shape indices. All data seem to confirm our initial hypothesis, thus, our results aid to reduce the taxonomic gap existing in Sciaenidae.

Keywords: Sciaenidae, *Stellifer*, taxonomy, otolith morphology

Resumo

Sciaenidae (corvinas, pescadas) é uma família conhecida por especializações nos sistemas sensoriais, como linha lateral e otólitos. Dentro dessa família, alguns membros de Stelliferinae permanecem com sua taxonomia não resolvida devido à característica críptica. *Stellifer punctatissimus* supostamente compreende um complexo de espécies formado por três espécies

(o "cesto de pescadinhas"), mas os dados moleculares têm indicado apenas duas linhagens evolutivas. Aqui, testamos a hipótese de que esse cesto é composto por *Stellifer gomezi* (GM), *S. menezesi* (MN), e *S. punctatissimus* (PC), usando a forma e morfologia do otólito para diferenciá-las. Setenta e sete otólitos sagitta (GM= 30, MN= 30, PC= 17) foram fotografados para detectar o contorno do otólito pelos descritores Elípticos de Fourier (EFDs). Dez otólitos foram usados para detectar a variação de forma no *sulcus acusticus* através dos *semilandmarks*. Foram registradas diferenças na forma do otólito entre as espécies através da PerANOVA ($F= 4,75$, $p < 0,001$) e pela LDA, demonstrando três grupos altamente segregados (reclassificação acima de 94%). Também foram registradas pequenas variações no *sulcus acusticus*, na morfologia do otólito e nos índices de forma. Todos os dados parecem confirmar nossa hipótese inicial; portanto, nossos resultados ajudam a reduzir a diferença taxonômica existente em Sciaenidae.

Palavras-chave: Sciaenidae, *Stellifer*, taxonomia, morfologia do otólito

Running Head

Disentangling the croaker basket

Introduction

Sciaenidae is one of the most speciose families within Percomorphaceae, including almost 300 species, and members from this family are widely known as ‘croakers’ or ‘drums’ (i.e., they produce sound) (Chao, 1978; Fricke et al., 2021). The diversity of morphological traits in the family has enabled the adaptation of the species to a variety of habitats, such as estuaries, sand bottoms, and surf zones, while a few species are strictly freshwater or reef-associated (Chao, 1978). Although recent evidence based on morphological and molecular approaches has supported the monophyly of this family, the evolutionary relationships in lower taxonomic ranks remain uncertain (Chao, 1978; Sasaki, 1989; Lo et al., 2015; Hughes et al., 2018). As an example, the status of the majority of genera of the monophyletic subfamily Stelliferinae (also known as ‘*Stellifer*-group’ sensu Chao, 1978) is still unsolved due to their great morphological similarity or even the lack of diagnostic characters to distinguish them (Chao et al., 2015; Silva et al., 2018).

A paucity of informative characters has led to shifts in the generic positioning of morphologically similar species, such as those originally described as *Stellifer* Oken 1817 and later changed to *Ophioscion* Gill 1863, or vice versa (Chao et al., 2021). Both genera are common or abundant, particularly in coastal waters of North-Northeastern Brazil, frequently

found as bycatch in shrimp trawls. Despite their abundance, the taxonomic status of several of those species remains undefined (Chao et al., 2015; Silva et al., 2018). A particular case of uncertainty is *Stellifer punctatissimus* (Meek & Hildebrand, 1925), initially described as *Ophioscion* by Meek, Hildebrand (1925). Later, a species complex with two additional species was recognized by Chao (2002); however, molecular data have pointed out only two evolutionary lineages within this complex (Barbosa et al., 2014; Silva et al., 2018). Finally, one of these species was described as new and another redescribed, both now included in *Stellifer*, which is considered a junior synonym of *Ophioscion* (see Chao et al., 2021).

Internal characters may be valuable surrogates for discriminating closely related sciaenid species. In particular, studies using otoliths and swimbladders have aided in resolving taxonomic incongruencies, especially separating genera or supra-generic groups (Casatti, 2001; Chao et al., 2019). In addition, croakers are well known for the relatively large otoliths, and both otoliths and swimbladders possess diverse shape patterns and specializations. This diversity yields fine-scale results in the differentiation of morphologically similar species, once those characters come from an evolutionary perspective of specialization of the sensory system (Trewavas, 1977; Schwarzhans, 1993).

Otoliths are calcified structures located in the inner ear of bony fishes (Teleostei) disposed into the three semicircular canals (utricle, saccule, and lagena), which correspond to the lapillus, sagitta, and asteriscus pairs (Schulz-Mirbach et al., 2019). They are metabolically inert, surrounded by endolymph and connected to the macula (which holds the sensory hair cells and nerves) by the otolithic membrane, which lies on the otoliths acusticus (Popper et al., 2005; Schulz-Mirbach et al., 2019). Due to their higher density when compared to the fish body, otoliths have a different response (i.e., distinct amplitudes and phases) to sound- or motion-induced movements (e.g., angular acceleration); thus, shape variations in otoliths, as well as differences in the features of their sensory cells (e.g., stereocilia number, cell orientation), may be correlated with directional sound sensitivity (Ramcharitar et al., 2001; Popper et al., 2005; Ramcharitar et al., 2006; Popper, Fay, 2011; Schulz-Mirbach et al., 2019). Furthermore, otolith shape is influenced by extrinsic factors, such as salinity and temperature, and intrinsic, such as physiology and ontogeny. As a result, selective pressure may lead to a specific shape for each species (Campana, Thorrold, 2001; Vignon, Morat, 2010; Hoff et al., 2020; Clark et al., 2021) and this has been considered a driver of evolution of the hearing (i.e., sensory drive hypothesis) by the effect of environmental factors on the evolution of signals and signaling dynamics (Tuset et al., 2016b); this process might have taken place in a context where the sight is not so effective - due to the turbidity and the properties of light propagation itself -

thus, the hearing would act better than sight in locating prey (or other objects) and in avoidance of predators (Ramcharitar et al., 2001; Popper, Schilt, 2008; Schulz-Mirbach et al., 2019). Additionally, this specific shape coupled with otolith size may have coevolved to avoid overstimulation in swimbladder possessors that use it for communication, as well as a result of different species having distinct hearing demands; however, there is some speculation about it because the size could also be related to the balance and swimming instead of hearing (Popper et al., 2005; Schulz-Mirbach et al., 2019). Although sciaenids are well known for their sensory specializations, and despite this aspect appearing to have a positive effect in avoiding predators, they are largely eaten by dolphins that use passive listening to search for their prey, such as sciaenids or haemulids (i.e., both sound producers); conversely, either the change in behavior regarding sound production (e.g., diminished loudness of choruses) or the high availability of those fish families in coastal zones may act as a trade-off to the maintenance of those groups under such predation pressure (Ramcharitar et al., 2006; Pansard et al., 2011; Rodrigues et al., 2019; Ladich, 2022).

In addition to the previously cited variations, by growing throughout the fish life cycle, otoliths seem to also respond to other factors, such as ontogenetic shifts and those linked to environmental gradients (Volpedo, Fuchs 2010; Schulz-Mirbach et al., 2019). Likewise, as they carry a signal of those traits, surveys that use otolith shape provide an indirect and effective way to investigate the living habits of such species and to seek diagnostic details in cryptic species. Such analyses contrast with traditional taxonomic approaches, which generally show more overlap than otolith shape analyses (Galley et al., 2006; Lombarte et al., 2006; Capoccioni et al., 2011). There are many techniques to delineate the otolith shape contour (e.g., shape indices, wavelet, Fourier descriptors). Despite being frequent in those kinds of studies or the ones that look into broader comparisons (i.e., at genus or family level), the shape indices are powerless to differentiate cryptic species due to their resolution being lower than required. In addition, they provide valuable biological information by shedding light to the association of shape patterns with habits such as feeding and water depth (Tuset et al., 2006; Wong et al., 2016; Assis et al., 2020; Ghanbarifardi et al., 2020). Fourier descriptors are more efficient in distinguishing the level of subtle differences in cryptic species than other indices, particularly because they decompose the otolith's outline into several harmonics, which encompass almost the entire variation across that border (Rohlf, Archie, 1984; Ferguson et al., 2011; Avigliano et al., 2018). In contrast, methodological constraints impair the application of geometric morphometric methods (GMM) in this context. This method likely achieves a fine resolution in the resolution of cryptic species or species-rich groups (Anjos et al., 2020; Argolo et al.,

2020), but due to the lack of homologous points, its use in otolith analysis is mostly restricted to outline descriptions with semi-landmarks (Ramírez-Pérez et al., 2010; Tuset et al., 2016), and such a method displays lower resolution than Fourier descriptors (Wong et al., 2016). However, it provides additional data when applied to structures such as the *sulcus acusticus* (i.e., ostium and cauda); as a result, such information could be applied to discuss hearing capabilities, taxonomy, and prey identification (Farré et al., 2016; Byrd et al., 2020; Granados-Amores et al., 2020).

In this context, this study aimed to test the following hypothesis: *Stellifer punctatissimus* species complex is formed by three distinct species and they can be distinguished by otolith shape analysis.

Material and methods

Sampling sites and otolith preparation. The otoliths were sampled along the coast of Bahia state, and 77 right sagittal otoliths from three *Stellifer* species were sampled as follows: *Stellifer gomezi* (GM) - 30; *Stellifer menezesi* (MN) - 30; and *Stellifer punctatissimus* (PC) – 17 (Tab. 1). The sampling was carried out at four sample sites: Itaparica Island, Porto Seguro (#2), and Caravelas (Fig. 1). The surveys were conducted in April 2018 and February 2019 on Itaparica Island and May and March 2016 in Porto Seguro and Caravelas, respectively. The vouchers were deposited at the fish collection in Universidade Estadual de Feira de Santana (UEFS - MZFS) under the numbers 17694, 18115, 18116, 18117, 18119, 18124, 18125, 18126, 18127, 18128, 18129, 18131, 18133, 18135. The samplings were authorized by Collection Permit SISBIO 47993-1. In the survey, five trawls parallel to the coast (totaling about 250 m) were conducted using a manual beach-seine net (9 meters in length, 1.7 meters in height, 13 mm mesh on the lateral, and 5 mm mesh in the center). At the Caravelas site, fish sampling was performed after regular shrimp trawling, and specimens were caught as bycatch.

The otoliths were extracted preferentially by cutting through the upper end of the right gill cover; herein, only the sagitta was used in the analyses. Then, the otoliths were manually cleaned, washed in distilled water, dried, and stored in individually labeled Eppendorf® tubes. Right otoliths were photographed using a stereomicroscope Leica EZ4 HD (for outline analysis) and Leica M205 A (for description and geometric morphometrics), broken otoliths were disregarded, and then were chosen from the left side. All pictures had their contrast improved in Adobe Photoshop CC 2019 and were digitally cleaned to avoid errors in contour analysis. Otolith's descriptions nomenclature (Fig. 2) were based on Chao (1978), Schwarzzhans (1993), and Aguilera et al. (2016).

Statistical analyses. The images were initially processed using ImageJ software (Schneider et al., 2012) to calculate the pixel-cm ratio of each one. To describe the otolith shape, the following shape indices were calculated: aspect ratio, circularity, ellipticity, form factor, rectangularity, and roundness (see Avigliano et al., 2018). A MANOVA test was used to determine differences among species. Additionally, Elliptical Fourier descriptors (EFDs) were used to quantify the otolith shape using “*shapeR*” package (Libungan, Palsson, 2015) in the R platform (R Core Team, 2020). An ANOVA-like permutation test (PerANOVA) was used to find differences in the shape indices (dependent variable) among the three species analyzed (categorical variables). Finally, a Linear Discriminant Analysis (LDA) was performed to describe the variation in EFDs among the species within a morphospace. Reclassification rates were calculated to measure the accuracy degree of segregation among the species, using the MASS package (Venables, Ripley, 2002)

For the geometric morphometric methods (GMM), ten photographs of each species were analyzed using the Tps series (Rohlf, 2017a, 2021). To account for the variation within the *sulcus acusticus*, a curve was drawn on its entire border, having a landmark as an initial and final point on that curve. The original curve was resampled to 35 points (by length), which were posteriorly assigned as landmarks (LM), by using the function of `append tps curves to landmarks`. The semilandmarks (sLM) at the initial and final points of the curve were deleted from the dataset, remaining only the 33 points from the curve (semilandmarks - sLM) plus the two landmarks, in the sequence, the sliding step was performed on those curve based on the minimum bending energy method (Figure 2). All data were initially subjected to a Generalized Procrustes Analysis (GPA) using `tpsRelw` (Rohlf, 2017b). To describe *sulcus acusticus* morphology, a Principal Component Analysis (PCA) was performed using the Procrustes residuals. Because our dataset presented many more variables (33 sLM + 2 LM) than specimens (10 by species), we achieved low statistical power. Thus, in all GMM analyses, we consider the description side of such analysis more valuable than its statistical significance in regard to distinction among groups.

Results

Otoliths description. Sagittal otoliths’ outline somewhat rectangular. Inner face strongly convex. A well-marked dorsal furrow. Postdorsal spine broad, relatively short. Dorsal depression not well defined, smooth, and shallow; a curve follows between predorsal spine and predorsal angle. The ontogenetic variation shows a more rounded otolith in juveniles (vs. more rectangular in adults), a smoother ostium in juveniles, postdorsal spine shorter in juveniles (Fig. 3).

Stellifer gomezi: Predorsal spine is relatively long, straight to slightly curved, outwards in the dorsal view. Dorsal margin smooth, slightly concave; forming an angle of approximately 130° with predorsal angle. Predorsal angle rounded, occasionally projecting posteriorly. Postventral notch smooth, with an angle of approximately 130° . Ostium short, shallow, and wide; narrowed close to the ostial-caudal joint. A spout-like groove between the ostium and dorsal depression, bent at approximately 100° . Cauda deep, widened, strongly bent; rounded on its tip. Outer face rather straight, except for the posterior margin, slightly convex. A well-defined mid-dorsal projection; rounded to slight sharp and backward oriented. The ontogenetic variation shows the cauda tip slightly pointed in juveniles, projection on the outer face less pronounced in juveniles (Fig. 3a).

Stellifer menezesi: Predorsal spine is relatively long, straight, also nearly straight in dorsal view. Dorsal margin smooth, slightly concave; forming an angle of approximately 140° with predorsal angle. Predorsal angle rounded, occasionally projecting outwards. Postventral notch smooth, with an angle of approximately 130° . Ostium short, generally shallow (except for a depression on its mid-posterior section), faint ventrally widened, narrowed close to the ostial-caudal joint. A spout-like groove between the ostium and dorsal depression, bent at approximately 130° . Deep, widened, strongly bent cauda; slightly forward-pointed on its tip. Outer face rather straight, except by the posterior margin slightly convex. A well-defined projection on the mid-dorsal; its margin squarish to rhomboidal and backward oriented. The ontogenetic variation shows the cauda slightly less bent in adults and its tip somewhat pointed in juveniles, predorsal angle less pronounced in juveniles, projection on the outer face less pronounced in juveniles (Fig. 3b).

Stellifer punctatissimus: Predorsal spine is relatively long, straight, sharp to slightly rounded, nearly outwards directed in dorsal view. The dorsal margin is rather smooth or faint sinuate and forms an angle of approximately 135° with predorsal angle. Predorsal angle rounded, occasionally projecting outwards. Postventral notch smooth, with an angle of approximately 135° . Ostium short, surface irregular (a depression on its mid-posterior section), faint ventrally widened, narrowed close to the ostial-caudal joint. A shallow, rather inconspicuous spout-like groove between the ostium and dorsal depression, bent at approximately 130° . Cauda deep, widened, strongly bent; slightly forward-pointed on its tip. Outer face flat to somewhat irregular, posterior margin slightly convex. A well-defined projection on the mid-dorsal margin; its margin C-shaped to somewhat backward oriented. The ontogenetic variation shows the cauda tip somewhat pointed in juveniles, predorsal spine more rounded in adults, predorsal

angle less pronounced in juveniles, projection on the outer face with its margin squarish to rhomboidal and backward oriented in adults (Fig. 3c).

Shape indices and shape analyses. Only the circularity and rectangularity exhibited statistically significant differences (MANOVA: $F= 3.9$, $p< 0.05$ and $F= 5.3$, $p<0.01$, respectively), which displayed differences in allometry (Figs. 4–5). Differences in otolith allometry were found among the species: negative in *Stellifer gomezi* and positive in *S. menezesi* and *S. punctatissimus*, the latter with the highest rectangularity value among all species (Fig. 5).

From all otolith sections, shape analysis (wavelet) showed a higher variation to the anterior margin: *S. gomezi* exhibited a most concave *ostium* border, while *S. menezesi* had a more elongated predorsal spine and a rounded predorsal angle (Fig. 6). These differences in otolith shape (EFDs) were also recorded among the species by PerANOVA ($F=4.75$; $p<0.001$), indicating that such differences might correspond to distinct groups - the species evaluated here. This was corroborated by the LDA, which demonstrated each species as nearly non-overlapping groups; thus, it may reinforce the hypothesis of each group as distinct species once they formed three highly segregated groups (Fig. 7). Moreover, this high segregation led to strong reclassification accuracy for each species: GM= 96.7%, MN= 100%, PC= 94.1% (Figure 4).

In respect to geometric morphometrics, the PCA explained the major variation of shape in the otolith's *cauda*. The first two components of the PCA accounted for 65.1% of the shape variation in the *sulcus acusticus*; PC1 corresponded to a narrower/larger *cauda*, angle at the *cauda* almost straight, slightly bent *cauda* tip, and a narrower *ostium* (on the dorso-ventral axis). The second component (PC2) showed a more narrowed ostial-caudal joint, a wider *ostium* (on the antero-posterior axis), and an expansion on the *cauda*. On the PCA plot, most of the morphospace overlapped among the species. However, slight differences were found among the species, especially for *Stellifer gomezi* (GM) and *S. menezesi* (MN). The GM/MN group was allocated in the positive values of the PC2, while PC exhibited the highest negative values and a more spread distribution, and *S. menezesi* (MN) had an almost centered distribution. On the pair comparisons, GM-PC displayed the higher variation - linked to the expansion of the *cauda*, *sulcus*, and *ostium* and a less straight caudal curve; followed by MN-PC, with slight expansion on the *ostium* and caudal tip; finally, the pair GM-MN presented a lower distinction, which was restricted to small variations in caudal curve and *ostium* expansion (Fig. 8).

Discussion

Integrative approaches have increasingly been used to distinguish cryptic species of shore fishes (e.g., Carvalho et al., 2020a; Figueiredo-Filho et al., 2021). An initial morphological study indicated the existence of a species complex in *Stellifer punctatissimus* (Chao, 2002), but this hypothesis has not been confirmed by molecular evidence, which suggested instead recent speciation and only two evolutionary lineages in this complex (Silva et al., 2018). Recently, all these species were formally recognized through a morphological basis (Chao et al., 2021), but complementary studies were still needed to elucidate such cases.

Herein, elliptic Fourier descriptors (EFDs) provided a robust result with a high reclassification rate for all species (more than 94%). In contrast, surveys at distinct levels such as spatiotemporal or stock levels showed lower values than those found here (Avigliano et al., 2018; Hoff et al., 2020; Kikuchi et al., 2021). Despite variation in reclassification rates, values closer to the found here (~94%) seem to be rare but were already recorded (Bani et al., 2013; Zischke et al., 2016; Hoff et al., 2020). An example is the Bigtooth corvina (*Isopisthus parvipinnis*) in SW Atlantic, where well-marked groups based on otolith shape were found (e.g., populations, years) reflecting probably fishery pressure and changes in population structure toward a metapopulation structure (Hoff et al., 2020). Therefore, these results demonstrate the utility of this method to discriminate closely related species, for aging in fishes, detecting stocks, ontogenetic variation, and patterns related to environmental gradients (Beyer, Szedlmayer, 2010; Assis et al., 2020; Carvalho et al., 2020b; Kikuchi et al., 2021). However, as this is a method for an outline, it has constraints in “inner” structures such as the *sulcus acusticus*, which can be used as a proxy for prey identification (e.g., in dolphins’ diet studies - Rodrigues et al., 2019; Byrd et al., 2020).

The geometric morphometric method (GMM), however, provided a contrasting result, particularly a more spread and overlapped pattern among the species. Meanwhile, few changes in shape were printed in the species’ otolith description. Interestingly, the observed pattern exhibits a “gradient” from *Stellifer punctatissimus* (PC) to *S. gomezi* and *S. menezesi* (GM, MN), which is in agreement with its external similarity. Accordingly with this external overlapping, such as in body depth, eye size, and pectoral-fin length (Chao et al., 2021; unpublished data), it would be expected a pattern as the one found here. Indeed, previous studies have shown that similar species (i.e., external morphology) may occupy a similar place in the morphospace, either when otolith shape or body shape is analyzed, as seen in the genus *Centropomus*, although its morphotypes were also separated by showing distinct allometry (Granados-Amores et al., 2020; Figueiredo-Filho et al., 2021; Medeiros et al., 2021). However, the association between otolith shape and body morphological convergence is not often a rule

within Teleostei (Lombarte et al., 2010; Tuset et al., 2016b; Assis et al., 2020; Pavlov, 2021); in fact, they often seem uncoupled (Tuset et al., 2016b; Pavlov, 2021). Although the shape may be affected by the phylogenetic inertia - similar shape among closely related species coming from a common ancestor - it could present distinct growth rates that might allow distinguishing such species (Lombarte, Cruz 2007; Lombarte et al., 2010).

Variations in otolith shape of the *Stellifer* complex can also result from unmeasured factors herein, such as the growth and metabolic rates (Alewijnse et al., 2021; Jónsson et al., 2021). As Geller (1999) argues, these aspects would also help to evaluate cryptic species because they could reveal the masking effect in species complexes. This seems to be achieved in our results, that show each species with a specific rate of otolith weight, which could suggest a distinct size at first maturity for each species (results not shown), and in agreement with our initial hypothesis. Additionally, our results show that at least one of the species (GM) has a distinct allometric pattern in the rectangularity index, also supporting the hypothesis of three distinct species in the *Stellifer punctatissimus* species complex. It has been proven that either accretion rates or growth rates in otolith shape can be used as a proxy for differentiating species or even stocks due to the assumed distinct intrinsic factors by species (Hamer, Jenkins 2007; Pavlov, 2016; Zischke et al., 2016; Kikuchi et al., 2021). In the same way, the shape indices can be linked to traits such as depth preference, use of habitat, and feeding habit (Volpedo, Echeverría 2003; Volpedo, Fuchs 2010; Assis et al., 2020). In doing so, we could apply the differences in ecological niches into a taxonomic approach to achieve a better resolution in taxonomic issues, as discussed here. Our data show values above 65% of the aspect-ratio, which may classify all these species as associated with demersal behavior in unconsolidated substrates, but does not suggest strict benthic behavior, such as that occurring in *Menticirrhus* (Aguirre, Lombarte 1999; Volpedo, Echeverría 2003; Jaramillo et al., 2014; Carvalho et al., 2020b). These findings are consistent with recent data on this species complex, which have changed the incorrect assignment from zoobenthivorous guild (closely related to the bottom) to zooplanktivorous (Santos et al., 2021).

Studies on species delimitation must consider a broad source of data to yield a reliable taxonomic recommendation; in doing so, a better understanding of the evolutionary process would be achieved and taxonomic issues would be solved (Carstens et al., 2013). It is known that to reject the null hypothesis in species delimitation, a much higher amount of data should be used in a well-studied species than to describe/record a new species (Hillis et al., 2021). An example of such incongruence is found in snappers (Lutjanidae), which provide some cases that either have led to subsequent splitting and adjoin species or to an endless doubtful

taxonomic status that harms taxonomic stability (Pinna et al., 2018; Pedraza-Marrón et al., 2019; Andrews et al., 2021). In such situations, only the combined use of approaches and data review lead to some resolution; as discussed before, different growth rates and otolith shapes aid in a well-based result that places certainty on taxonomic status (Pedraza-Marrón et al., 2019; Andrews et al., 2021). Despite most of our data being from a single source (otoliths), they were not appraised through a single view. For instance, its description reveals some agreement with the current phylogeny, namely, the closer relationship between the *Stellifer punctatissimus* species complex and *S. scierus*/*S. strabo* (both from the Pacific ocean); they shared a well-marked spout-like groove, with almost a right angle, and shared with fossil species a backward oriented projection on its otolith's outer face (Aguilera et al., 2016; Silva et al., 2018). This would be better explored as an ancestral state reconstruction - in a systematic review - because by coming from an evolutionary perspective of specialization on the sensory system in Sciaenidae, those characters would help solve incongruencies within Stelliferinae phylogeny (Trewavas, 1977; Schwarzhans, 1993; Pagel, 1999). Additionally, a few differences, such as *sulcus acusticus* shape/size and outline angles, add evidence to refute the null hypothesis (herein, only two species on its complex); therefore, it agrees with the other methods' results that indicate the occurrence of three species on its complex.

Conversely, of all shape indices, likely resulting of high multicollinearity among them, only the circularity and rectangularity were statistically significant (Tuset et al., 2021). This low contribution to differentiation among the species is not unexpected; these indices present an unsuitable resolution to detect small differences at the species level (Pavlov, 2016; Wong et al., 2016; Avigliano et al., 2018). As discussed by Tuset et al. (2021), the shape indices only provide good results if clearly distinct species are compared - this is not the case of cryptic species. We suggest therefore that Elliptical Fourier descriptors perform better than shaped indices to distinguish cryptic and congeneric species. On the other hand, once the application of homologous landmarks in otoliths is unlikely, we needed to apply several semilandmarks on the *sulcus acusticus*, as a result, we lost statistical power. Thus, our GMM results would be improved by adding specimens, which could give a balance between variables (semilandmarks) and specimens (otoliths) (Gunz, Mitteroecker 2013; Cardini et al., 2015).

As the otolith shape is known to be species-specific (Campana, Casselman 1993), it responds to environmental gradients; thus, at the same time that we could indicate habitat use through otoliths. We cannot disregard the likelihood of those differences to indicate some distinctions in the otolith as holding a signal of a putatively different occupation in the coastal zone; this could retrieve a recent speciation process likely by ecological divergence (Carvalho-

Filho et al., 2009; Silva et al., 2018; Caires et al., 2019). As these shapes vary (e.g., outline, *sulcus acusticus*) among the species, they can be applied for taxonomic purposes to fulfill the gaps within the family Sciaenidae and in ecological surveys, once otoliths are one of the most informative remains to identify bony fishes in diet studies (Rodrigues et al., 2019; Byrd et al., 2020).

As the croakers produce sound, they are supposed to be more efficient in locating prey, hearing predators, and attracting partners in the spawning season when compared to nonsound-producing taxa (Deary et al., 2016; Taylor et al., 2020). However, sound production can have a negative effect on avoiding predators, once croakers are targeted by coastal dolphins, which might present several feeding behaviors, but seem to feed generally upon sound-producing fishes (e.g., Sciaenidae, Haemulidae) in likely an opportunistic way. This is may be driven by the use of passive listening to locate those prey and sciaenids' high availability in the coastal zone (Pansard et al., 2011; Secchi et al., 2017; Tellechea et al., 2017; Rodrigues et al., 2019). On the other hand, a trade-off should occur in calling benefits in an adaptative way; it has been shown that sciaenids can perceive predators' presence and, as a result, reduce their calling activity and diminish the loudness of their choruses (Luczkovich et al., 2000; Ramcharitar et al., 2006; Ladich, 2022).

Both of them - prey and predators - are caught as bycatches in shrimp fisheries, with the former (*S. punctatissimus*) being classified as Least concern (LC) and Data deficient (DD) according to IUCN and MMA/IBAMA, respectively (Tellechea et al., 2017; ICMBio, 2018; Passarone et al., 2019; IUCN, 2020). To date, *S. menezesi* was not evaluated either by IUCN or ICMBIO, and *S. gomezi* was classified as LC by the last available IUCN's assessment (IUCN, 2020). Despite their lack of commercial value, we could not dismiss the ecological importance of these species because some effects of fisheries pressure on marine food webs remain unclear (Lira et al., 2021; Márquez-Velásquez et al., 2021). Due to the possibility of differences in habitat use among those species, such as discussed for the Tonkin weakfish (Caires et al., 2019), the existence of distinct conservation statuses by species in a future assessment is presumable due to the likely specific threats to each species. For this reason, it is essential to continue pursuing for additional data that could elucidate if those species truly have a degree of distinct habitat use throughout their life cycle, which would also help to solve uncertainties in their recent speciation process.

Acknowledgments

We are grateful to Pedro Romano and Ilver Alabat for their suggestions on early version of this manuscript. Special thanks to Natália Souza, Hemille Mariane, Marcelo Carvalho-Júnior,

Rafael Oliveira, Verônica Costa, and Leonardo Moraes for their help in fieldwork. We are also grateful to LABICT/UEFS, LAPAQ/UFSB, and CEPENE-Caravelas teams for allowing the use of their facilities and logistic assistance. JAS thanks Jéssica Prata for the otolith's photos. This work was partially supported by the Coordenação de Aperfeiçoamento de Pessoal de Nível Superior, Brazil (CAPES – finance code 001) and Fundação de Amparo à Pesquisa do Estado da Bahia (FAPESB) through the project “Migrações ontogenéticas entre ecossistemas costeiros e o papel de estuários como berçários para espécies de peixes marinhos comerciais através de análise microquímica de otólitos” (PAM 0019/2014).

References

- Aguilera OA, Schwarzhans W, Béarez, P. Otoliths of the Sciaenidae from the Neogene of tropical America. *Palaeo Ichthyologica*. 2016; 14:7–90.
- Aguirre H, Lombarte A. Ecomorphological comparisons of sagittae in *Mullus barbatus* and *M. surmuletus*. *J Fish Biol*. 1999; 55:105–14. <https://doi.org/10.1111/j.1095-8649.1999.tb00660.x>
- Alewijnse SR, Stowasser G, Saunders RA, Belcher A, Crimmen OA, Cooper N, Trueman CN. Otolith-derived field metabolic rates of myctophids (Family Myctophidae) from the Scotia Sea (Southern Ocean). *Mar Ecol Prog Ser*. 2021; 675:113–131. <https://doi.org/10.3354/meps13827>
- Andrews KR, Fernandez-Silva I, Randall JE, Ho HC. *Etelis boweni* sp. nov., a new cryptic deepwater eteline snapper from the Indo-Pacific (Perciformes: Lutjanidae). *J Fish Biol*. 2021; 99(2):335–44. <https://doi.org/10.1111/jfb.14720>
- Anjos MS, Bitencourt JA, Nunes LA, Sarmiento-Soares LM, Carvalho DC, Armbruster JW, et al. Species delimitation based on integrative approach suggests reallocation of genus in Hypostomini catfish (Siluriformes, Loricariidae). *Hydrobiologia*. 2020; 847:563–78. <https://doi.org/10.1007/s10750-019-04121-z>
- Argolo LA, López-Fernández HL, Batalha-Filho H, Affonso PRAM. 2020. Unraveling the systematics and evolution of the '*Geophagus*' *brasiliensis* (Cichliformes: Cichlidae) species complex. *Mol Phylogenet Evol*. 2020; 150:e106855. <https://doi.org/10.1016/j.ympev.2020.106855>
- Assis IO, Silva VEL, Souto-Vieira D, Lozano AP, Volpedo AV, Fabrè NN. Ecomorphological patterns in otoliths of tropical fishes: Assessing trophic groups and depth strata preference by shape. *Environ Biol Fishes*. 2020; 103(4):349–61. <https://doi.org/10.1007/s10641-020-00961-0>
- Avigliano E, Rolón ME, Rosso JJ, Mabragaña E, Volpedo AV. Using otolith morphometry for the identification of three sympatric and morphologically similar species of *Astyanax* from the Atlantic Rain Forest (Argentina). *Environ Biol Fish*. 2018; 101:1319–28. <https://doi.org/10.1007/s10641-018-0779-2>
- Bani A, Poursaeid S, Tuset V. Comparative morphology of the sagittal otolith in three species of south Caspian gobies. *J Fish Biol*. 2013; 82:1321–32. <https://doi.org/10.1111/jfb.12073>

- Barbosa AJB, Sampaio I, Schneider H, Santos S. Molecular phylogeny of weakfish species of the *Stellifer* group (Sciaenidae, Perciformes) of the Western South Atlantic based on mitochondrial and nuclear data. PLoS One. 2014; 9(7):e102250. <https://doi.org/10.1371/journal.pone.0102250>
- Beyer SG, Szedlmayer ST. The use of otolith shape analysis for ageing juvenile red snapper, *Lutjanus campechanus*. Environ Biol Fish. 2010; 89:333–40. <https://doi.org/10.1007/s10641-010-9684-z>
- Byrd BL, Hohn AA, Krause JR. Using the otolith sulcus to aid in prey identification and improve estimates of prey size in diet studies of a piscivorous predator. Ecol Evol. 2020; 10(8): 3584–3604. <https://doi.org/10.1002/ece3.6085>
- Caires RA, Santos WCR, Machado L, Oliveira C, Cerqueira NNCD, Rotundo MM, et al. The Tonkin weakfish, *Cynoscion similis* (Sciaenidae, Perciformes), an endemic species of the Amazonas-Orinoco Plume. Acta Amazonica. 2019; 49:197–207. <https://doi.org/10.1590/1809-4392201803481>
- Campana SE, Casselman JM. Stock identification using otolith shape analysis. Can J Fish Aquat Sci. 1993; 50:1062–83. <https://doi.org/10.1139/f93-123>
- Campana SE, Thorrold SR. Otoliths, increments, and elements: keys to a comprehensive understanding of fish populations?. Can J Fish Aquat Sci. 2001; 58:30–8. <https://doi.org/10.1139/f00-177>.
- Cappocionni F, Costa C, Aguzzi J, Menesatti P, Lombarte A, Ciccotti E. Ontogenetic and environmental effects on otolith shape variability in three Mediterranean European eel (*Anguilla anguilla*, L.) local stocks. J Exp Mar Biol Ecol. 2011; 397(1):1–7. <https://doi.org/10.1016/j.jembe.2010.11.011>
- Cardini A, Seetah K, Barker G. How many specimens do I need? Sampling error in geometric morphometrics: testing the sensitivity of means and variances in simple randomized selection experiments. Zoomorphology. 2015; 134:149–63. <https://doi.org/10.1007/s00435-015-0253-z>
- Carstens BC, Pelletier TA, Reid NM, Satler JD. How to fail at species delimitation. Mol Ecol. 2013; 22:4369–83. <https://doi.org/10.1111/mec.12413>
- Carvalho CO, Marceniuk AP, Oliveira C, Wosiacki WB. Integrative taxonomy of the species complex *Haemulon steindachneri* (Eupercaria; Haemulidae) with a description of a new species from the western Atlantic. Zoology. 2020a; 141:e125782. <https://doi.org/10.1016/j.zool.2020.125782>
- Carvalho BM, Volpedo AV, Fávaro LF. Ontogenetic and sexual variation in the sagitta otolith of *Menticirrhus americanus* (Teleostei; Sciaenidae) (Linnaeus, 1758) in a subtropical environment. Pap Avulsos Zool. 2020b; 60:e20206009. <https://doi.org/10.11606/1807-0205/2020.60.09>
- Carvalho-Filho A, Ferreira CEL, Craig M. A shallow water population of *Pronotogrammus martinicensis* (Guichenot, 1868) (Teleostei: Serranidae: Anthiinae) from South-western Atlantic, Brazil. Zootaxa. 2009; 2228(1):29–42. <https://doi.org/10.11646/zootaxa.2228.1.2>

Casatti L. *Petilipinnis*, a new genus for *Corvina grunniens* Schomburgk, 1843 (Perciformes, Sciaenidae) from the Amazon and Essequibo river basins and redescription of *Petilipinnis grunniens*. Pap Avulsos Zool. 2001; 42(7):169–81. <https://doi.org/10.1590/S0031-10492002000700001>

Chao LN, Chang CW, Chen MH, Guo CC, Lin BA, Liou YY, et al. *Johnius taiwanensis*, a new species of Sciaenidae from the Taiwan Strait, with a key to *Johnius* species from Chinese waters. Zootaxa. 2019; 4651(2):259–70. <https://doi.org/10.11646/zootaxa.4651.2.3>

Chao LN. A basis for classifying western Atlantic Sciaenidae (Pisces: Perciformes). NOAA (National Oceanic and Atmospheric Administration) Technical Report NMFS (National Marine Fisheries Service); 1978: Circular No. 415, p. 1–64.

Chao NL, Carvalho-Filho A, Santos JA. Five new species of Western Atlantic stardrums, *Stellifer* (Perciformes: Sciaenidae) with a key to Atlantic *Stellifer* species. Zootaxa. 2021; 4991(3):434–66. <https://doi.org/10.11646/zootaxa.4991.3.2>

Chao NL, Frédou FL, Haimovici M, Peres MB, Polidoro B, Raseira M, et al. A popular and potentially sustainable fishery resource under pressure – extinction risk and conservation of Brazilian Sciaenidae (Teleostei: Perciformes). Glob Ecol Conserv. 2015; 4:117–26. <https://doi.org/10.1016/j.gecco.2015.06.002>

Chao NL. Sciaenidae. In: Carpenter KE, editor. The living marine resources of the Western Central Atlantic. FAO Species Identification Guide for Fishery Purposes and American Society of Ichthyologists and Herpetologists. Special Publication No. 5. Rome: FAO. p. 1583–1653.

Clark FJK, Lima CSS, Pessanha ALM. Otolith shape analysis of the Brazilian silverside in two northeastern Brazilian estuaries with distinct salinity ranges. Fish Res. 2021; 243:e106094. <https://doi.org/10.1016/j.fishres.2021.106094>

Deary AL, Metscher B, Brill RW, Hilton EJ. Shifts of sensory modalities in early life history stage estuarine fishes (Sciaenidae) from the Chesapeake Bay using X-ray micro computed tomography. Environ Biol Fish. 2016; 99:361–75. <https://doi.org/10.1007/s10641-016-0479-8>

Farré M, Tuset VM, Maynou F, Recasens L, Lombarte A. Selection of landmarks and semilandmarks in fishes for geometric morphometric analyses: a comparative study based on analytical methods. Sci Mar. 2016; 80(2):175–86. <https://doi.org/10.3989/scimar.04280.15A>

Ferguson GJ, Ward TM, Gillanders BM. Otolith shape and elemental composition: complementary tools for stock discrimination of mulloway (*Argyrosomus japonicus*) in southern Australia. Fish Res. 2011; 110(1):75–83. <https://doi.org/10.1016/j.fishres.2011.03.014>

Figueiredo-Filho JM, Marceniuk AP, Feijó A, Siccha-Ramirez R, Ribeiro GS, Oliveira C, et al. Taxonomy of *Centropomus* Lacépède, 1802 (Perciformes: Centropomidae), with focus on the Atlantic species of the genus. Zootaxa. 2021; 4942(3):301–38. <https://doi.org/10.11646/zootaxa.4942.3.1>

Fricke R, Eschmeyer WN, Van der Laan R. Eschmeyer's catalog of fishes: genera/species by family/subfamily [Internet]. San Francisco: California Academy of Science; 2021. Available from: <http://researcharchive.calacademy.org/research/ichthyology/catalog/fishcatmain.asp>

- Galley EA, Wright PJ, Gibb FM. Combined methods of otolith shape analysis improve identification of spawning areas of Atlantic cod. *ICES J Mar Sci.* 2006; (63)9:1710–17. <https://doi.org/10.1016/j.icesjms.2006.06.014>
- Geller JB. Decline of a native mussel masked by sibling species invasion. *Conserv Biol.* 1999; 13(3):661–64. <https://doi.org/10.1046/j.1523-1739.1999.97470.x>
- Ghanbarifardi M, Gut C, Gholami Z, Esmaeili HR, Gierl C, Reichenbacher B. Possible link between the structure of otoliths and amphibious mode of life of three mudskipper species (Teleostei: Gobioidae) from the Persian Gulf. *Zool Middle East.* 2020; 66(4):311–20. <https://doi.org/10.1080/09397140.2020.1805140>
- Granados-Amores E, Granados-Amores J, Zavala-Leal OI, Flores-Ortega JR. Geometric morphometrics in the *sulcus acusticus* of the *sagittae* otolith as tool to discriminate species of the genus *Centropomus* (Centropomidae: Perciformes) from the southeastern Gulf of California. *Mar Biodivers.* 2020; 50:e10. <https://doi.org/10.1007/s12526-019-01030-1>
- Gunz P, Mitteroecker P. Semilandmarks: a method for quantifying curves and surfaces. *Hystrix It J Mamm.* 2013; 24(1):103–109. <https://doi.org/10.4404/hystrix-24.1-6292>
- Hamer PA, Jenkins GP. Comparison of spatial variation in otolith chemistry of two fish species and relationships with water chemistry and otolith growth. *J Fish Biol.* 2007; 71(4):1035–55. <https://doi.org/10.1111/j.1095-8649.2007.01570.x>
- Hillis DM, Chambers EA, Devitt TJ. Contemporary methods and evidence for species delimitation. *Ichthyol Herpetol.* 2021; 109(3):895–903. <https://doi.org/10.1643/h2021082>
- Hoff NT, Dias JF, Zani-Teixeira ML, Correia AT. Spatio-temporal evaluation of the population structure of the bigtooth corvina *Isopisthus parvipinnis* from Southwest Atlantic Ocean using otolith shape signatures. *J Appl Ichthyol.* 2020; 36:439–50. <https://doi.org/10.1111/jai.14044>
- Hughes LC, Ortí G, Huang Y, Sun Y, Baldwin CC, Thompson AW, et al. Comprehensive phylogeny of ray-finned fishes (Actinopterygii) based on transcriptomic and genomic data. *Proc Natl Acad Sci U S A.* 2018; 115(24):6249–54. <https://doi.org/10.1073/pnas.1719358115>
- ICMBio. Livro vermelho da fauna brasileira ameaçada de extinção: Volume I/1. ed. Brasília: ICMBio; 2018.
- IUCN. 2020. The IUCN Red List of Threatened Species. Version 2020-1. Available at: www.iucnredlist.org. (Accessed: 19 March 2020).
- Jaramillo AM, Tombari AD, Benedito Durá V, Rodrigo Santamalia ME, Volpedo AV. Otolith eco-morphological patterns of benthic fishes from the coast of Valencia (Spain). *Thalassas.* 2014; 30(1):57–66.
- Jónsson EP, Campana SE, Sólmundsson J, Jakobsdóttir KB, Bárðarson H. The effect of growth rate on otolith-based discrimination of cod (*Gadus morhua*) ecotypes. *PLoS One.* 2021; 16(9):e0247630. <https://doi.org/10.1371/journal.pone.0247630>
- Kikuchi E, Cardoso LG, Canel D, Timi JT, Haimovici M. Using growth rates and otolith shape to identify the population structure of *Umbrina canosai* (Sciaenidae) from the Southwestern Atlantic. *Mar Biol Res.* 2021; 17(3):272–85. <https://doi.org/10.1080/17451000.2021.1938131>

- Klingenberg CP. MorphoJ: an integrated software package for geometric morphometrics. *Mol Ecol Resour.* 2011; 11:353–357. <https://doi.org/10.1111/j.1755-0998.2010.02924.x>
- Ladich F. Shut up or shout loudly: Predation threat and sound production in fishes. *Fish Fish.* 2022; 23(1):227–38. <https://doi.org/10.1111/faf.12612>
- Libungan LA, Pálsson S. ShapeR: An R package to study otolith shape variation among fish populations. *PLoS One.* 2015; 10(3):e0121102. <https://doi.org/10.1371/journal.pone.0121102>
- Lira AS, Lucena-Frédou F, Ménard F, Frédou T, Gonzalez JG, et al. Trophic structure of a nektonic community exploited by a multispecific bottom trawling fishery in Northeastern Brazil. *PLoS One.* 2021; 16(2):e0246491. <https://doi.org/10.1371/journal.pone.0246491>
- Lo PC, Liu SH, Chao NL, Nunoo FKE, Mok HK, Chen WJ. A multi-gene dataset reveals a New World origin and Oligocene diversification of croakers (Perciformes: Sciaenidae). *Mol Phylogenet Evol.* 2015; 88:132–43. <https://doi.org/10.1016/j.ympev.2015.03.025>
- Lombarte A, Chic Ò, Parisi-Baradad V, Olivella R, Piera J, García-Ladona E. A web-based environment for shape analysis of fish otoliths. The AFORO database. *Sci Mar.* 2006; 70:147–52. <https://doi.org/10.3989/scimar.2006.70n1147>
- Lombarte A, Cruz A. Otolith size trends in marine fish communities from different depth strata. *J Fish Biol.* 2007; 71(1):53–76. <https://doi.org/10.1111/j.1095-8649.2007.01465.x>
- Lombarte A, Palmer M, Matallanas J, Gómez-Zurita J, Morales-Nin B. Ecomorphological trends and phylogenetic inertia of otolith sagittae in Nototheniidae. *Environ Biol Fish.* 2010; 89:607–18. <https://doi.org/10.1007/s10641-010-9673-2>
- Luczkovich JJ, Dahle HJ, Hutchinson M, Jenkins T, Johnson SE, Pullinger RC, et al. Sounds of sex and death in the sea: Bottlenose dolphin whistles suppress mating. *Bioacoustics*, 2000; 10(4):323–34. <https://doi.org/10.1080/09524622.2000.9753441>
- Márquez-Velásquez V, Raimundo RLG, Rosa RS, Navia AF. The use of ecological networks as tools for understanding and conserving marine biodiversity. In: Ortiz M, Jordán F, editors. *Marine Coastal Ecosystems Modelling and Conservation*. Cham: Springer; 2021. p.179-202. https://doi.org/10.1007/978-3-030-58211-1_9
- Medeiros R, Oliveira CD, Souto D, Rangely J, Fabré NN. Growth stanza in fish life history using otoliths shape: the protandric *Centropomus* case (Carangaria: Centropomidae). *Neotrop Ichthyol.* 2021; 19(4):e200145. <https://doi.org/10.1590/1982-0224-2020-0145>
- Meek SE, Hildebrand SF. The marine fishes of Panama. Part II. Field Museum of Natural History Publications 226. Zoological Series 15. Chicago: Field Museum of Natural History; 1925.
- Pagel M. Inferring the historical patterns of biological evolution. *Nature.* 1999; 401:877–84. <https://doi.org/10.1038/44766>
- Pansard KCA, Gurgel HDCB, Andrade LCDA, Yamamoto ME. Feeding ecology of the estuarine dolphin (*Sotalia guianensis*) on the coast of Rio Grande do Norte, Brazil. *Mar Mammal Sci.* 2011; 27:673–87. <https://doi.org/10.1111/j.1748-7692.2010.00436.x>

- Passarone R, Aparecido KC, Eduardo LN, Lira AS, Silva LVSS, Justino AKS, et al. Ecological and conservation aspects of bycatch fishes: An evaluation of shrimp fisheries impacts in Northeastern Brazil. *Braz J Oceanogr.* 2019; 67:e19291. <https://doi.org/10.1590/s1679-87592019029106713>.
- Pavlov DA. Differentiation of three species of the genus *Upeneus* (Mullidae) based on otolith shape analysis. *Journal of Ichthyology*, 2016; 56(1):37–51. <https://doi.org/10.1134/S0032945216010094>
- Pavlov DA. Otolith morphology and relationships of several fish species of the suborder Scorpaenoidei. *J Ichthyol.* 2021; 61:33–47. <https://doi.org/10.1134/S0032945221010100>
- Pedraza-Marrón CR, Silva R, Deeds J, Van Belleghem SM, Mastretta-Yanes A, Domínguez-Domínguez O, et al. Genomics overrules mitochondrial DNA, siding with morphology on a controversial case of species delimitation. *Proc R Soc.* 2019; 286:e20182924 <https://doi.org/10.1098/rspb.2018.2924>
- Pinna PH, Fernandes DS, Passos P. “If you choose not to decide you still have made a choice”. *Bionomina*, 2018; 13:65–8. <https://doi.org/10.11646/bionomina.13.1.5>
- Popper AN, Fay RR. Rethinking sound detection by fishes. *Hear Res.* 2011; 273:25–36. <https://doi.org/10.1016/j.heares.2009.12.023>
- Popper AN, Ramcharitar J, Campana SE. Why otoliths? Insights from inner ear physiology and fisheries biology. *Mar Freshw Res.* 2005; 56:497–504. <https://doi.org/10.1071/MF04267>
- Popper AN, Schilt CR. Hearing and acoustic behavior: basic and applied considerations. In: Webb JF, Fay RR, Popper AN, editors. *Fish Bioacoustics*. New York: Springer; 2008. p.17–48. https://doi.org/10.1007/978-0-387-73029-5_2
- R Core Team. R: A language and environment for statistical computing. [internet] R Foundation for Statistical Computing. 2020. Available from: <https://www.R-project.org/>
- Ramcharitar J, Gannon DP, Popper AN. Bioacoustics of fishes of the family Sciaenidae (Croakers and Drums). *Trans Am Fish Soc.* 2006; 135:1409–31. <https://doi.org/10.1577/T05-207.1>
- Ramcharitar JU, Higgs DM, Popper AN. Sciaenid inner ears: a study in diversity. *Brain Behav Evol.* 2001; 58:152–62. <https://doi.org/10.1159/000047269>
- Ramirez-Perez JS, Quinonez-Velazquez C, Garcia-Rodriguez FJ, Felix-Uraga R, Melo-Barrera FN. Using the shape of sagitta otoliths in the discrimination of phenotypic stocks in *Scomberomorus sierra* (Jordan and Starks, 1895). *J Fish Aquat Sci.* 2010; 5(2):82–93. <https://doi.org/10.3923/jfas.2010.82.93>
- Rodrigues VLA, Wedekin LL, Marcondes MCC, Barbosa L, Farro APC. Diet and foraging opportunism of the Guiana dolphin (*Sotalia guianensis*) in the Abrolhos Bank, Brazil. *Mar Mamm Sci.* 2020; 36(2):436–50. <https://doi.org/10.1111/mms.12656>
- Rohlf FJ, Archie JW. A comparison of Fourier methods for the description of wing shape in mosquitoes (Diptera: Culicidae). *Syst Biol.* 1984; 33(3):302–17. <https://doi.org/10.2307/2413076>

- Rohlf FJ. tpsDig2 v.2.27. State University of New York at Stony Brook. 2017a
- Rohlf FJ. tpsRelw, v. 1.69. State University of New York at Stony Brook. 2017b
- Rohlf FJ. tpsUtil v.1.69. State University of New York at Stony Brook. 2021
- Santos JA, Oliveira RL, Guedes APP, Santos ACA, Moraes LE. Do macrophytes act as restaurants for fishes in a tropical beach? An approach using stomach content and prey availability analyses. *Reg Stud Mar Sci.* 2021; 47: e101920. <https://doi.org/10.1016/j.rsma.2021.101920>
- Sasaki K. Phylogeny of the family Sciaenidae, with notes on its zoogeography (Teleostei, Perciformes). *Memoirs of the Faculty of Fisheries Sciences.* 1989; 36(1/2):1–137. <https://doi.org/10.1007/BF02905681>
- Schneider C, Rasband W, Eliceiri K. NIH Image to ImageJ: 25 years of image analysis. *Nat Methods* 2012; 9:671–75. <https://doi.org/10.1038/nmeth.2089>
- Schulz-Mirbach T, Ladich F, Plath M, Heß M. Enigmatic ear stones: What we know about the functional role and evolution of fish otoliths. *Biol Rev.* 2019; 94:457–82. <https://doi.org/10.1111/brv.12463>
- Schwarzhan W. A comparative morphological treatise of recent and fossil otoliths of the family Sciaenidae (Perciformes). *Piscium Catalogus, Otolithi Piscium*, 1993; 1:1-245.
- Secchi ER, Botta S, Wiegand MM, Lopez LA, Fruet PF, Genoves RC, et al. Long-term and gender-related variation in the feeding ecology of common bottlenose dolphins inhabiting a subtropical estuary and the adjacent marine coast in the western South Atlantic. *Mar Biol Res.* 2017; 13(1):121–34. <https://doi.org/10.1080/17451000.2016.1213398>
- Secchi ER, Cremer MJ, Danilewicz D, Lailson-Brito J. A synthesis of the ecology, human-related threats and conservation perspectives for the endangered Franciscana dolphin. *Front Mar Sci.* 2021; 8:e617956. <https://doi.org/10.3389/fmars.2021.617956>
- Silva TF, Schneider H, Sampaio I, Angulo A, Brito MFG, Santos ACA, et al. Phylogeny of the subfamily Stelliferinae suggests speciation in *Ophioscion* Gill, 1863 (Sciaenidae: Perciformes) in the western South Atlantic. *Mol Phylogenet Evol.* 2018; 125:51–61. <https://doi.org/10.1016/j.ympev.2018.03.025>
- Taylor MD, Fowler AM, Suthers IM. Insights into fish auditory structure–function relationships from morphological and behavioural ontogeny in a maturing sciaenid. *Mar Biol.* 2020; 167:e21. <https://doi.org/10.1007/s00227-019-3619-9>
- Tellechea JS, Perez W, Olsson D, Lima M, Norbis W. Feeding habits of franciscana dolphins (*Pontoporia blainvillei*): echolocation or passive listening? *Aq Mamm.* 2017; 43(4):430–38. <https://doi.org/10.1578/AM.43.4.2017.430>
- Trewavas E. The sciaenid fishes (croakers or drums) of the Indo-West-Pacific. *Trans Zool Soc London.* 1977; 33:253–541. <https://doi.org/10.1111/j.1096-3642.1977.tb00052.x>
- Tuset VM, Farré M, Otero-Ferrer JL, Vilar A, Morales-Nin B, Lombarte A. Testing otolith morphology for measuring marine fish biodiversity. *Mar Freshw Res.* 2016a; 67:1037–48. <https://doi.org/10.1071/MF15052>

- Tuset VM, Otero-Ferrer JL, Gómez-Zurita J, Venerus LA, Stransky C, Imondi R, et al. Otolith shape lends support to the sensory drive hypothesis in rockfishes. *J Evol Biol*, 2016b; 29:2083–97. <https://doi.org/10.1111/jeb.12932>
- Tuset VM, Otero-Ferrer JL, Siliprandi C, Manjabacas A, Marti-Puig P, Lombarte A. Paradox of otolith shape indices: routine but overestimated use. *Can J Fish Aquat Sci*. 2021; 78(6):681–92. <https://doi.org/10.1139/cjfas-2020-0369>
- Tuset VM, Rosin PL, Lombarte A. Sagittal otolith shape used in the identification of fishes of the genus *Serranus*. *Fish Res*. 2006; 81:316–25. <https://doi.org/10.1016/j.fishres.2006.06.020>
- Venables WN, Ripley BD. *Modern Applied Statistics with S*. 4th ed. New York: Springer; 2002. <https://doi.org/10.1007/978-0-387-21706-2>
- Vignon M, Morat F. Environmental and genetic determinant of otolith shape revealed by a nonindigenous tropical fish. *Mar Ecol Prog Ser*. 2010; 411:231–41. <https://doi.org/10.3354/meps08651>
- Volpedo AV, Echeverría DD. Ecomorphological patterns of the sagitta in fish on the continental shelf off Argentine. *Fish Res*. 2003; 60(2-3):551–60. [https://doi.org/10.1016/S0165-7836\(02\)00170-4](https://doi.org/10.1016/S0165-7836(02)00170-4)
- Volpedo AV, Fuchs DV. Ecomorphological patterns of the lapilli of Paranoplatense Siluriforms (South America). *Fish Res*. 2010; 102(1-2):160–65. <https://doi.org/10.1016/j.fishres.2009.11.007>
- Wong JY, Chu C, Chong VC, Dhillon SK, Loh KH. Automated otolith image classification with multiple views: an evaluation on Sciaenidae. *J Fish Biol*. 2016; 89(2):1324–44. <https://doi.org/10.1111/jfb.13039>
- Zischke MT, Litherland L, Tilyard BR, Stratford NJ, Jones EL, Wang YG. Otolith morphology of four mackerel species (*Scomberomorus* spp.) in Australia: Species differentiation and prediction for fisheries monitoring and assessment. *Fish Res*. 2016; 176:39–47. <https://doi.org/10.1016/j.fishres.2015.12.003>

Table captions

Tab. 1. Number of specimens analyzed per site and their size by species.

Species	Sites			Body length	
	Itaparica	Porto Seguro	Caravelas	Mean \pm SD	Range
<i>Stellifer gomezi</i>	21	9	-	67.24 \pm 14.31	46.43-111 mm
<i>Stellifer menezesi</i>	15	15	-	65.50 \pm 15.05	38.57-99.98 mm
<i>Stellifer punctatissimus</i>	4	12	1	60.45 \pm 20.32	35.33-109 mm

Figure captions

Fig. 1. A. Map of the study area highlighting the sampling sites in the Bahia state. B. Specimens of the species studied. Top: *Stellifer gomezi*; Middle: *S. gomezi*; Bottom: *S. punctatissimus* (Scale bars = 10 mm).

Fig. 2. Illustration of representative sagitta otolith. Filled dots = landmarks, empty circles = semilandmarks; A = anterior, M = medial, D = dorsal; **sulcus acusticus* = *ostium* + *cauda*.

Fig. 3. Otoliths of *Stellifer punctatissimus* complex. A. *S. gomezi*. B. *S. menezesi*. C. *S. punctatissimus*. Left: Inner face, Right: Dorsal view. Arrow indicates spout-like groove; asterisk indicates projection on the outer face (Scale bars = 1 mm).

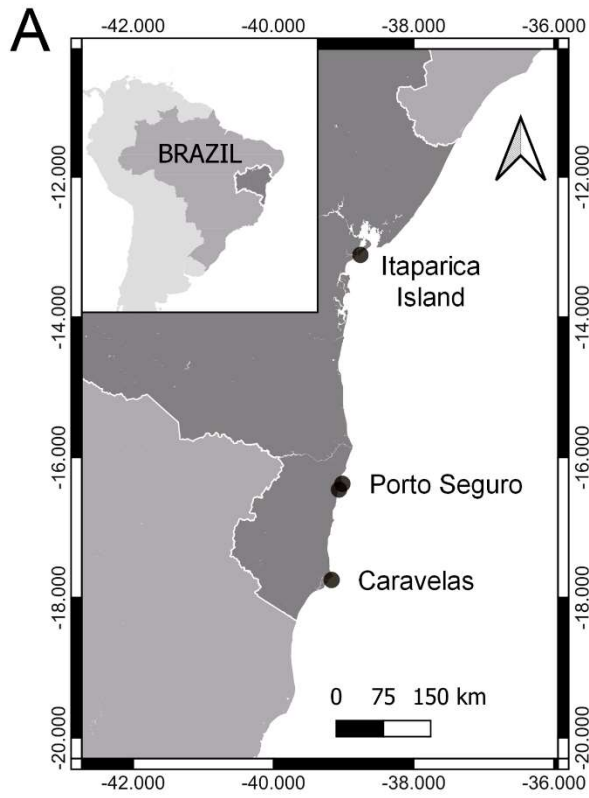
Fig. 4. Boxplot of shape indices by species. GM = *S. gomezi*, MN = *S. menezesi*, PC = *S. punctatissimus*.

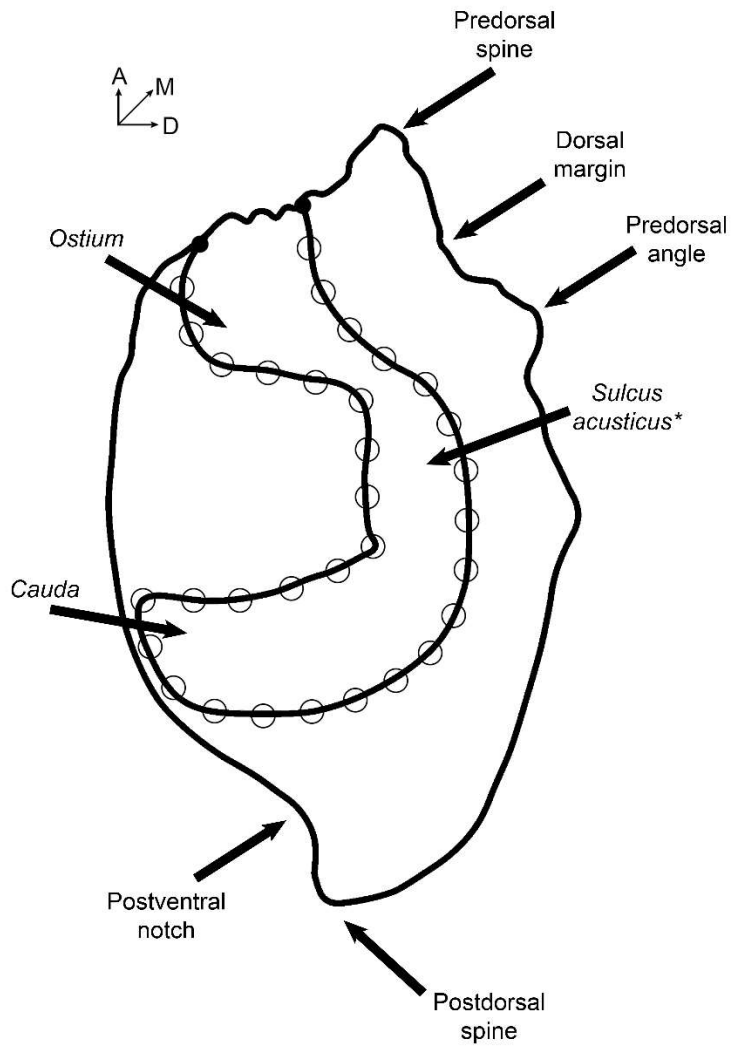
Fig. 5. Scatterplot of rectangularity indice. GM = *S. gomezi*, MN = *S. menezesi*, PC = *S. punctatissimus*.

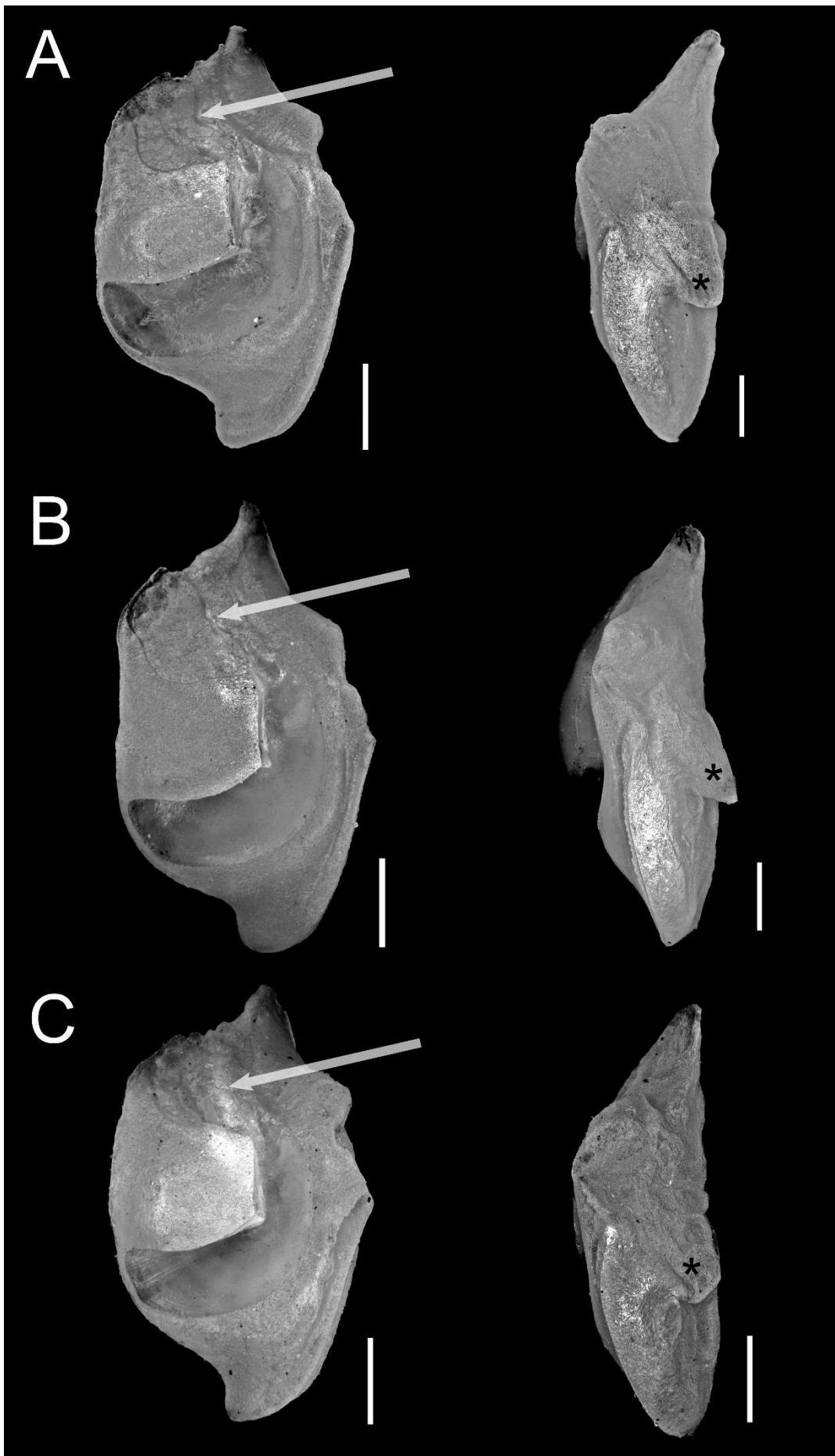
Fig. 6. Otolith's outline reconstruction (wavelet) and its angle. GM = *S. gomezi*, MN = *S. menezesi*, PC = *S. punctatissimus*.

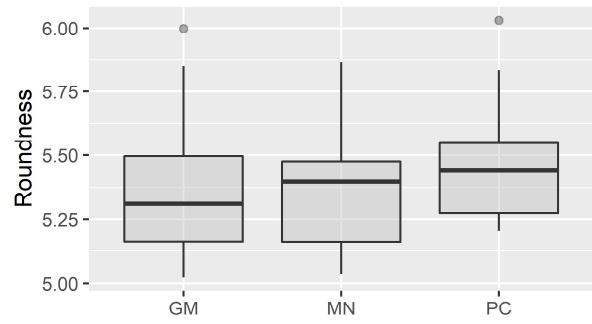
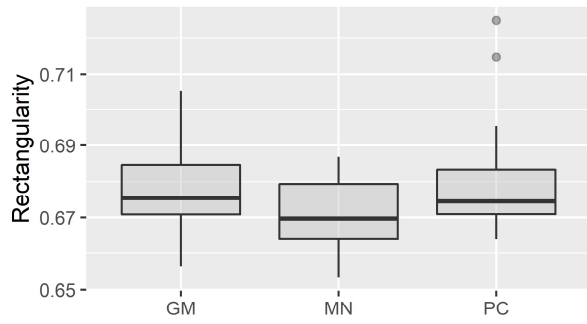
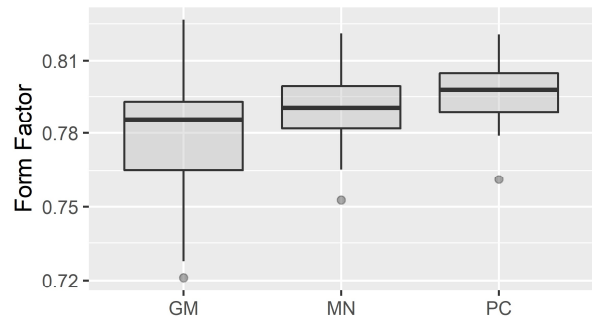
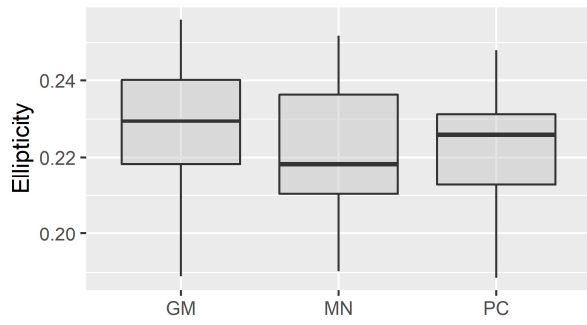
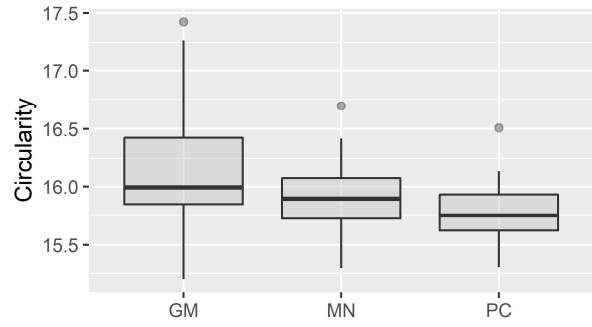
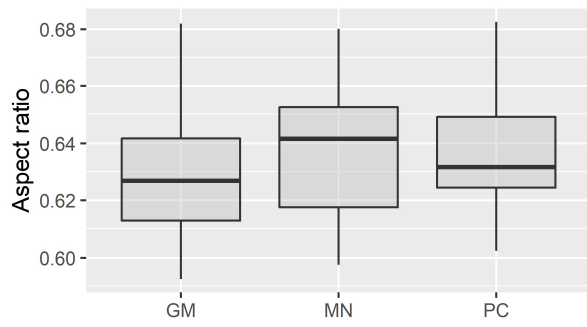
Fig. 7. Linear Discriminant Analysis (LDA) of outline shape accordingly to elliptical Fourier descriptors (EFDs). GM = *S. gomezi*, MN = *S. menezesi*, PC = *S. punctatissimus*.

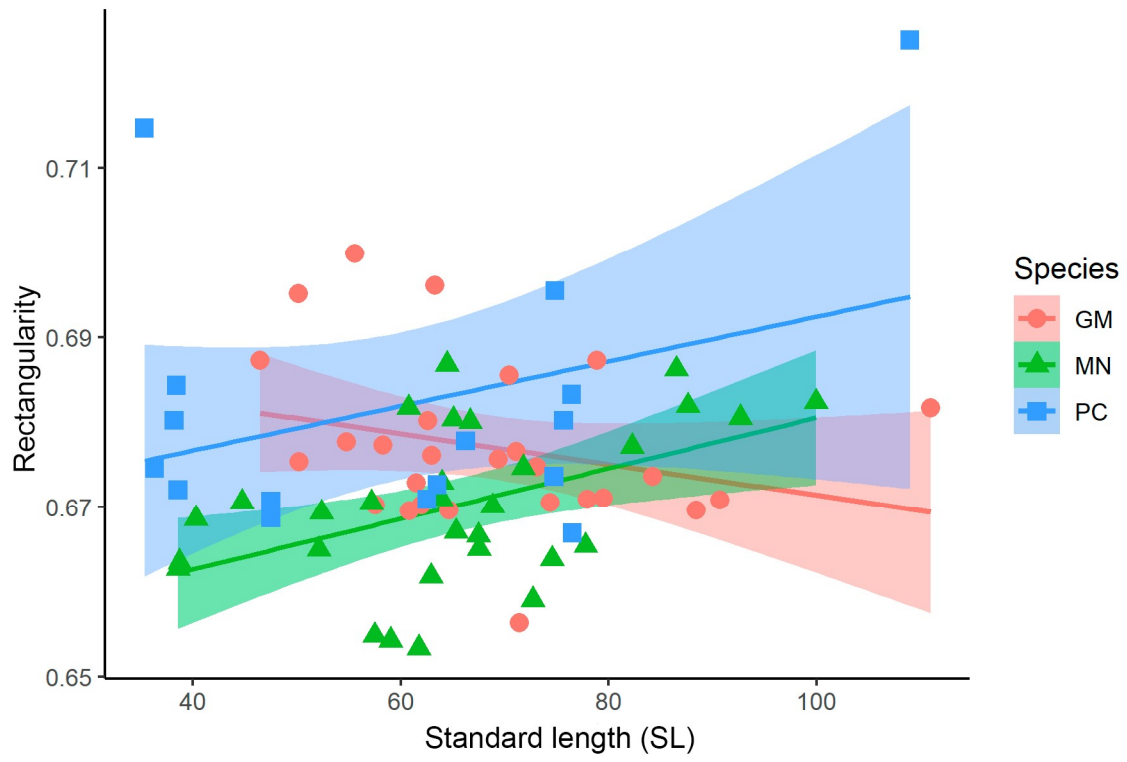
Fig. 8. A. Biplot resulting from Principal Component Analysis (PCA) of *sulcus acusticus*'s shape variation using geometric morphometric data (GMM). B. Shape variation in each principal component, PC1 in the horizontal and PC2 in the vertical. GM = *S. gomezi*, MN = *S. menezesi*, PC = *S. punctatissimus*.

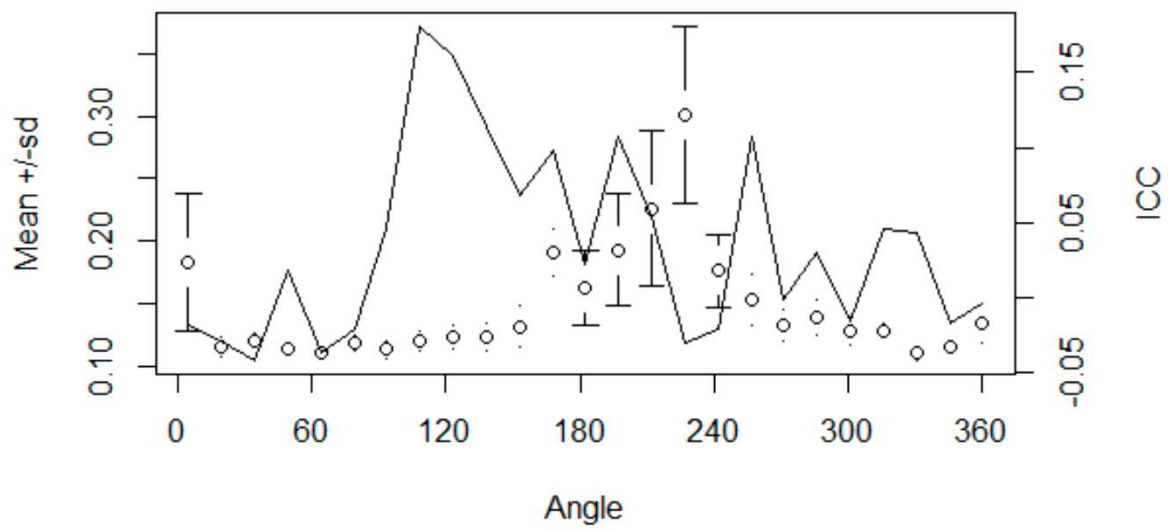
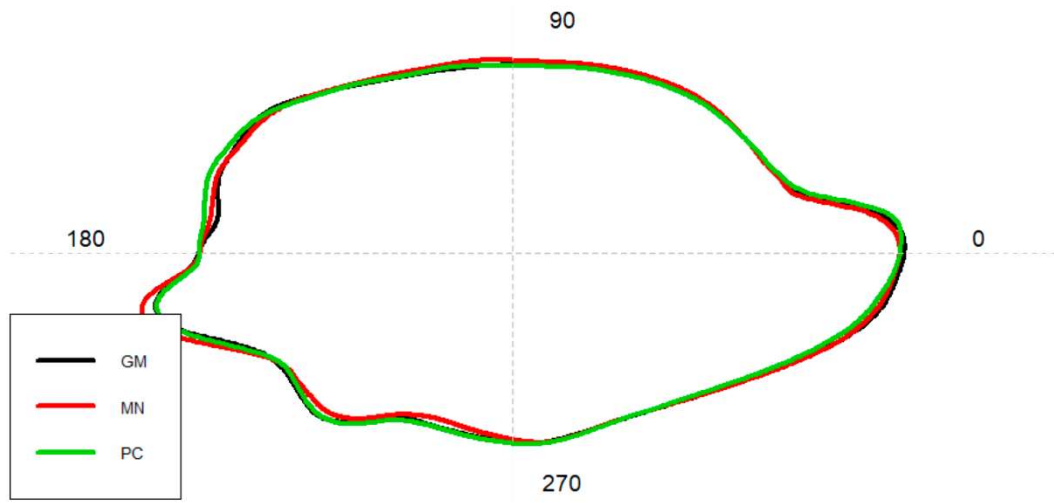


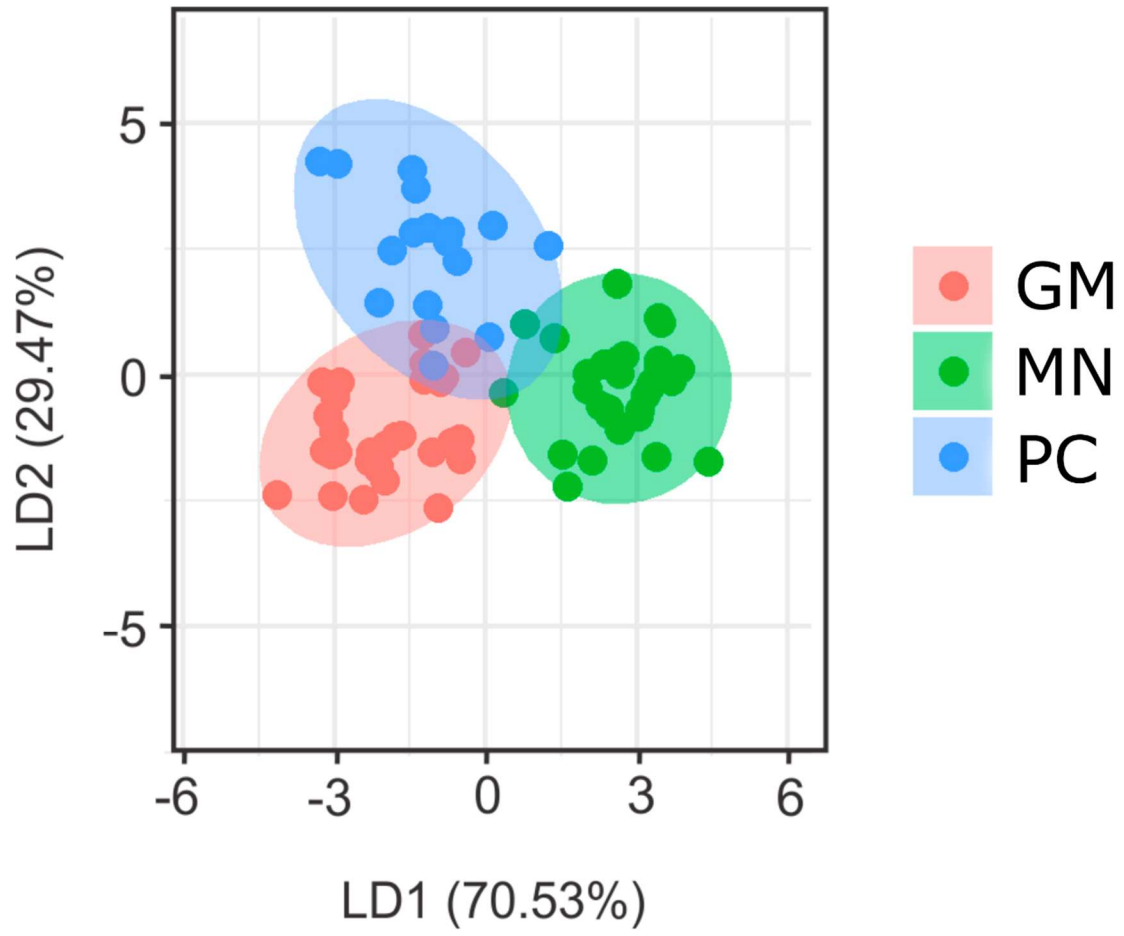


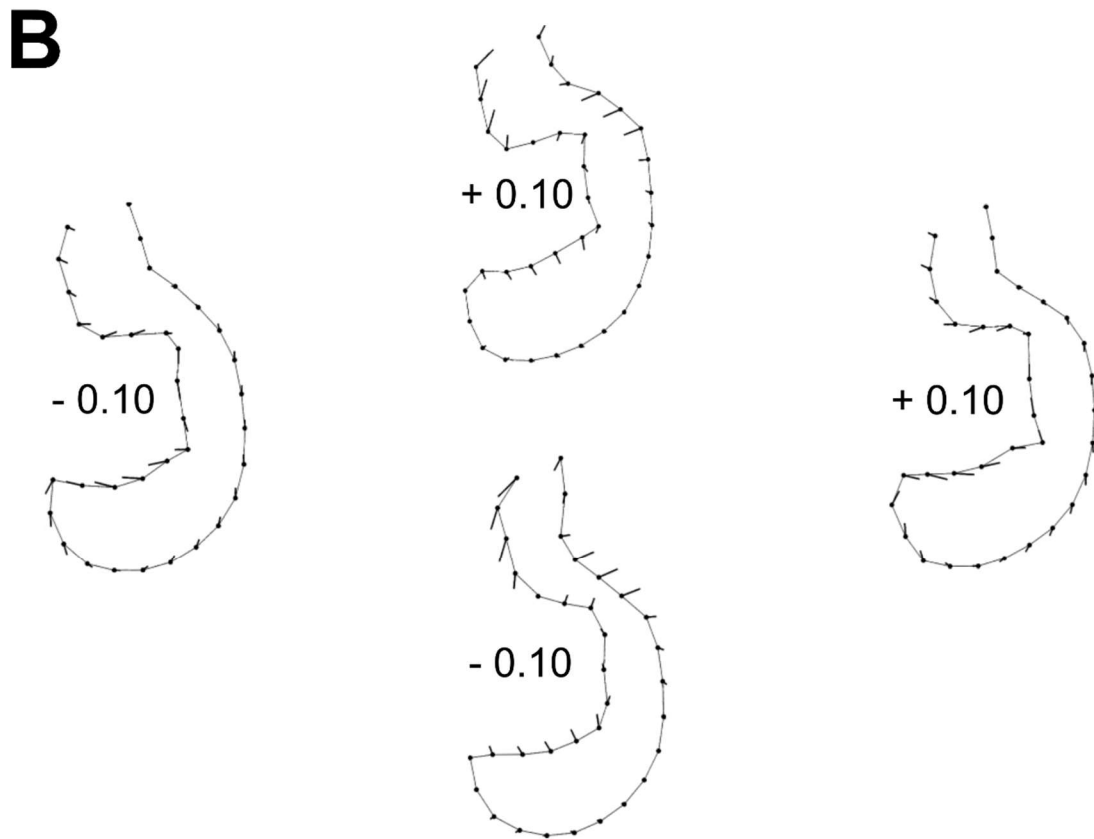
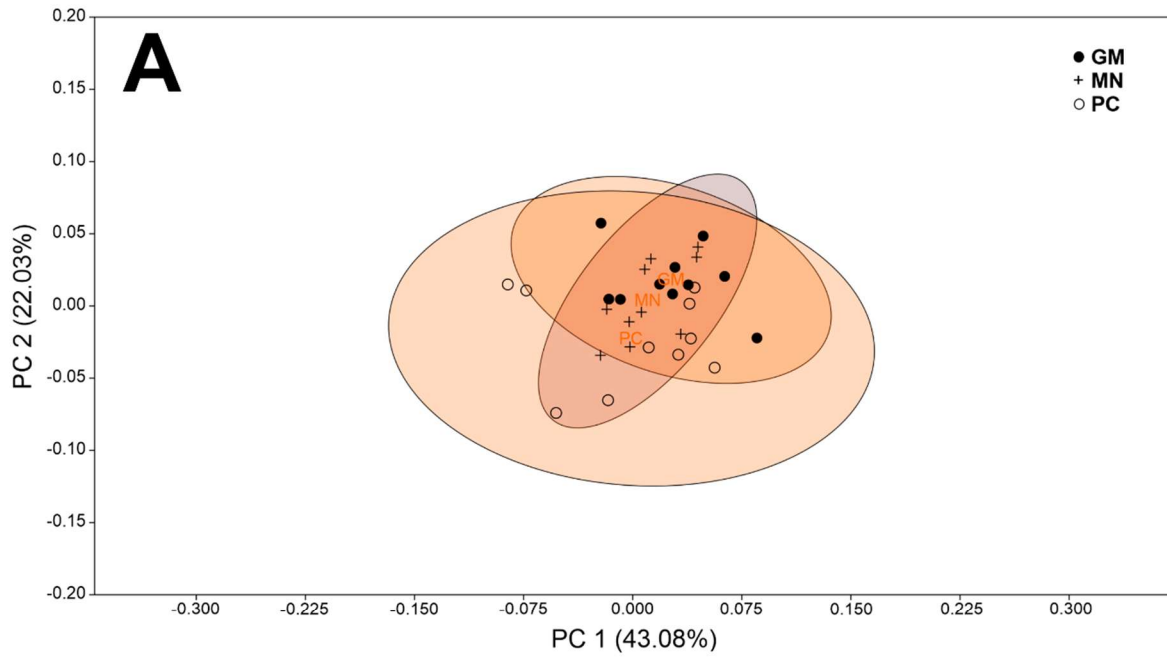












3 CONCLUSÕES

A descoberta de padrões ou variações no dimorfismo sexual e em alometria confirma que o déficit Linneano limita as ações futuras, como o avanço do conhecimento da biodiversidade e avaliação de estado de conservação. No início do século XX, o status taxonômico de *Stellifer punctatissimus* (Meek & Hildebrand, 1925) era restrito à resumida descrição. Posteriormente, o que na verdade se tratava de juvenis de *S. punctatissimus* foi descrito como outra espécie. Aqui mostramos que, dentro do complexo de espécies, existe uma distinção entre os juvenis e os adultos, incluindo os padrões de crescimento de estruturas de forma não linear. A junção dos resultados mostra que, como muitas vezes retratado em espécies crípticas, o formato do corpo recupera essa grande similaridade (i.e., baixa disparidade fenotípica) na morfologia externa. Através da análise de padrões alométricos e de dimorfismo, conseguimos detectar variações que indicam três espécies distintas nesse complexo.

Comparativamente, o mesmo pode ser analisado através do formato e morfologia dos otólitos. Eles mostram muita similaridade em métodos de baixa resolução (e.g., índices de forma), ao passo que, em métodos mais refinados, como morfometria geométrica e descritores de Fourier, notam-se variações mais finas que confirmam a hipótese de três espécies no complexo. Apesar da baixa resolução dos índices de forma, eles também indicam, assim como os padrões alométricos no formato do corpo, padrões divergentes entre as espécies. A descrição morfológica também adiciona evidências que auxiliam na distinção entre as espécies, mas que, por serem compartilhadas com espécies viventes e fósseis, tanto do Atlântico quanto do Pacífico, podem também funcionar em análises de reconstrução do estado ancestral, auxiliando, assim, a resolução de outros déficits, como o Darwiniano (i.e., resolução do processo evolutivo em filogenias).

A análise conjunta de diversos métodos em formato do corpo e otólitos se mostrou eficiente em representar os padrões dentro do complexo e auxiliou na resolução taxonômica, por demonstrar que são realmente espécies distintas, apesar da baixa disparidade fenotípica, especialmente entre *Stellifer menezesi* e *Stellifer gomezi*. Isso está de acordo com outros casos de espécies crípticas e outras que mostram conservantismo morfológico.

APÊNDICE

Five new species of Western Atlantic stardrums, *Stellifer* (Perciformes: Sciaenidae) with a key to Atlantic *Stellifer* species

NING LABBISH CHAO¹, ALFREDO CARVALHO-FILHO² & JONAS DE ANDRADE SANTOS^{3*}

1National Museum of Marine Biology, Pingtung, Taiwan; Bio-Amazonia Conservation International, Brookline, MA, USA.

https://orcid.org/0000-0002-0474-8740

2Fish Bizz Ltda, R. D. Maria Garcez, n. 39, 05424-070, Pinheiros, São Paulo, Brazil.

https://orcid.org/0000-0002-2903-7355

3Programa de Pós-Graduação em Ciências Biológicas (Zoologia) - Laboratório de Ictiologia, Departamento de Sistemática e Ecologia, Universidade Federal da Paraíba, João Pessoa, PB, Brazil. https://orcid.org/0000-0001-9245-1121

***Corresponding author: jonasandradebio@gmail.com**

Zootaxa 4991 (3): 434–466. <https://doi.org/10.11646/zootaxa.4991.3.2>

** A formatação original da publicação foi ligeiramente alterada para acomodar as regras de formatação da UFPB.

Five new species of Western Atlantic stardrums, *Stellifer* (Perciformes: Sciaenidae) with a key to Atlantic *Stellifer* species

NING LABBISH CHAO¹, ALFREDO CARVALHO-FILHO² & JONAS DE ANDRADE SANTOS^{3*}

¹National Museum of Marine Biology, Pingtung, Taiwan; Bio-Amazonia Conservation International, Brookline, MA, USA.

<https://orcid.org/0000-0002-0474-8740>

²Fish Bizz Ltda, R. D. Maria Garcez, n. 39, 05424-070, Pinheiros, São Paulo, Brazil. <https://orcid.org/0000-0002-2903-7355>

³Programa de Pós-Graduação em Ciências Biológicas (Zoologia) - Laboratório de Ictiologia, Departamento de Sistemática e Ecologia, Universidade Federal da Paraíba, João Pessoa, PB, Brazil. <https://orcid.org/0000-0001-9245-1121>

*Corresponding author: jonasandradebio@gmail.com

Abstract

Five new species of *Stellifer* are described from the Caribbean Sea and tropical southwestern Atlantic. Among the previously recognized stelliferine genera, *Stellifer* is unique by having a pair of variably developed appendages on the posterior margin of the anterior gas chamber, which is lacking in *Bairdiella*, *Corvula*, *Elattarchus*, *Odontoscion* and *Ophioscion*. However, recent genetic studies indicated that *Stellifer* and *Ophioscion* are not monophyletic. The genus *Ophioscion* Gill, 1863 is recognized herein as a junior synonym of *Stellifer* Oken, 1817. Of the five new species described, *Stellifer cervigoni* n. sp., *S. collettei* n. sp., and *S. musicki* n. sp. have a pair of knob-like diverticula along the posterior margin of the anterior gas chamber, which is absent in *S. macallisteri* n. sp., and *S. menezesi* n. sp. *Stellifer cervigoni* n. sp. is found along the southern Caribbean coast of Colombia and Venezuela; it can be distinguished from other species by having a jet-black roof of mouth and inner opercular lining. *Stellifer collettei* n. sp. is found from Surinam to southeastern Brazil, while *S. musicki* n. sp. is endemic to northern Brazil. *Stellifer macallisteri* n. sp. has an oblique, terminal mouth and it is found in Colombia, Venezuela and Dominican Republic. *Stellifer menezesi* n. sp. has a subterminal mouth and is found from northeastern to southeastern Brazil. These results bring the number of valid species of *Stellifer* in the Atlantic to 18, and a key to the identification of these species is included.

Key words: Cryptic species, Taxonomy, Stelliferinae, *Ophioscion*, West Atlantic

Introduction

Sciaenidae is a large family in the order Perciformes, with nearly 300 species distributed in about 70 genera worldwide (Chao *et al.* 2015; Parenti 2020; Fricke *et al.* 2021). The subfamily Stelliferinae (Sasaki 1989), or the *Stellifer*-group (Chao 1978), is endemic to the Americas and comprises the genera *Bairdiella*, *Corvula*, *Elattarchus*, *Odontoscion*, *Ophioscion* and *Stellifer*. These genera are unique in having a two-chambered gas-bladder (Fig. 1), the anterior one yoke-shaped and the posterior one carrot-shaped, and two of the three otoliths (sagitta & lapillus) are enlarged (Fig. 2) (Chao 1978). Sasaki (1989) listed seven additional synapomorphies for the subfamily Stelliferinae: auditory bulla notched-*Stellifer* type; exoccipital condyles not broadly joined to each other-*Stellifer* type; basioccipital projecting backwards-*Stellifer* type; Baudelot's ligament attached to exoccipital; retractor dorsalis originating from basicranial region and first vertebra; ventral modification of anterior abdominal vertebra-*Stellifer* type; sulcus head situated on anterior surface of sagitta.

The genus *Stellifer*, or stardrums, can be distinguished from other stelliferines by having an oval-elongate to quadrilateral shaped sagitta (Fig. 3B & C) and often with a pair of variably developed diverticula on the posterior margin of the anterior gas chamber (Fig. 1). The vertebral counts are 10 abdominal and 15 caudal in *Stellifer* and *Ophioscion*, 11+14 in *Bairdiella*, and 12+13 in *Corvula*, *Elattarchus*, and *Odontoscion* (Fig. 4). *Stellifer* is further distinguished from *Bairdiella*, *Elattarchus*, and *Odontoscion* by lacking large, sharp teeth on the jaws.

Molecular studies have shown that *Stellifer* forms a sister group with *Bairdiella* + (*Corvula* + *Odontoscion*)

(Vinson *et al.* 2004; Santos *et al.* 2013; Lo *et al.* 2015). Recent molecular studies indicate that *Stellifer* and *Ophioscion* are non-monophyletic genera (Santos *et al.* 2013; Barbosa *et al.* 2014; Lo *et al.* 2015; Silva *et al.* 2018). Barbosa *et al.* (2014) and Silva *et al.* (2018) found two distinct groups of *Stellifer* species. Herein, we consider all species of *Ophioscion* and *Stellifer* to be in a single clade, the genus *Stellifer*, based on the overlap of previously considered diagnostic characters and the non-monophyly of the genera in molecular studies.

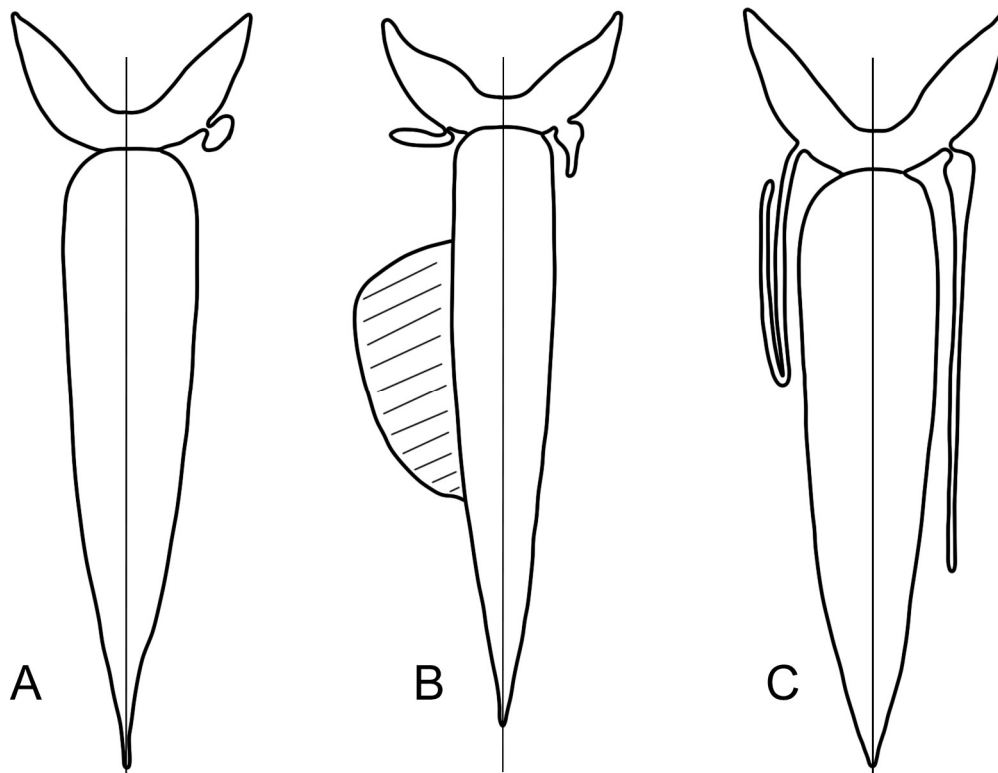


FIGURE 1. Two-chambered gas bladders of Stelliferinae, left & right halves represent different forms or taxa. A. left, *Bairdiella*, *Corvula*, *Elattarchus*, *Odontoscion* & *Stellifer* (*Ophioscion*); right, *S. naso* & *S. venezuelae*. B. left, *S. microps*, hatched area indicates drumming muscle patch; right, small knob-like such as *S. griseus*, *S. colonensis*, *S. lanceolatus*, etc. C. left, *S. brasiliensis*; right, *S. rastrifer*.

Stardrums are medium- to small-sized fishes and are abundant in fishery by-catch along the warm shallow coasts of the Americas. This paper describes five new species of *Stellifer* from the tropical western Atlantic, increasing the number of valid species from the region to 18. Of the 18, only one species, *S. lanceolatus* (Holbrook, 1855), occurs in the North America; the remaining are from the Caribbean Sea and South America. An artificial key to the Atlantic species of *Stellifer* is provided. Taxonomic remarks are included to clarify misidentified species or synonyms of *Stellifer*. A major range extension for *S. gomezii* (Cervigón, 2011), from Venezuela to Brazil, is recognized and a description based on Brazilian specimens is included. In the tropical Eastern Pacific, there are 13 species of *Stellifer* and six of *Ophioscion*, found from Chile to Mexico. We recognize potentially undescribed species of *Stellifer* from Peru, Panama, and Mexico.

Materials and methods

Specimens were deposited and examined from several museum collections. Museum collection acronyms follow Sabaj (2020). Methods of counting and measuring follow Hubbs & Lagler (2004), except as follows, and some specific terms for morphological structures of sciaenids follow Chao (1978; 2019) and Sasaki (1989).

Counts. Dorsal fin-ray counts, e.g. D. X+I, 20, indicates ten spines on the anterior portion of the dorsal fin, followed by a notch, and continued by one spine and 20 soft rays on the posterior portion. The pectoral-fin ray count excludes the one to three short axillary rays preceding the uppermost and longest ray. The gill-raker count is that of the first arch and includes rudimentary rakers. Counts are expressed numerically in the formula: number of rakers on

upper limb plus number of rakers on lower limb, which includes the raker straddling the angle of the arch. Lateral-line scale count is the number of scales perforated by lateral-line pores excluding those distal to the structural base of the caudal fin (hypural plate). Vertebral counts were based on radiographs of one to several specimens of every species included. The first vertebral centrum is ankylosed to the basioccipital and the urostyle was counted as the last centrum.

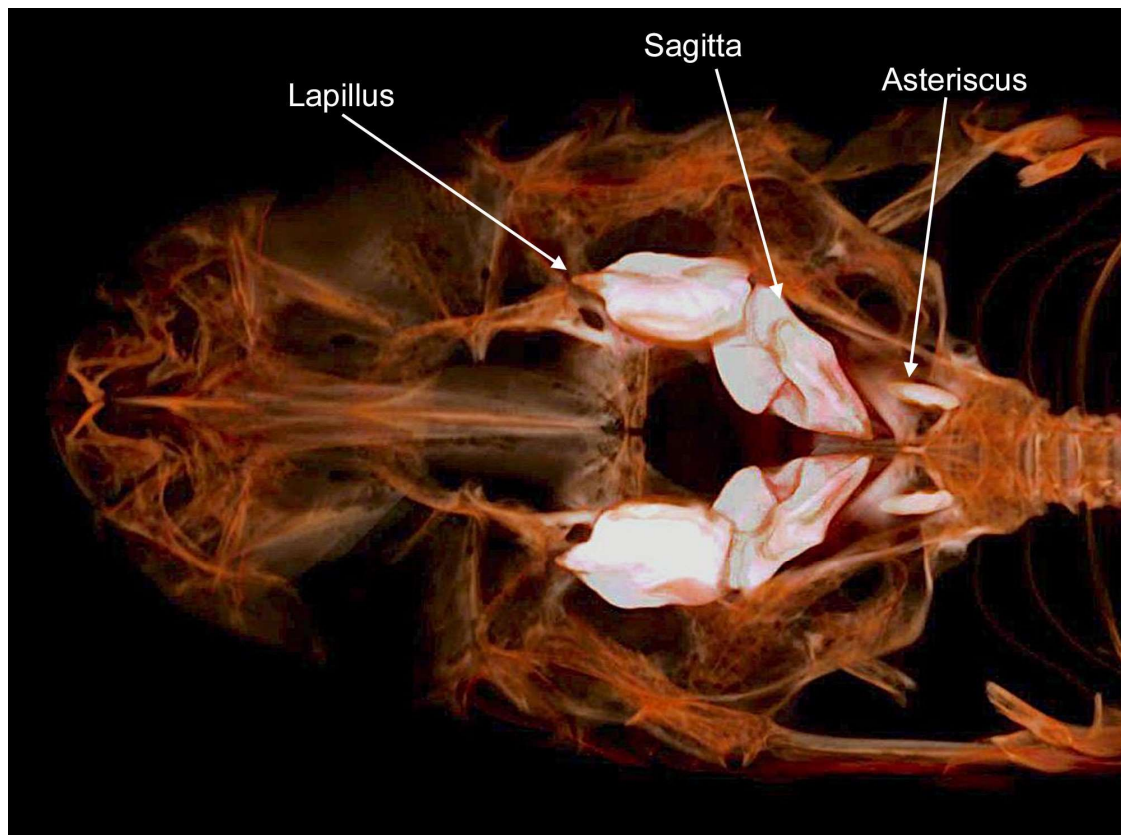


FIGURE 2. CT scan of the ventral region of the head of *Stellifer collettei* new species (paratype: MCZ 157278, 76.2 mm SL) showing the *in situ* positions of three pairs of otoliths; a large lapillus located anteriorly, a large triangular-shaped sagitta in the middle, and a thin asteriscus located post-laterally (CT Scan by Andrew Williston, MCZ, Harvard University).

Measurements. Lengths of all specimens are given as standard length (SL) and measurements are given in number of times in SL or head length (HL). All measurements were made with flat-pointed dividers and recorded to the nearest 1.0 mm or to the nearest 0.1 mm when the measured distance was less than 100 mm. The head length is the distance between the anterior most tip of the snout and the membranous hind edge of the opercular flap. The bony interorbital width is the distance across the frontal bone as measured with the divider points pressed lightly against its edges directly above the middle of the orbits. The body width is measured between the axillae of the pectoral fins. Maxilla length is measured from tip of snout to the posterior margin of the maxilla, while the upper-jaw length is measured from the tip of the premaxilla to the lower corner of the maxilla. Caudal-peduncle length is measured from the insertion of the anal fin to the middle of the posterior margin of the hypural plate.

Gas bladder. The anterior horn of the *Stellifer* gas bladder is often visible under the skin of upper gill cover anterior to the cleithrum. In order to examine the anterior chamber of the gas bladder and appendages, an extensive incision is often cut through the isthmus of the cleithrum. Gas bladders were extracted and illustrated with the position of the vent and anal fin origin indicated. Drumming muscles along the side of viscera (under the peritoneal membrane) were checked thoroughly as some are not conspicuous during non-spawning season or are absent in females (Fig. 1B, hatched area).

Otoliths. Otoliths were extracted by cutting through the cranial base from the upper end of the right gill cover. The three pairs of otoliths: the sagitta, lapillus, and asteriscus, were obtained from fresh specimens whenever possible. Illustrations were made using a camera lucida. A cranial CT scan radiograph of *Stellifer collettei* new species (Fig. 2) was taken at the MCZ (by Andrew Williston, Harvard University, with permission to use one time here). Otolith terminology follows Frizzell & Dante (1965) and Chao (1978).

Sensory pores on the head. Sensory pores at the tip of the snout and on the ventral region of the lower jaw (mandible) of *Stellifer* are the openings of well-developed cavernous lateral-line canals on the head (Chao 1978). Here, we followed the patterns of description of sensory pores based on Chao (1978).

Results

Genus *Ophioscion* Gill, 1863 as a junior synonym of *Stellifer* Oken, 1817

Gill (1863) designated the genus *Ophioscion* with the eastern Pacific species, *O. typicus* Gill, 1863, as the type species, which was distinguished only from *Bairdiella* by having an oblong head, a narrow and prominent snout with a small, inferior mouth. The gas bladder of *O. typicus* has two chambers, as present in all stelliferines, but lacks appendages on the hind margin of the anterior chamber (Fig. 1A, left). Chao (1978) distinguished the genus *Ophioscion* from *Stellifer*, by lacking a pair of variably developed appendages on the hind margin of the anterior chamber (Fig. 1). Sasaki (1989) incorrectly assigned the tooth plate on pharyngobranchial 2, enlarged and anteriorly located, as an autapomorphic character of *Ophioscion*; when in fact they share this derived condition with other closely related genera (e.g. *Bairdiella*), and this should be considered a homoplasy. Additionally, Sasaki added the medially concave ventral margin of the palatine as an autapomorphy of *Stellifer*. Therefore, the morphological features separating the current *Stellifer* genus from other genera within Stelliferinae are the enlarged lapillus that is about the same size of the oval shaped sagittal otoliths (Fig. 2) vs. shorter and triangular in *Bairdiella*, *Corvula*, *Elattarchus* and *Odontoscion* (Fig. 3), and the vertebral counts of 10 abdominal and 15 caudal in *Stellifer* (*Ophioscion*), vs. either 12+13 or 11+14 in other stelliferine genera (Fig. 4). Recent molecular studies (Santos *et al.* 2013; Barbosa *et al.* 2014; Lo *et al.* 2015; Silva *et al.* 2018) have confirmed that Stelliferinae is a monophyletic group, but the monophyly of *Ophioscion* and *Stellifer* are not supported. We agree with the suggestion of Silva *et al.* (2018) that *Ophioscion* is a junior synonym of *Stellifer*.

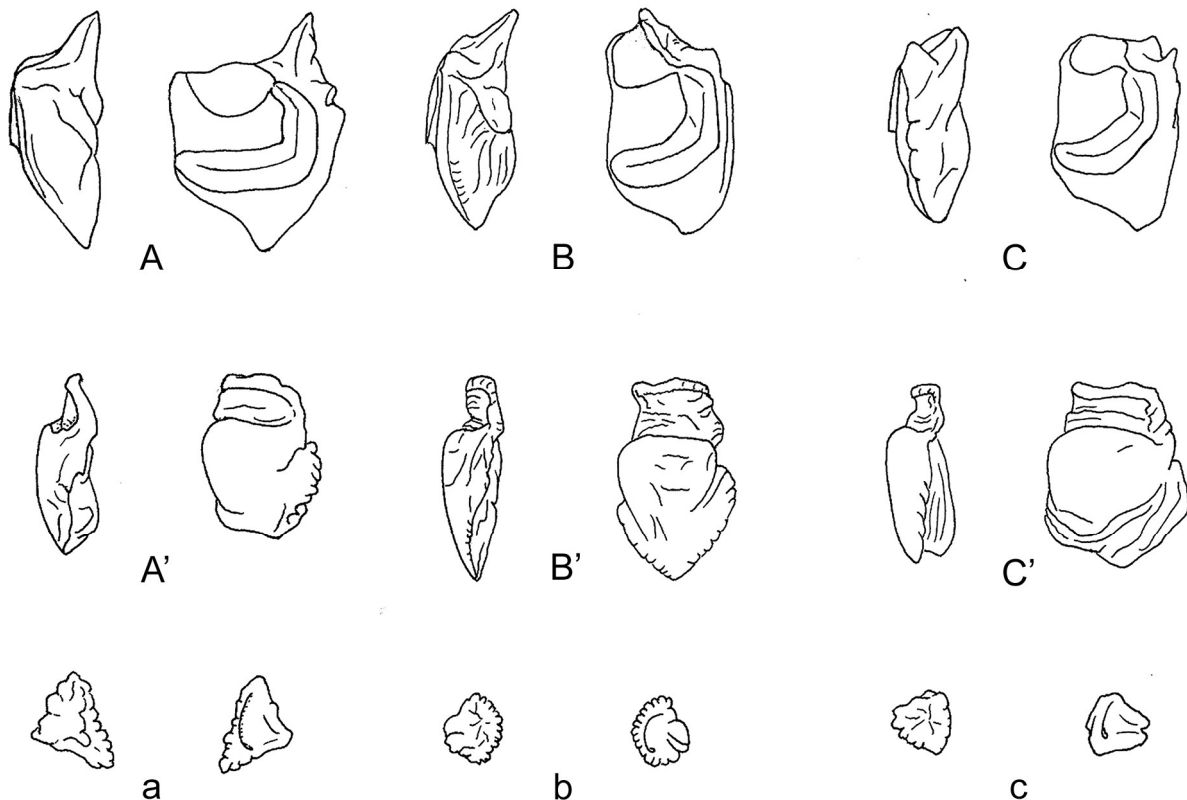


FIGURE 3. Otoliths of Stelliferinae. A. *Bairdiella chrysoura*. B. *Stellifer punctatissimus*. C. *Stellifer rastrifer*. A, B, C, Sagitta: left image, lateral view with medial surface facing to the left; right image, medial surface view. A', B', C', Lapillus: left image, lateral view with medial surface facing to the left; right image, medial surface view. a, b, c, Asteriscus: left image, lateral surface, right image, medial surface (otolith orientations follow *in situ* position in Fig. 2).

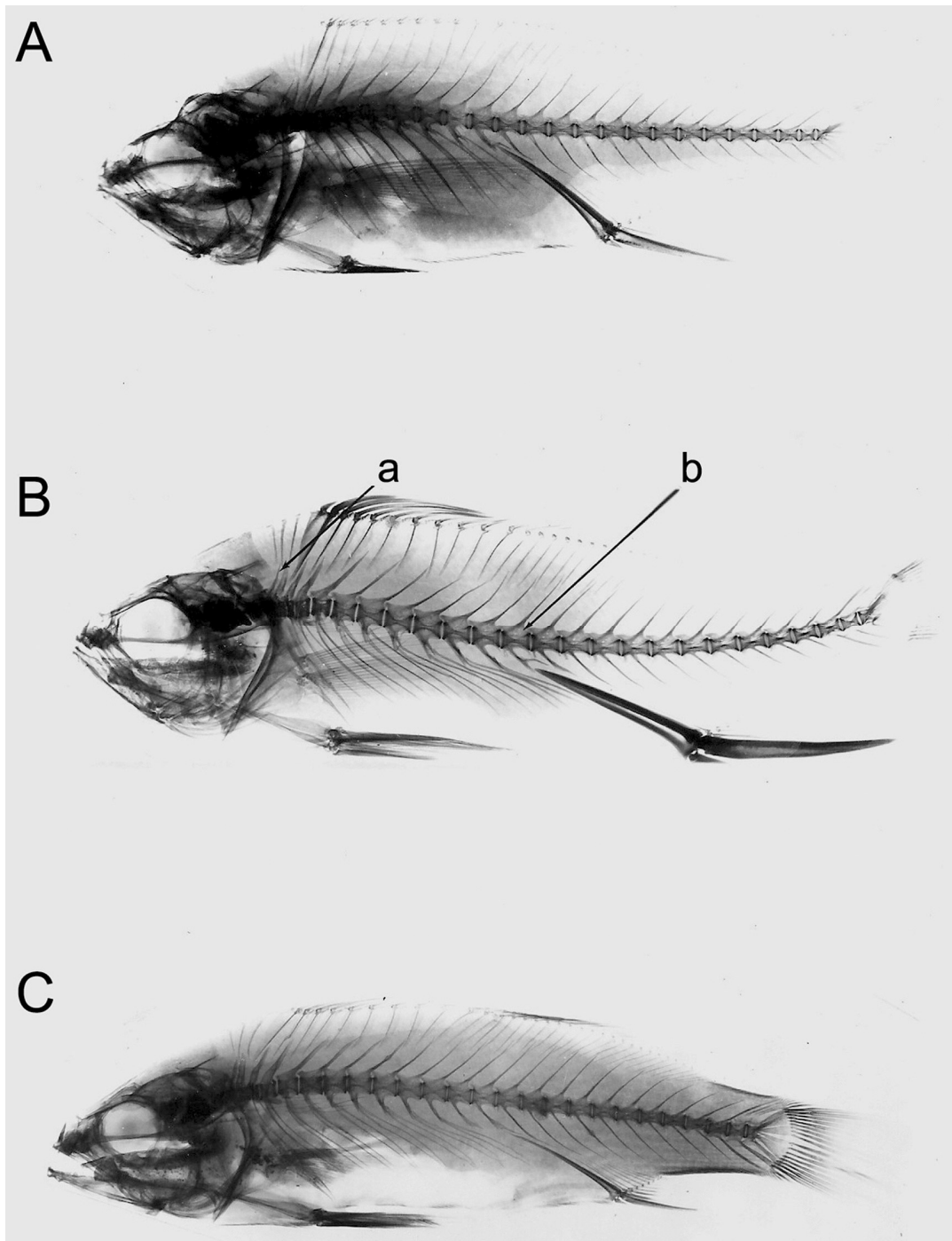


FIGURE 4. Stelliferinae vertebral columns with a total of 25 vertebrae (precaudal + caudal). A. *Bairdiella* (11+14); B. *Corvula*, *Elattarchus* & *Odontoscion* (12+13); C. *Stellifer* (10+15). a. indicates the first vertebrae; b. the first caudal vertebrae.

Synonyms and invalid names of nominal species of *Ophioscion* Gill, 1863

Corvina adusta Agassiz, 1831 is often referred to as *Ophioscion adustus* (Agassiz, 1831) (Chao 1978); it has a dorsal-ray count of 28, greater than all nominal species of *Ophioscion* and *Stellifer* (22–24 soft dorsal rays). The original color plate (70) in Agassiz (1831) shows that the specimen has an inferior mouth and a golden-colored back. The only Brazilian sciaenid with high soft dorsal ray counts (27–29), inferior mouth, and golden back is *Micropogonias furnieri* (Desmarest, 1823). We found that some specimens identified as *O. adustus* from Puerto Rico (e.g. USNM 50161, USNM 126188) are *Ophioscion punctatissimus* Meek & Hildebrand, 1925.

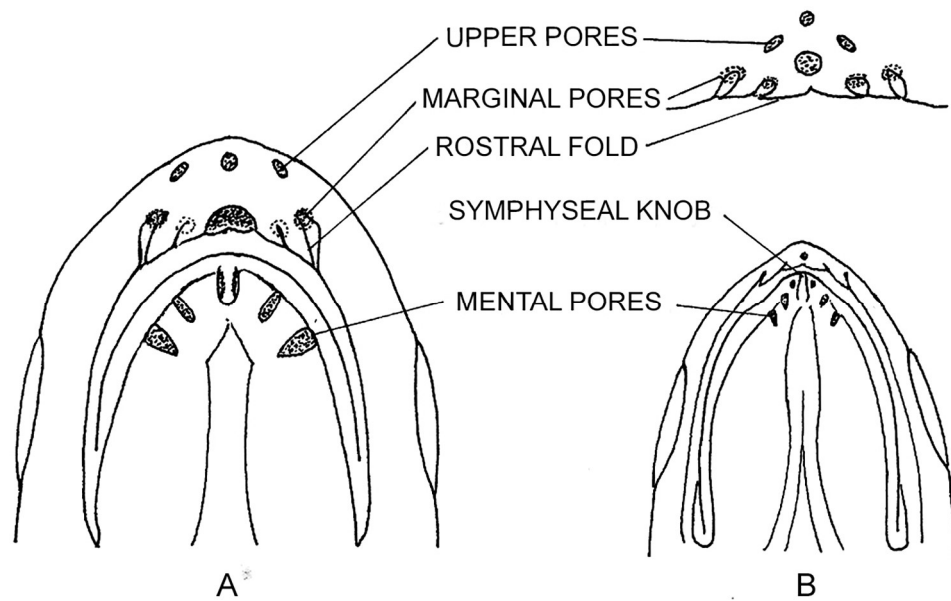


FIGURE 5. *Stellifer* sensory pore system at the tip of the snout and on the ventral region of the lower jaw. A. species with subterminal or inferior mouth; B. species with oblique mouth (front view of snout pores on top).

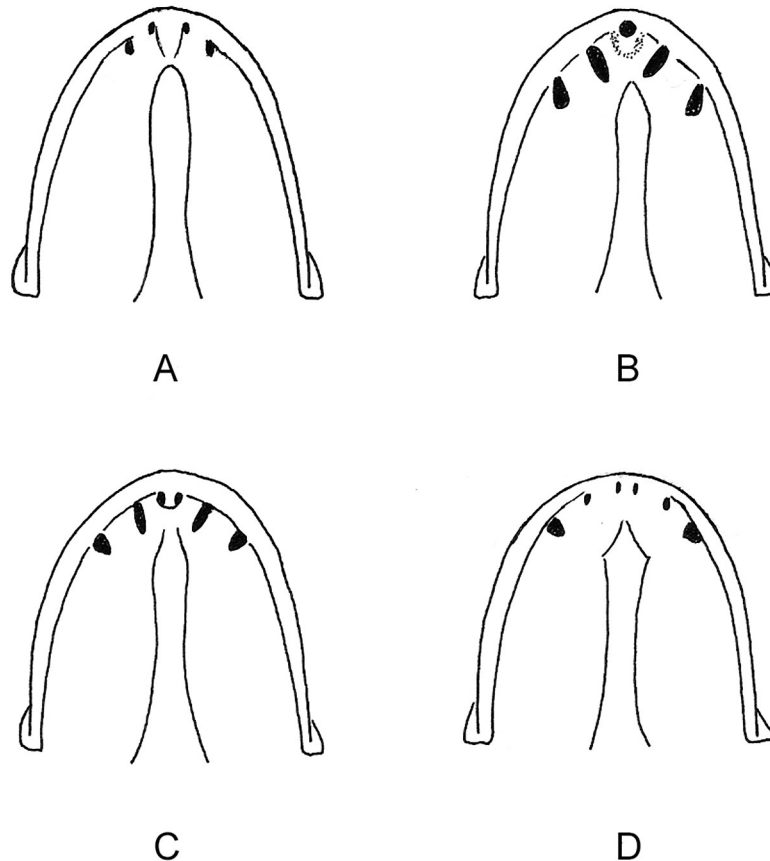


FIGURE 6. Mental pore patterns of *Stellifer* species. A. Four pores (*S. collettei* new species); B. Five pores (*S. stellifer*); C. Six pores with the medial pair set in a pit (*S. rastrifer*); D. Six pores (*S. colonensis*).

Corvina gillii Steindachner, 1867, was tentatively assigned as a synonym of *Ophioscion adustus* by Chao (1978). The original description was based on one specimen of 165 mm TL (6.5 inches) from La Plata River, Argentina (Steindachner 1867). Although the general description resembles a sciaenid, the combination of 16 soft dorsal-fin rays and seven anal-fin rays does not match any known sciaenid from the southwestern Atlantic. The

holotype cannot be located at NMW (pers. comm., Anja Palandacic). Therefore, *Corvina gillii* is considered a *nomen nudum*.

Sciaena unicirrata Larrañaga, 1923 from Uruguay was included as a synonym of *O. adustus* by Devincenzi (1925). After comparing the meristics, morphometrics, coloration, and the figure presented in that study, we determined this species is actually *Micropogonias furnieri*. Also, *Ophioscion woodwardi* Fowler, 1937 from Port-au-Prince, Haiti, West Indies, is a junior synonym of *M. furnieri* (Chao 1978; this study).

Stellifer brasiliensis (Schultz, 1945) was considered the valid name for *Ophioscion brasiliensis* Schultz, 1945 by Chao (1978) on morphological grounds. *Ophioscion costaricensis* Caldwell, 1958 was included as a junior synonym of *Stellifer microps* (Steindachner, 1864) by Chao (1978) and Parenti (2020).

Ophioscion punctatissimus is considered the only valid species of *Ophioscion* from the Western Atlantic (Fig. 7A). *Ophioscion panamensis* Schultz, 1945, is herein considered a junior synonym of *O. punctatissimus*, based on comparative study of the type specimens at the USNM and additional specimens of *O. punctatissimus* that indicate that specimens of *O. panamensis* are in fact the juvenile phase of *O. punctatissimus* (Fig. 7) (Chao 1978; this study). Compared type specimens are: *O. panamensis* Holotype: USNM 122612, 60 mm SL; Paratypes: USNM 81204–07 (3, 4, 1, 1), 128260 (1), all between 35 and 45 mm SL. Examined type specimens for *O. punctatissimus* are: Holotype: USNM 81766, 157 mm SL. Paratypes: USNM 80765–66 (1, 137 mm SL & 1, 185 mm SL).



FIGURE 7. *Stellifer punctatissimus*. A. Holotype USNM 81766, 157 mm SL, from Panama; B. UFPB 601, 147 mm SL, Paraíba State - Brazil. Scale: 10 mm.

Currently, six species of *Ophioscion* are recognized from Eastern Pacific, they are now: *S. imiceps* (Jordan & Gilbert, 1822), *S. scierus* (Jordan & Gilbert, 1884), *S. simulus* (Gilbert, 1898), *S. strabo* (Gilbert, 1897), *S. typicus*, and *S. vermicularis* (Günther, 1867). Additional undescribed species of *Stellifer* (*Ophioscion*) may be found in this region (Chao 1995; Chao 2001). As stated by Chao (1995) and Parenti (2020), these are the junior synonyms of *Ophioscion* in the Eastern Pacific: *Corvina ophioscion* Günther, 1868 as *S. typicus*; *Ophioscion obscurus* Hildebrand, 1946 as *S. scierus*; *Corvina miacanthus* Boulenger, 1899 as *S. strabo*.

Species descriptions

Stellifer cervigoni new species

(Figure 8)

urn:lsid:zoobank.org:act:058E6CB6-B2FC-4999-B8CC-FA5BE8147168

Ophioscion sp. Cervigón (1966): 511, 515, Fig. 211 (key; description; northern coast of Araya, Venezuela).

Stellifer sp. A. Chao (1978): 55 (key); Chao, 2002 (key, description).

Holotype: USNM 435344, 108 mm SL, Morro de Puerto Santo, Estado Sucre, Venezuela, collected by F. Cervigón, 21 September 1961; formerly MHNLS 344, Venezuela.

Paratypes: ANSP 109636, 10 (67–103 mm SL), Peninsula de Araya, between Punta Horno and Punta Cardon, Estado Sucre, Venezuela, collected by William A. Lund, Jr., 06 March 1962. MCZ 4581, 3 (53.5–65.0 mm SL), near Belém, Pará, Brazil, 1°27'S, 48°29'W, collected by Agassiz, L. & D. Bourget, 10 August 1865. NMMBP 21565, 96.5 mm SL, formerly USNM 435344, collected with the holotype. USNM 208558, 2 (96.8–105 mm SL), collected with the holotype. USNM 283764, 3 (47.6–50.7 mm SL), Mouth of Blenheim River, Dominica, collected by V.G. Springer & R.H. Reckweg, 7 November 1964.

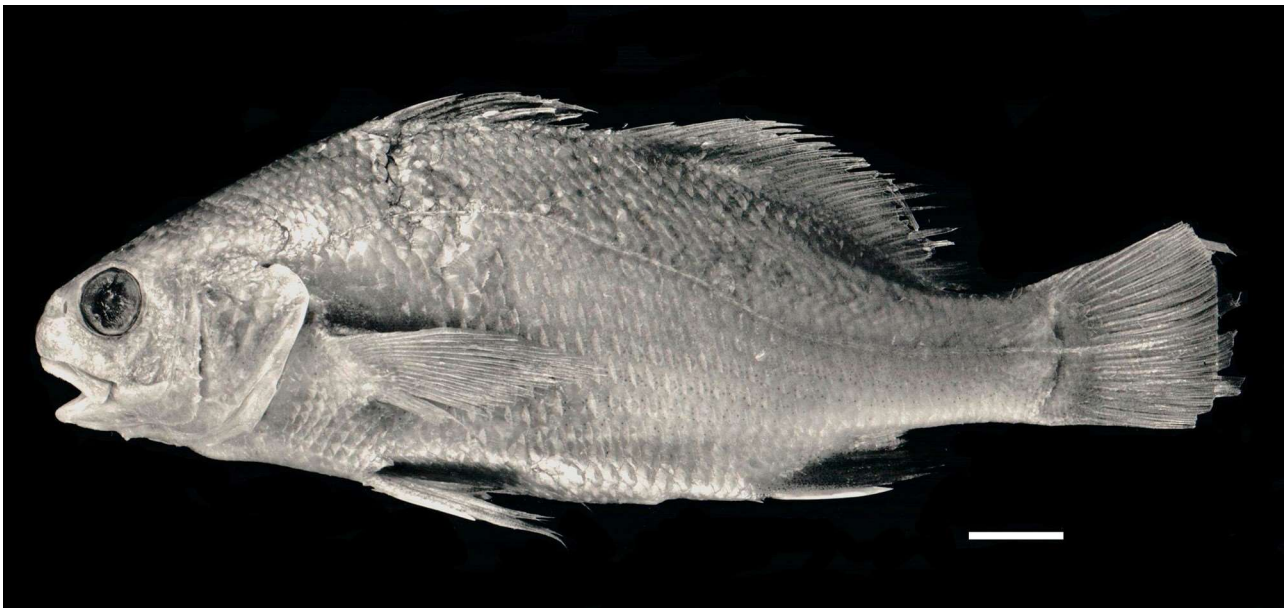


FIGURE 8. *Stellifer cervigoni* new species Holotype USNM 435344, 108 mm SL, Morro de Puerto Santo, Estado Sucre, Venezuela. Scale: 10 mm.

Diagnosis. *Stellifer cervigoni* can be distinguished from all other Atlantic species of the genus by having a jet-black mouth roof and inner opercular lining, except *S. rastrifer*, which also has a dark grayish lining, but never jet-black. In addition, *S. cervigoni* has a slightly oblique, subterminal mouth (vs. oblique in *S. rastrifer*), usually 36–38 total gill-rakers on the first arch (vs. 44–50 in *S. rastrifer*), and a shorter pelvic fin (4.8–5.3 times in SL vs. 4.0–4.8 times in *S. rastrifer*); finally, the hind margin of the anterior chamber of the gas bladder has a pair of small knob-like, hammerhead-shaped diverticula (Fig. 9), while *S. rastrifer* has a pair of tubular appendages (Fig. 1C, right).

Description. Dorsal-fin rays XI+I or II, 22–25; anal-fin rays II, 9 (occasionally 8); pectoral-fin rays 17–19;

gill rakers 11–15 + 24–26 = 35–41; preopercular spines 6–9; lateral-line scales 54–56. Anterior chamber of gas bladder with hammerhead-shaped posterior diverticula pair (Fig. 9). Posterior tip of posterior chamber reaching first anal–spine base. Drumming muscles in males only (Fig. 1B, hatched area). Sagitta (Fig. 10A) elongate with rostrum at middle of anterior margin; sulcus with oval ostium, deeply grooved, L-shaped cauda, and conspicuous marginal groove; outer surface elevated at center. Lapillus (Fig. 10B) smaller than sagitta, oval, with thin anterior flange; inner surface smoothly elevated, outer surface irregularly grooved. Asteriscus (Fig. 10C) triangular, with lanceolate groove near ventral margin of inner surface. Preopercular spines strong, sharp. Lowermost spine longest and strongest, directed obliquely downward and back at about 45°, occasionally slightly antrorse; upper spines progressively shorter and weaker. Head low and broad, interorbital region wide and gently arched, 2.9–3.1 in HL. Head cavernous but moderately firm. Snout 4.0–4.3 in HL, projecting beyond upper lip, its tip with three upper and five marginal pores (Fig. 5A); rostral fold slightly indented below marginal pores. Eye moderately large, 4.5–5.1 in HL, orbit round. Mouth small, slightly oblique, subterminal, upper jaw 2.9–3.1 in HL, lower jaw included within gape forming angle of about 20°. Anterior tip of upper lip, horizontally, passing below ventral margin of orbit by about half eye diameter.

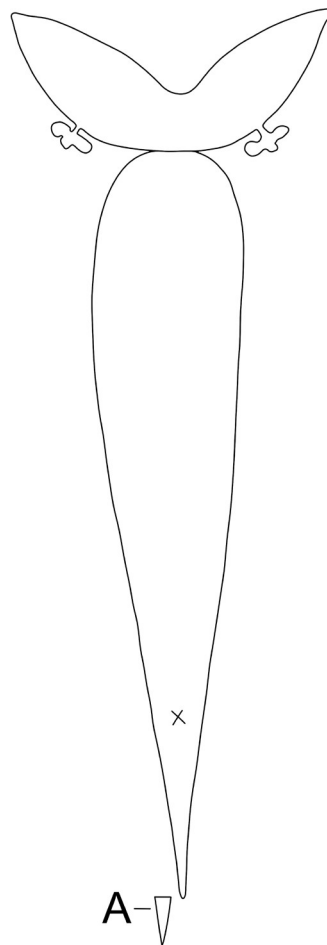


FIGURE 9. Gas bladder of *Stellifer cervigoni* new species with a pair of small hammer-like appendages on the posterior margin of anterior chamber. X indicates position of vent; A indicates base of first anal spine.

Posterior end of maxilla extending to vertical through center of pupil. Underside of lower jaw with six pores (Fig. 6C), medial pair lying together in common pit. Upper jaw with outer row of slender, nearly contiguous, slightly enlarged, conical teeth bordered medially by very fine villiform teeth band. Lower jaw teeth villiform, set in narrow bands, none noticeably enlarged. Gill rakers, moderately long and slender, longest about equal to length of filament at angle of arch or about three-quarters of eye diameter. Anal fin truncate, second spine moderately long and fairly stout, 2.0–2.3 in HL. Caudal fin rounded, about three-quarters of HL. Vertical from tip of pectoral fin passing through or just anterior to vent. Tip of pelvic fin, exclusive of filamentous prolongation, reaching from half distance between pelvic base to anal fin insertion or to as far as first anal spine. Scales large, thin and ctenoid below

lateral line posteriorly, ctenoid patch reducing and occasionally disappearing anteriorly. Scales above lateral line with small ctenoid patch posteriorly, scales becoming smooth in advance of soft dorsal origin. Head squamation cycloid, scales becoming reduced and embedded on snout and suborbital region. Spinous dorsal with one and a half irregular rows of cycloid scales forming basal sheath; membrane naked except for row of minute, elongated, cycloid scales along posterior border of each spine in anterior portion of fin. Soft dorsal and anal membranes heavily and uniformly covered from base to edge with small cycloid scales. Pectoral, pelvic and caudal fins with small cycloid scales at bases, naked distally. Lateral line pored scales smooth anteriorly, but with small patch of ctenii posteriorly. Canal systems usually with single dorsal and ventral branch, occasionally more arborescent.

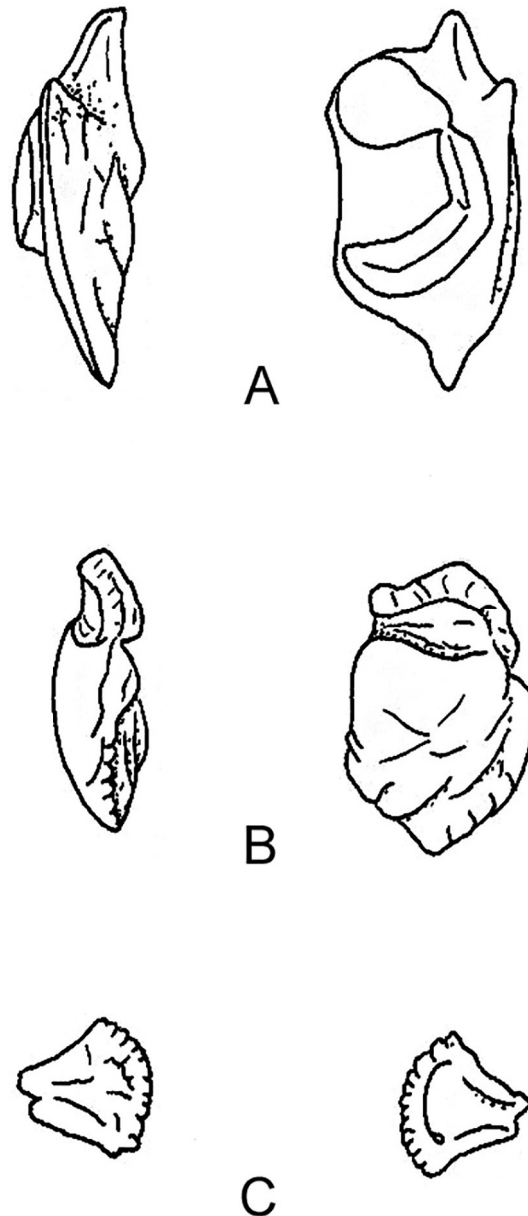


FIGURE 10. Otoliths of *Stellifer cervigoni* new species A. Sagitta; B. Lapillus; C. Asteriscus (layout as in Fig. 3).

Coloration. Preserved specimens with ground color light beige fading to yellowish white ventrally. Snout, top of head, nape, dorsum and sides above level of pectoral fin base profusely dusted with very small brown chromatophores, becoming larger and more widely dispersed ventrally, and disappearing from ventral body surface. Suborbital region and upper half of upper lip sprinkled with large brown chromatophores. Lower lip, tongue and floor of mouth pale. Roof of mouth interior to the oral valve and throat, jet black. Inner side of opercle jet black, appearing externally as a D-shaped blotch bordered by vertical portion of preopercle and following the contour but not extending to the edge of the opercle. Ramus of first gill-arch dark brownish at the angle or extends to entire length. Spinous

dorsal finely stippled, chromatophores concentrated distally at apex of fin appearing dusky. Soft dorsal similarly colored, not finely stippled. Pectoral fin coarsely stippled. Posterior two-thirds of pelvic fins stippled, trailing edges appearing dusky; pelvic filament speckled. Anal fin peppered with chromatophores, dusky in appearance. Caudal fin lightly and evenly dusted. Peritoneum variably sprinkled with large, stellate, chromatophores, especially at the anterior portion of the body cavity.

Distribution. North coast of the Araya Peninsula and the Gulf of Paria, Venezuela, the Caribbean Islands, Lesser Antilles, Dominica and north coast of Brazil, Pará State. Additional collections probably will extend its range.

Etymology. In honor of late Dr. Fernando Cervigón M. formerly at Universidad de Oriente, Venezuela, for his contributions to ichthyology and for discovering the species.

Stellifer collettei new species

(Figure 11)

urn:lsid:zoobank.org:act:AE55EBA9-F72D-4E10-B47E-95585EC92AA9

Stellifer sp. B. Chao (1978): 55 (key); Chao (1981): 1598 (key); Chao (2002): 1598 (key).

Stellifer sp. Menezes & Figueiredo (1980): 58 (key); Casatti & Menezes (2003): 89.

Holotype: USNM 218075, 100 mm SL, off coast of French Guiana, 04°44.7'N, 51°37'W, R/V Oregon II, Station 17622 and 17623, 32.9 m, collected by B.B. Collette, 5 May 1975.

Paratypes: AZUSC 5960, 5 (74–92 mm SL), Ilha das Cabras, Guarujá, São Paulo, Brazil, 24°00'26"S, 46°12'49"W. CMNFI 1977-0361, 10 (46.8–61.8 mm SL) off coast of northern Brazil, 03°16'N, 50°12'W, R/V Oregon II Station 17660, 17661, 20 m, collected by B.B. Collette, 9 May 1975. MCZ 90694, 2 (50.3–68.2 mm SL), off coast of Trinidad and Tobago, 10°45'00"N, 60°53'30"W, RV Eastward St. Station 23754, 28 February 1974. MCZ 157279, 62.5 mm SL, off coast of Trinidad and Tobago, 10°45'42"N, 60°53'30"W, RV Eastward 23754, 28 February 1974. MCZ 157276, 15 (33.0–72.0 mm SL), off coast of Guyana, 08°08'30"N, 58°45'39"W, RV Eastward 23727, 26 February 1974. MCZ 157277, 19 (32.2–76.2 mm SL), off coast of Guyana, 07°11'48"N, 57°59'36"W, RV Eastward 23712, 23 m, 25 February 1974. MCZ 157278, 4 (35.3–62.3 mm SL), off coast of Guyana, 07°49'30"N, 57°47'30"W, RV Eastward 23706, 25 February 1974 (CT scanned 62.3 mm SL). MZUSP 13837, 73.8 mm SL, Praia do Itaguá, Ubatuba, São Paulo, Brazil, collected by J.L. Figueiredo, 02 January 1970. MZUSP 13838, 5 (51.7–60.1 mm SL), Praia da Avenida, Maceió, Alagoas, Brazil, collected by J.G. Marques, 16 October 1978. MZUSP 13845, 3 (67.2–74.5 mm SL), Praia do Camburi, Vitória, Espírito Santo, Brazil, collected by A.V. Alcântara, 24–25 January 1972. MZUSP 13842, 5 (61–68 mm SL), Praia do Itaguá, Ubatuba, São Paulo, Brazil, collected by J.L. Figueiredo, 02 January 1970. MZUSP 13844, 8 (50.7–60.6 mm SL), Ilha da Moela, Santos, São Paulo, Brazil, collected by C. Jesus, 14 July 1961. MZUSP 13847, 30 (38–72 mm SL), Atafona, Rio de Janeiro, Brazil, otter trawl, collected by Expedição do Departamento de Zoologia, 08 April 1964. NMMB-P 21571, 3 (47.2–62.5 mm SL), off coast of Amapá State coast, northern Brazil, 03°16'N, 50°12'W, R/V Oregon II 1664 and 65, 18 m, collected by B.B. Collette, 9 May 1975. NMMB-P 31974, 3 (57.6–62.7 mm SL), Ilha das Cabras, Guarujá, São Paulo, Brazil, 24°00'47"S, 46°12'45"W, 15.5 m, bottom trawl, collected by Matheus Rotundo, 23 February 2019. NMMB-P 319775, 2 (49.2–56.8 mm SL), same data as NMMB-P 31974. USNM 218212, 81.0 mm SL, off coast of French Guiana collected with holotype. USNM 325186, 98.8 mm SL, off coast of French Guiana collected with holotype. USNM 325187, 3 (45.3–52.7 mm SL), off coast of northern Brazil, 03°33'N, 50°17'W, R/V Oregon II Station 17660 and 17661, 20 m, collected by B.B. Collette, 9 May 1975. USNM 218211, 11 (48–65 mm SL), off coast of northern Brazil, 03°16'N, 50°12'W, R/V Oregon II Station 1664 and 65, 18 m, collected by B.B. Collette, 9 May 1975.

Additional, non type specimens: Brazil: Paraíba State: UFPB 5640, 66.78 mm SL, Praia de Pitimbu. UFPB 3081, 62.7 mm SL, Lucena. MZFS 5648, 63.87 mm SL, Praia de Manaíra. Bahia State: MNRJ 549517, 6 (50.1–53.4 mm SL), Rio das Contas estuary, Itacaré, collected by P.S. Young & M.C. Brito, 11 February 1993. MZFS 12275, 3 (62.2–65.9 mm SL), Praia do Malhado, Ilhéus. MZFS 16942, 7 (51.1–67.8 mm SL), Praia do Malhado, Ilhéus. MZFS 18089, 10 (57.9–69.7 mm SL). MZFS 18088, 9 (52.7–75.7 mm SL). MZFS 18086, 9 (59.9–71.0 mm SL), Praia do Malhado, Ilhéus. Rio de Janeiro State: MZUSP 13835, 39 (35.5–83.8 mm SL) and MZUSP 13839, 8 (42–60.1 mm SL), both from Atafona, Rio de Janeiro, Brazil, collected by Expedição do Departamento de Zoologia. MZFS 12275, 55.0 mm SL, Atafona, Rio de Janeiro, no date. São Paulo State: MZUSP 13840, 2 (64.8–65.3 mm SL), Enseada de Ubatuba, Ubatuba, São Paulo, Brazil, collected by J. de Abreu, 01 January 1975. MZUSP 13843, 2

(53.7–66.5 mm SL), Enseada de Ubatuba, Ubatuba, São Paulo, Brazil, collected by J. de Abreu, 18 December 1973. MZUSP 13841, 5 (56–74 mm SL), Ponta Grossa, Ubatuba, São Paulo, Brazil, collected by J. de Abreu, 01 January 1975. MZUSP 13846, 33 mm SL, Boqueirão, Santos, São Paulo, Brazil, collected by Seção Biologia da Pesca – IO, 12 March 1960. *Guyana*: MCZ 157277, 20 (33.0–72.0 mm SL), off coast of Guyana, 07°11'48"N, 57°59'36"W, RV Eastward St. 23712, 25 February 1974.

Diagnosis. *Stellifer collettei* can be distinguished from all other Atlantic species of the genus by the combination of a strong oblique mouth, six to nine short spines on the preopercular margin, and four pores on the underside of the lower jaw, except the Venezuelan *S. chaoi*, which is similar in external appearance, but has 42–48 total gill rakers on the first arch (vs. 28–37 in *S. collettei*).

Description. Dorsal-fin rays X–XII+I–III, 19–23; anal-fin rays II, 8 (rarely 7 or 9); pectoral-fin rays 18–20; gill rakers 10–12 + 18–25 = 29–36; preopercular spines 6–9; lateral-line pored scales 45–50; 4–5 transverse scale rows from lateral line to dorsal fin origin and 7–8 rows to anal fin origin. Anterior chamber of gas bladder with short knob-like, pear-shaped posterior diverticula pair (Fig. 12). Posterior tip of posterior chamber reaching to base of first anal spine. Drumming muscles in males only (Fig. 1B, hatched area). Sagitta (Fig. 13A) thick and broad, deep notched anterodorsally; sulcus with narrow ostium, deeply grooved L-shaped cauda, and marginal groove along dorsal margin; outer surface rough, with crest-like projections. Lapillus (Fig. 13B) ovoid, with thin anteroventral flange; inner surface smooth, outer surface with irregular grooves. Asteriscus (Fig. 13C) triangular, with lanceolate groove near ventral margin of inner surface (Fig. 2). Preopercular spines strong, sharp, lower three longest and strongest; direction of lowermost spine varying from straight and angled down and back at about 45° to curved, the tip pointing vertically down; upper spines often reduced to thin, flat, flexible points. Head low, dorsal profile rather straight, interorbital region nearly flat; rather cavernous but not spongy with moderately strong frontal bone ridges. Snout 3.9–4.6 in HL, not projecting beyond upper lip, its tip with three upper and five marginal pores; rostral fold slightly indented below marginal pores. Eye moderate to small 4.7–6.2 in HL (Table 1), orbit usually rounded, sometimes oval with oblique axis in small specimens. Mouth large, terminal, upper jaw 2.0–2.3 in HL; jaws subequal, gape forming angle of about 30°. Anterior tip of upper lip, horizontally, passing through or above ventral margin of orbit. Posterior end of maxilla reaching to vertical between posterior borders of pupil and orbit. Underside of lower jaw with four pores, medial pair minute and separated by symphyseal ridge (Fig. 6A). Teeth in upper jaw subequal, in narrow villiform band, outer row slightly enlarged, the longest not exceeding one quarter of pupil diameter. Teeth in lower jaw in narrow villiform band, inner row of closely set, slightly enlarged teeth. Gill rakers long and slender, longest 1.5 to 2.1 times that of gill filament at angle, greater than eye diameter. Anal fin truncate, second spine long, strong, about equal length of first soft ray, 1.6–1.9 in HL. Caudal fin rhomboidal to pointed in juveniles, about equal to head length. Pectoral fin long, its tip passing beyond vent. Tip of pelvic fin, exclusive of filamentous prolongation, reaching to within one eye diameter of vent. Scales large, thin and strongly ctenoid everywhere on body, except for one or two rows of cycloid scales beneath opercular flap. Head squamation cycloid, except for patch of ctenoid scales on opercle; scales reduced and somewhat embedded on snout. Spinous dorsal with three or four rows of reduced cycloid scales at base. Interspinous membrane naked except for row of minute, elongated scales along posterior border of each spine. Soft dorsal and anal fins uniformly covered by small cycloid scales. Caudal, pectoral, and pelvic fins finely scaled. Lateral line pored scales ctenoid, indented in middle of posterior margin, much smaller than scales of adjacent rows. Lateral-line scales marked with arborescent sensory canals.

Coloration. Preserved specimens with body brownish becoming darker dorsally through dense stippling of tiny chromatophores. Opercle above level of angle sprinkled with large chromatophores. Some chromatophores concentration on snout and around orbit. Dorsal margin of anterior half of upper lip with conspicuous dark band, few chromatophores scattered posteriorly. Anterior part of lower lip sprinkled with chromatophores. Tongue and inside of mouth pale, except for dark band medial to teeth rows in anterior half of jaws. Inside opercle, posterior portion of mouth and cleithrum variably dusky or punctuate elsewhere. First gill arch densely punctuated, chromatophores forming dark band along base of filaments. Exterior of cleithrum heavily dusted with large chromatophores. Spinous dorsal covered with large chromatophores, concentrated distally, apex dark; soft dorsal similarly colored but less densely dusted. Caudal fin evenly dusted with small chromatophores. Anal fin punctuated, becoming dark toward trailing edge. Upper half of pectoral fin sprinkled with chromatophores, densely pigmented patch just above fin-base. Pelvic fin generally pale at base but densely punctuate distally. Peritoneum silvery.

Distribution. Coastal waters from southeastern Venezuela to southeastern Brazil.

TABLE 1. Key morphological characters and total gill rakers of Western Atlantic *Stellifer* spp. with a large, oblique mouth. N=Total sample

Species	Characters					28
	Eye in HL	Inteorbital in HL	Pelvic fin in SL	Mental pores	Inteorbital scales	
<i>S. chaoi</i> *	5.8–6.4	3.4	4.1–5.0	4	Cycloid	
<i>S. collettei</i>						
Trinidad						
Guyana						1
NE Brazil						
SE Brazil						
Total range	5.2–6.1	3.0–3.7	3.8–4.8	4	Cycloid	1
<i>S. griseus</i>	4.1–5.6	2.8–3.0	4.1–5.0	6	Cycloid	
<i>S. lanceolatus</i>	4.5–5.5	2.8–3.3	4.5–5.0	6	Cycloid	
<i>S. macallisteri</i>	4.4–5.3	2.7–3.2	3.9–4.9	6	Ctenoid	2
<i>S. musicki</i>	3.8–4.5	2.5–3.0	4.3–5.3	6	Cycloid	
<i>S. rastrifer</i>	4.0–5.3	2.7–3.2	4.0–4.8	6	Cycloid	
<i>S. stellifer</i>	4.2–4.6	2.5–2.7	3.7–5.0	4	Cycloid	

Continued.

Species	Gill-raker count																
	37	38	41	42	43	44	45	46	47	48	49	50	51	52	53	54	55
<i>S. chaoi</i> *			4	16	15	24	17	6	1	2							
<i>S. collettei</i>																	
Trinidad																	
Guyana																	
NE Brazil																	
SE Brazil																	
Total range																	
<i>S. griseus</i>													1	2	3	5	4
<i>S. lanceolatus</i>																	
<i>S. macallisteri</i>																	
<i>S. musicki</i>	2	1															
<i>S. rastrifer</i>					1	5	5	13	13	7	6	5	3	2		1	
<i>S. stellifer</i>																	

*including Aguilera *et al.* (1983) (n=73), current (n=13)

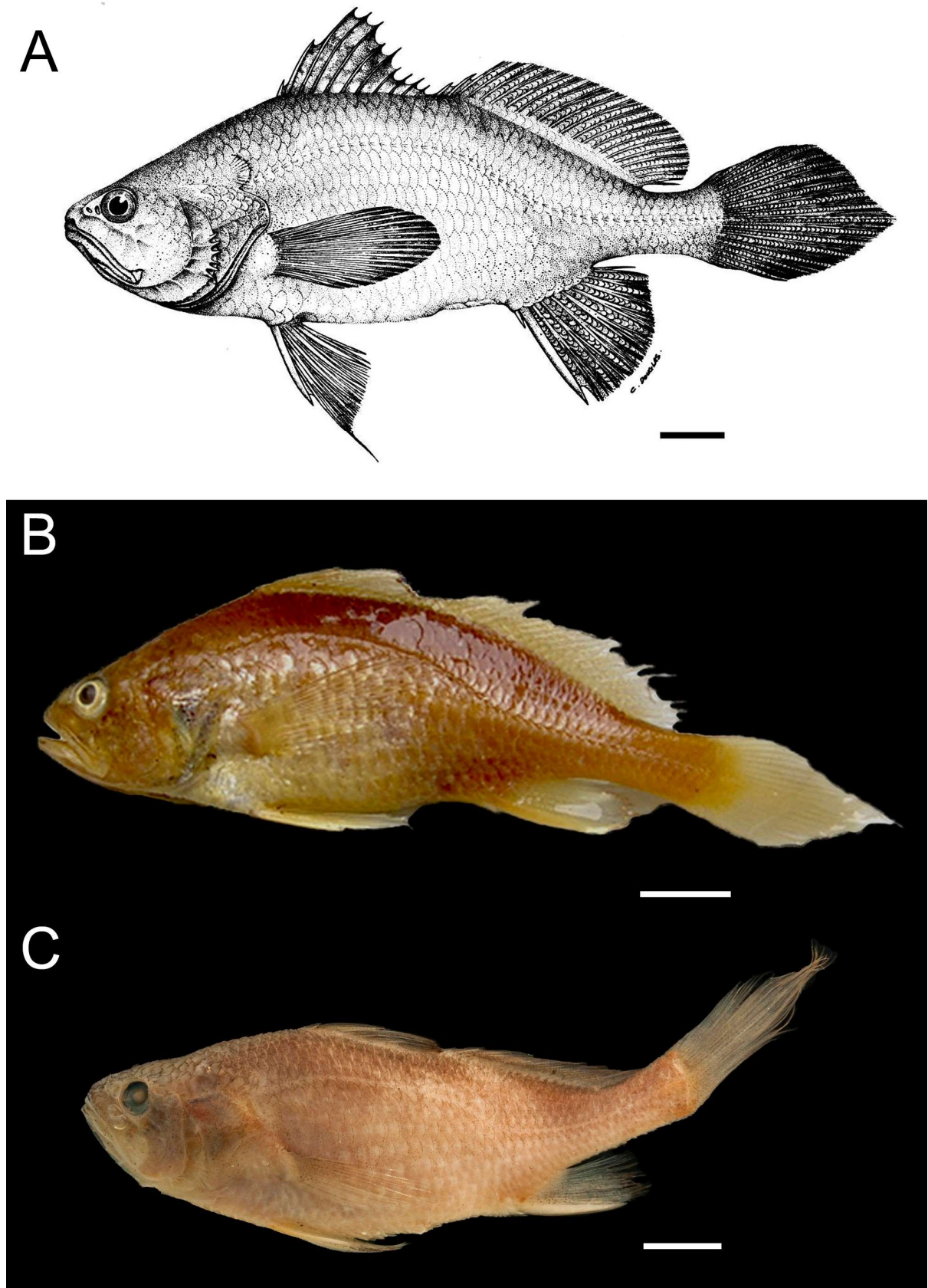


FIGURE 11. *Stellifer collettei* new species A. Holotype USNM 218075, 100 mm SL, off shore, French Guiana (Illustrated by C. Douglas, formerly at the Canadian Museum of Nature); B. Paratype MZUSP 13837, 73.8 mm SL, São Paulo, Brazil; C. MZFS 18088, 75.7 mm SL, Bahia, Brazil. Scale: 10 mm.

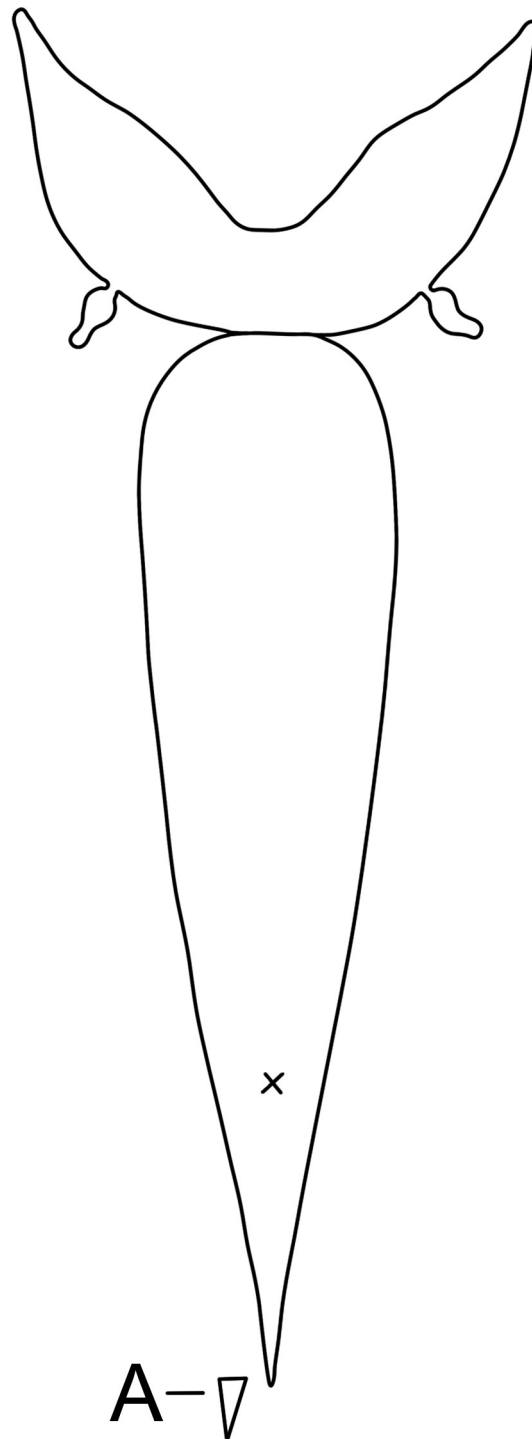


FIGURE 12. Gas bladder of *Stellifer collettei* new species with a pair of small knob-like, pear-shaped appendages on the posterior margin of the anterior chamber. X indicates position of vent; A indicates base of first anal spine.

Etymology. This species is named in honor of Dr. Bruce B. Collette, formerly of the Systematics Laboratory, National Marine Fisheries Service, NOAA, who collected the holotype, and is the principal mentor of N.L. Chao.

Remarks on geographic variation. *S. collettei* has a broad distribution from southeastern Venezuela to southeastern Brazil. Gill-raker counts on the first gill arch vary from 28 to 37 (Table 1). Also, there are some small variations in head length, pectoral-fin length and eye diameter along the distribution. Additional genetic information may reveal geographic forms or cryptic species along the Atlantic and Caribbean coasts.

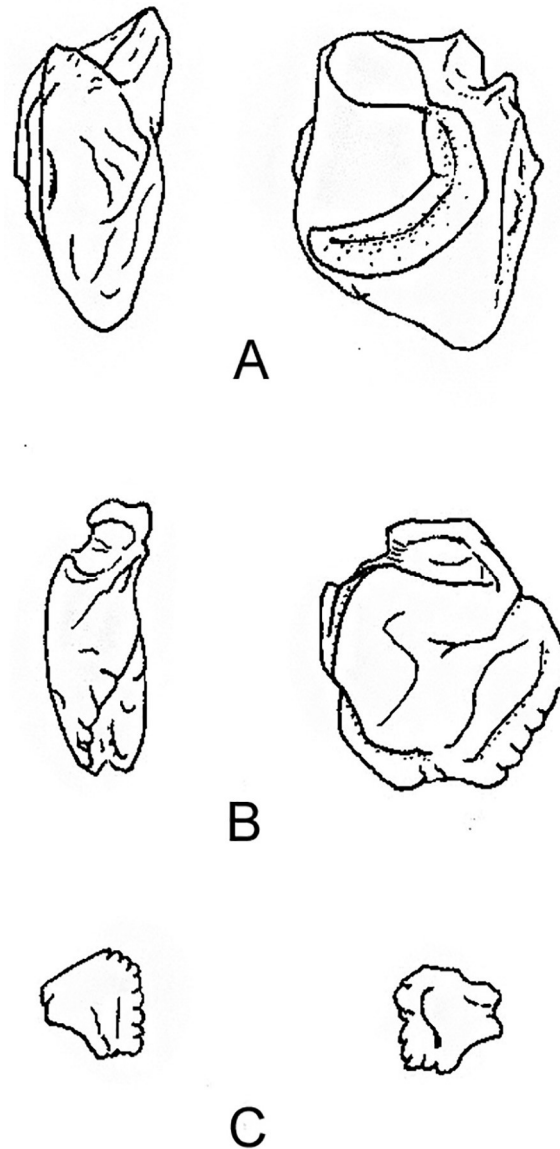


FIGURE 13. Otoliths of *Stellifer collettei* new species A. Sagitta; B. Lapillus; C. Asteriscus (layout as in Fig. 3).

***Stellifer macallisteri* new species**

(Figure 14)

urn:lsid:zoobank.org:act:FDE3B27B-01B7-4A56-95A1-741B4341C6C9

Stellifer sp. C. Chao (2002), p.1652.

Holotype: CMNFI 1986-500.1, 86.4 mm SL, Gulf of Venezuela, in front of Punta Capana, Península de Paraguana, 12°N, 70°W, Estado del Falcon, Venezuela, collected by J. Valdez & D. Diaz, bottom trawl, three nautical miles offshore, six fathoms, 8:00-11:30 a.m, 24 November 1984.

Paratypes: CMNFI 86-499.1, (63.0–94.0 mm SL), collected with the holotype. USNM 377173, 3 (79.3–84.1 mm SL), collected with the holotype. USNM 377174, 2 (75.4–96.0 mm SL), Santo Domingo, Dominican Republic; sent to the first author by D. Sang in 1984 (original collection number MNHN 417). USNM 287531, 4 (73.2–83.9 mm SL), Caribbean coast near Cartagena, Colombia, collected by D. Solano; received by the first author on May 30, 1983. MCZ 171873, 2 (74.2–78.8 mm SL) from USNM 377173, collected with the holotype. MCZ 157248, 5 (77.2–84.5 mm SL), collected with the holotype. NMMBA 20762, 110 mm SL (clear & stained), collected with the holotype. NMMBA 21566, 2 (79.1–85.5 mm SL), collected with the holotype. NMMBA 21567, 4 (77.0–87.0 mm

SL), Isla de Salamanca, Colombia, collected by A. Acero, October 1993. NMMBA 21568, 66.6 mm SL, Ciénaga Grande de Santa Marta, Colombia, collected by D. Solano, 31 May 1983. USNM 144665, 72.5 mm SL, Fort Sherman, Canal Zone, Limon Bay, Panama, collected by S.F. Hildebrand, April 1937.

Diagnosis. *Stellifer macallisteri* can be distinguished from all other Atlantic species of the genus by the combination of a terminal, slightly oblique mouth, XI spines in the first dorsal fin, and lack of diverticula on anterior chamber of gas bladder. In addition, it can be differentiated from the other species that lack diverticula as follows: *S. punctatissimus* has a deeper body, subterminal to inferior mouth; *S. menezesi* (described herein) and *S. gomezi* have a more elongated body, subterminal to inferior mouth.



FIGURE 14. *Stellifer macallisteri* new species Holotype CMNFI 1986-500.1, 86.4 mm SL, Gulf of Venezuela. Scale: 10 mm.

Description. Dorsal-fin rays XI+I, 22–24; anal-fin rays II, 8 (occasionally 7); pectoral-fin rays 17–18; gill rakers 9–11 + 19–20 = 28–31; preopercular margin with 6–7 spines; lateral-line pored scales 47–51. Anterior chamber of gas bladder yoke-shaped without appendages (Fig. 1A, left); posterior chamber carrot-shaped ending anterior to base of first anal spine. Drumming muscles in males only (Fig. 1B, hatched area). Sagitta (Fig. 15A) thick with antero-dorsally notch; sulcus with small ovoid ostium, deeply grooved L-shaped cauda, and shallow groove along dorsal margin; outer surface with crest-like elevations. Lapillus (Fig. 15B) ovoid, with thin anterior flange; inner surface smoothly convex, outer surface roughly concave. Asteriscus (Fig. 15C) triangular, thin, with lanceolate groove near ventral margin of inner surface. Preopercular spines short, three prominent at angle, directed obliquely down and back; 3–4 upper spines progressively shorter and weaker on upper part of preopercle, the uppermost appearing as flat points. Head conical and deep, interorbital region slightly convex and cavernous. Snout pointed, 3.9–4.4 in HL, projecting slightly in front of upper lip, its lower margin with three upper and five marginal sensory pores. Eye moderate, 4.4–5.1 in HL, orbit rounded, somewhat oval in small specimens. Mouth large, terminal, the upper jaw 2.1–2.3 in HL; jaws subequal, gape forming angle of about 30°. Anterior tip of upper lip, horizontally, passing through or above ventral margin of orbit. Posterior end of maxilla reaching vertical between posterior borders of pupil and orbit. Underside of lower jaw with six pores, medial pair minute and separated by symphyseal knob (Fig. 6D). Upper jaw teeth in narrow band, with clearly enlarged outer row of sparsely set of teeth, longest not exceeding one quarter of the pupil diameter. Teeth on lower jaw villiform, set in narrow bands, with slightly enlarged inner row. Gill rakers long and slender, longest much longer than gill filament at angle of gill arch, but shorter than eye diameter. Anal fin truncate, second spine long and strong, 1.6–1.9 in HL or more than 80% of first ray length. Caudal fin rhomboidal to point, about equal to HL. Pectoral fin tip reaching beyond pelvic fin and vent; pelvic fin tip with short filamentous prolongation, reaching to within one eye diameter of vent. Scales large, thin, and strongly ctenoid everywhere on body, except for one or two rows of cycloid scales beneath opercular flap. Head squamation cycloid, except for patch of ctenoid scales on opercle; scales reduced and somewhat embedded on snout. Base of spinous dorsal with three or four rows of reduced cycloid scales, basal sheath not well-defined. Interspinous membrane naked except for row of minute, elongated scales along posterior border of each spine. Soft dorsal and anal fins uniformly covered by small cycloid scales. Caudal, pectoral, and pelvic fins finely scaled.

Lateral line pored scales ctenoid, indented in middle of posterior margin, and much smaller than scales of adjacent rows. Lateral line scales marked with arborescent sensory canals.

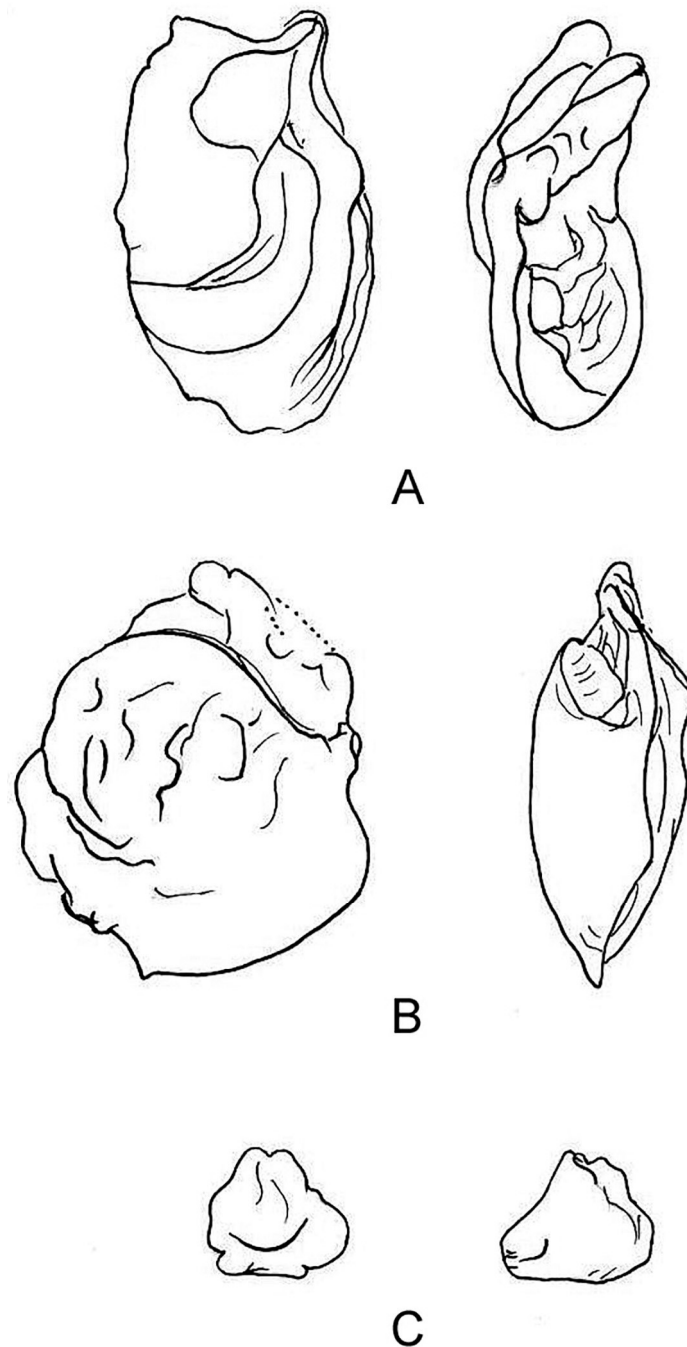


FIGURE 15. Otoliths of *Stellifer macallisteri* new species A. Sagitta; B. Lapillus; C. Asteriscus (layout as in Fig. 3).

Coloration. Preserved specimens with body brownish, slightly darker dorsally due to dense stippling of tiny chromatophores. Opercle with silvery reflection externally and narrow patch of chromatophores behind upper end of pre-opercle. Dorsal margin of anterior half of upper lip with conspicuous dark band, few chromatophores scattered posteriorly. Anterior part of lower lip sprinkled with chromatophores. Tongue and inside of mouth pale, roof dusky posteriorly. Inside of opercle silvery pale becomes darkish towards the pseudobranchiae, variably dusky or speckled elsewhere. First gill arch pale, medial skin cover cleithrum heavily dusted with large chromatophores. Tip of spinous dorsal fin darkish, distal margin of soft dorsal slightly dark. Caudal fin evenly dusted with small chromatophores. Anal fin punctuated, becoming dark toward trailing edge. Upper half of pectoral fins sprinkled with chromatophores and a densely pigmented patch just above pectoral-base. Pelvic fin generally pale at base but densely punctuate distally. Peritoneum silvery.

Distribution. Caribbean coast of South America from Cartagena, Colombia to Gulf of Venezuela. Also found in Dominican Republic and one record from Canal Zone, Limon Bay, Panama.

Etymology. In honor of the late Dr. Don E. McAllister, formerly of the National Museum of Natural History, Ottawa, Canada.

***Stellifer menezesi* new species**

(Figure 16)

urn:lsid:zoobank.org:act:FAC15843-74C0-49A5-B4CC-A29D6DD4EBB0

Holotype: MZUSP 123409, 102 mm SL, Ponta Grande Beach, Porto Seguro, Bahia, Brazil, collected by Moraes, L.E. and Costa, V.F., 10 May 2016.



FIGURE 16. *Stellifer menezesi* new species Holotype MZUSP 123409, 102 mm SL, Porto Seguro, Bahia, Brazil. Scale: 10 mm.

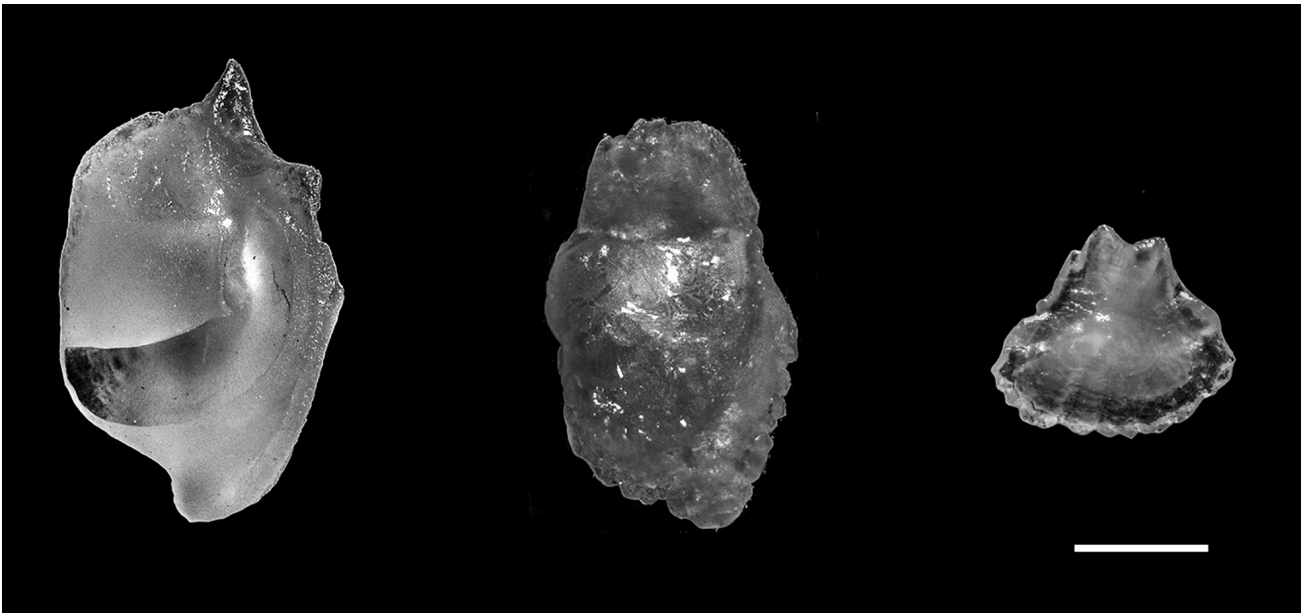


FIGURE 17. Otoliths of *Stellifer menezesi* new species. Medial surface of sagitta (left), lapillus (middle) and asteriscus (right). MZFS 18128, 82 mm SL (female). Scale: 1 mm.



FIGURE 18. Detail of nostrils shape for: A- *Stellifer menezesi* new species; B- *Stellifer gomezi*. Scale: 10 mm.

Paratypes: AZUSC 5950, 56 mm SL, Maracaípe, Pernambuco, Brazil, 8°31'31"S, 34°59'37"W, trawl, 11 m, collected by Flores, F.G., 26 November 2011. AZUSC 5963, 4 (72–101 mm SL), Ponta Grande, Porto Seguro, Bahia, Brazil, 16°22'40"S, 39°00'56"W, trawl, 12 m, collected by Moraes, L.E. and Costa, V.F., 29 August 2016. AZUSC 6060, 5 (98–129 mm SL), Barra Nova, Maceió, Alagoas, Brazil, 9°43'58"S, 35°47'11"W, trawl, 15 m, collected by Gardeni, M.R., 29 October 2016. AZUSC 6087, 2 (136–153 mm SL), Barra do Una, Peruíbe, São Paulo, Brazil, 24°29'18"S, 47°05'49"W, trawl, 20., collected by Souza, T.R., 15 December 2016. MZUSP 123405, 63.0 mm SL, and MZUSP 123406, 6 (63.8–81.2 mm SL), Praia de Ponta da Ilha – Ilha de Itaparica (Baía de Todos os Santos – Bahia), collected by Lopes, P.R.D, Oliveira-Silva, J.T., 3 March 2010. MZUSP 123407, 39.5 mm SL, Praia do Malhado, Ilhéus, Bahia, Brazil, local fishermen, October 2008. MZUSP 123408, 2 (54.6–67.1 mm SL), Praia de Berlinque, Ilha de Itaparica, Bahia, Brazil, collected by Lopes, P.R.D, Oliveira-Silva, J.T. and Moraes, L.E., 27 June 2002. MZFS 17125, 108 mm SL, Praia de Ponta da Ilha, Ilha de Itaparica, Bahia, Brazil, collected by Santos, J.A., Moura, P.E.S. and Bucheni, F., 14 December 2016. MZFS 18131, 84.9 mm SL, collected with the holotype. MZFS 16961, 6 (70.5–90.4 mm SL), Praia de Ponta da Ilha – Ilha de Itaparica (Baía de Todos os Santos – Bahia), collected by Lopes, P.R.D, Oliveira-Silva, J.T., 3 March 2010. UFPB 3228, 2 (40.9–87.7 mm SL), Lucena, Paraíba. NMMBA 27623, 3 (59.4–78.9 mm SL) Praia do Malhado, Ilhéus, Bahia, Brazil, local fishermen, November 2013. MNRJ 50825, 2 (61.2–69.5 mm SL), Praia de Ponta da Ilha, Ilha de Itaparica, Bahia, Brazil, collected by Santos, J.A. and M. Carvalho-Junior, 28 October 2015. MNRJ 50824, 4 (75–78.8 mm SL), Praia de Ponta da Ilha, Ilha de Itaparica, Bahia, Brazil, 11 September 2010. MNRJ 50823, 8 (35.0–45.2 mm SL), Praia de Berlinque, Ilha de Itaparica, Bahia, Brazil, collected by P.R.D. Lopes, J.T. Oliveira-Silva and L.E. Moraes, 27 June 2002. MZFS 17734, 3 (62.9–70.7 mm SL), Praia de Ponta da Ilha, Ilha de Itaparica, Bahia, Brazil, 3 October 2010. MZFS 18169, 2 (85.7–91.5 mm SL), Praia de Ponta da Ilha, Ilha de Itaparica, Bahia, Brazil, December 2009. MZFS 2100, 78.8 mm SL, Praia de Ponta da Ilha, Ilha de Itaparica, Bahia, Brazil, collected by Lopes, P.R.D, Silva, J.T.O. and Silva, I.S., 21 June 1997. MZFS 17650, 4 (64.6–73.5 mm SL) collected with the holotype. MZFS 9998, 2 (51.1–55.6 mm SL), Ilhéus, Bahia, Brazil, November 2003. ZUEC 147672, 5 (59.1–82.1 mm SL), Praia de Ponta da Ilha – Ilha de Itaparica (Baía de Todos os Santos – Bahia), collected by Lopes, P.R.D, Oliveira-Silva, J.T. 3 March 2010. ZUEC 147671, 56.8 mm SL, Praia de Ponta da Ilha, Ilha de Itaparica, Bahia, Brazil, collected by J.A. Santos et al., 26 December 2015. ZUEC 147673, 88.0 mm SL, Caravelas, Bahia, Brazil, collected by CEPENE team, 06 January 2015.

Diagnosis. *Stellifer menezesi* can be distinguished from other Atlantic species of the genus with a terminal or oblique mouth by the inferior mouth and elongated body. The absence of diverticula on the posterior margin of anterior gas bladder chamber distinguishes it from *S. microps*, *S. naso* and *S. venezuelae* (Fig. 1A, right). *Stellifer punctatissimus* has a strongly arched back, body depth much greater than HL and black pectoral and pelvic fins (Fig. 7). *S. gomezi* has a body depth equal to or shorter than HL and a protruding snout greater than the eye diameter (Fig. 21), while in *S. menezesi* the body depth is slightly greater than HL (Fig. 16) and the snout length is shorter than the eye diameter; also, in *S. menezesi* the anterior nostril is slightly oval and forward directed, and the posterior nostril is bean-shaped forming an angle between them, which differs from *S. gomezi* that has rounded nostrils and almost of the same height (Fig. 18).

Description. Dorsal-fin rays X+I, 23–24; anal-fin rays II, 7 (6–8); pectoral-fin rays 17–18; gill rakers 6–8 + 11–13 = 17–21; preopercular spines 8–10; pored lateral-line scales 48–51; 4–5 transverse scale rows from lateral line to dorsal fin origin and 6–8 rows to anal fin origin. Anterior chamber of gas bladder smooth without appendages (Fig. 1A, left); posterior tip of posterior chamber terminating anterior to base of first anal spine. Drumming muscles in males only (Fig. 1B, hatched area). Sagitta (Fig. 17) thick with notch anterodorsally; sulcus with small ovoid ostium, deeply grooved L-shaped cauda, and shallow groove along dorsal margin; outer surface with crest-like elevations. Lapillus ovoid, with thin anterior flange; inner surface smoothly convex, outer surface roughly concave. Asteriscus triangular, thin, with lanceolate groove near ventral margin of inner surface.

Preopercular spines short, sharp, usually 10, more prominent at the angle; upper spines progressively shorter and weaker, the uppermost appearing as flat points, lower margin of preopercle weakly serrated. Head conical, interorbital region slightly convex, not cavernous in appearance. Snout conical, 4.0–4.4 in HL, projecting beyond upper lip, its tip with three upper and five marginal pores. Eye moderate to large, 3.3–4.3 in HL, orbit rounded, its diameter equal to interorbital width, 3.1–4.4 (3.8 in HL), and snout length. Mouth inferior, moderately large, upper jaw 3.0–4.0 in HL; jaws subequal with nearly horizontal gap. Anterior tip of upper lip, horizontally, passing below ventral margin of orbit. Posterior maxilla ends below anterior half of eye. Underside of lower jaw with six sensory pores, medial pair set in common pit, often difficult to observe with naked eye (Fig. 6C). Teeth thin and short on

both jaws set in villiform bands, longest not exceeding one third of pupil diameter. Tooth band on upper jaw slightly broader than lower jaw. No teeth on mandibular symphysis area. Gill rakers moderately short and slender, longest at corner shorter than filament at angle of arch, less than one third of eye diameter. Nostrils below middle of eye, anterior slightly oval and forward directed, horizontally aligned with the larger oblong, bean-shaped posterior nostril, distance between them about the same as height of posterior nostril; angle of about 60° between them (Fig. 18A). Anal fin truncate, second spine long and strong, 1.5–1.8 in HL, slightly shorter than first ray. Caudal fin rhomboidal, much shorter than HL. Tip of pectoral fin vertically short or equal to pelvic-fin tip when depressed. Pelvic fin filamentous prolongation very short. Scales moderately large, strongly ctenoid on body and head; small cycloid scales on preorbital, infraorbital, and embedded under skin of lachrymal bones; tip of snout not scaled. Spinous dorsal with four or five rows of reduced cycloid scales along base, basal sheath not well-defined. Inter-spine membrane naked, soft dorsal and anal fins uniformly covered by small cycloid scales on membrane behind each soft ray, extending distally to at least half fin height. Pectoral fin base with small cycloid scales. Pelvic fin base with four or five rows of ctenoid scales, moderate in size. Caudal, pectoral, and pelvic fins finely scaled. Lateral line pored scales ctenoid, indented in middle of posterior margin, and much smaller than scales of adjacent rows. Lateral line canal system arborescent.

Coloration. Fresh specimens have silvery gray to brownish body with dusky pectoral fin; pelvic, anal, and lower part of caudal fins darker. Some concentration of chromatophores on snout, around orbit and at pectoral fin base. Margin of upper lip and lower jaw with slightly conspicuous dark band, few chromatophores scattered posteriorly. Tongue and inside of mouth pale. Inside of opercle black dorsally around the pseudobranchiae, variably dusky elsewhere. Skin covering cleithrum heavily dusted with large chromatophores. Spinous dorsal fin covered with large chromatophores, concentrated distally, apex of fin slightly dark. Soft dorsal similarly but less densely dusted. Pectoral fins densely covered with chromatophores, pale distally, and with oval dusky patch extending from axillae dorsally to upper end of gill cover. Pelvic fins pale at base, densely punctuated distally. Caudal fin evenly dusted with small chromatophores, lower half often darker. Peritoneum membrane silvery. Preserved specimens pale brown overall, fin-rays blackish, fin-spines pale.

Distribution. From Paraíba to São Paulo on the Brazilian coast, uncommon south of Bahia.

Ecological Notes. This species is rather common in inshore waters, from the surf zone to estuaries along the northeastern Brazilian coast. It is found near beaches with accumulations of detached macrophytes, mostly between September and February, feeding on amphipods and other crustaceans. Females mature at about 70 mm SL.

Etymology. In honor of Dr. Naércio A. Menezes, Professor Emeritus, Museum of Zoology, University of São Paulo, for his contributions to neotropical ichthyology and his mentorship of numerous students.

Stellifer musicki new species

(Figure 19)

urn:lsid:zoobank.org:act:1D782FAF-A50F-4487-A0A6-83E65C71122E

Holotype: UFPB 1932, 88.7 mm SL, Praia de Tambaú, João Pessoa, Paraíba, Brazil.

Paratypes: MZFS 17992, 4 (67.2–73.5 mm SL), Praia do Malhado, Ilhéus, Bahia, Brazil, collected by P.R.D. Lopes, December 2006. MZFS 18015, 2 (66.6–86.2 mm SL), Praia do Malhado, Ilhéus, Bahia, Brazil, collected by P.R.D. Lopes, October 2013. NMMBP 21570, 97.7 mm SL, Bragança, Pará, Brazil, collected by N.L. Chao, 28 June 2010. UFPB 11887, 6 (62.5–81.5 mm SL), Praia de Tambaú, João Pessoa, Paraíba, Brazil, collected with holotype. UFPB 0821, 6 (66.9–86 mm SL), Praia do Cabo Branco, João Pessoa, Paraíba, Brazil, collected by G. Melo, 08 July 1981. UFPB 3108, 85.4 mm SL, Lucena, Paraíba, Brazil, collected by NEPREMAR, 14 October 1994. UFPB 3213, 75.4 mm SL, Lucena, Paraíba, Brazil, collected by NEPREMAR, 19 January 1995. UFPB 2001, 7 (66.4–76.5 mm SL), Barra do Rio Mamanguape, Rio Tinto, Paraíba, Brazil, collected by J.C.C. Oliveira, 20 November 1988. UFPB 1905, 3 (47.91–64.03 mm SL), Praia do Cabo Branco, João Pessoa, Paraíba, Brazil, collected by R.S. Rosa, 07 August 1987. UFPB 1892, 73.5 mm SL, Praia de Tambaú, João Pessoa, Paraíba, Brazil, collected by J.C.C. Oliveira, 13 November 1986. UFPB 3082, 79.5 mm SL, Lucena, Paraíba, collected by NEPREMAR, 23 September 1994.

Non-type specimens: MZFS 12125, 70 mm SL, Ilhéus, Bahia, Brazil, December 2003. MZFS 18091, 2 (64.2–72.4 mm SL), Praia do Malhado, Ilhéus, Bahia, Brazil, collected by P.R.D. Lopes, October 2004. MZFS 18113, 3 (58.1–75.6 mm SL), Praia do Malhado, Ilhéus, Bahia, Brazil, collected by P.R.D. Lopes, October 2004.

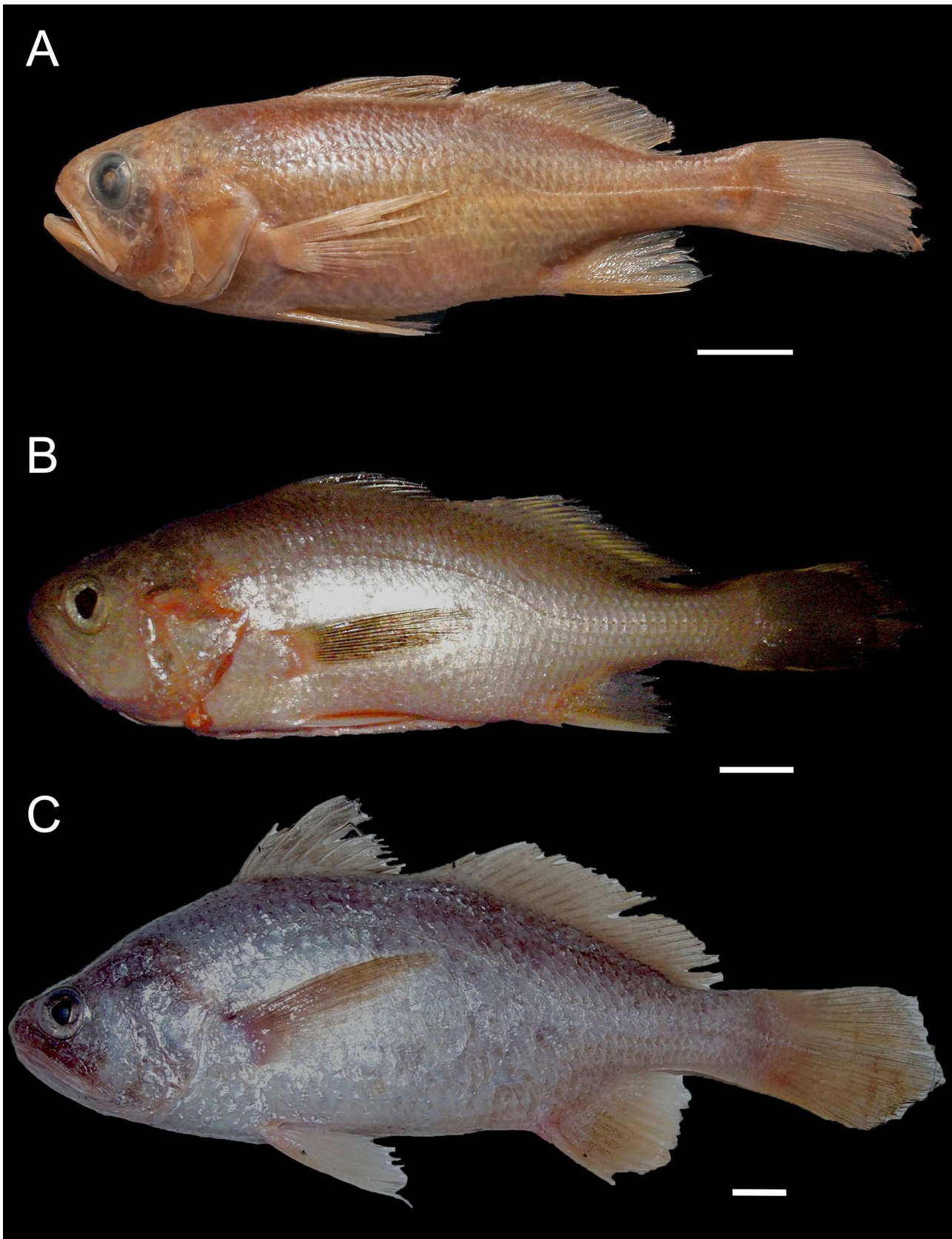


FIGURE 19. *Stellifer musicki* new species A. Holotype UFPB 1932, 88 mm SL, João Pessoa, Paraíba, Brazil; B. Paratype NMMBA 21570, 97.7 mm SL, Bragança, Pará, Brazil; C. A photo record from Rio Grande do Sul, Brazil (photo by Luciano G. Fischer). Scale: 10 mm.

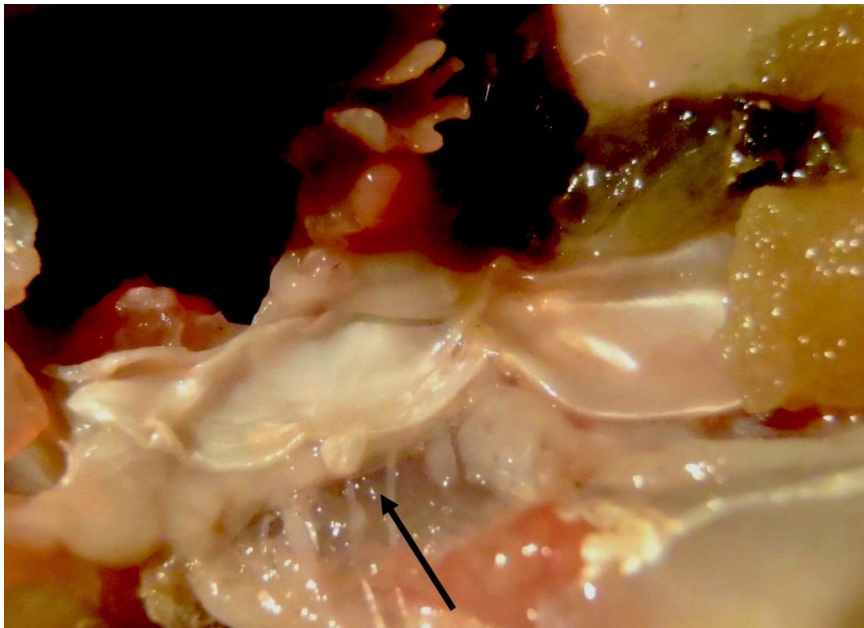


FIGURE 20. Anterior chamber of gas bladder of *Stellifer musicki* new species with a small knob-like diverticula (arrow) from paratype NMMBA 21570, 97.7 mm SL, Bragança, Pará, Brazil.

Diagnosis. *Stellifer musicki* can be distinguished from all other Atlantic species of the genus with a horizontal or inferior mouth by the large, oblique mouth and large eye (3.8–4.5 in HL). It can be differentiated from *S. collettei* and *S. macallisteri* by their smaller eye (5.0–7.1 and 4.4–5.4 in HL, respectively) and from other moderately large-eyed species as follows: from *S. griseus* by having fewer gill rakers (31–38 vs. 52–59); from *S. cervigoni* and *S. rastrifer* by their jet-black lining under gill cover, pale in *S. musicki*; from *S. stellifer* by the several small, finely serrated spines instead of 3 to 4 distinct strong spines at the lower corner of preopercle.

Description. Dorsal-fin rays X to XII+II to III, 19–21; anal-fin rays II, 8 (rarely 9); pectoral-fin rays 18–20; gill rakers 12–15 + 19–23 = 32–38; preopercular spines small, finely serrated, 6–9; lateral-line scales 48–50; 6–7 transverse scale rows from lateral line to dorsal fin origin and 9–11 rows to anal fin origin. Anterior chamber of gas bladder with short, knob-like diverticula pair (Fig. 20). Posterior tip of posterior chamber reaching base of first anal spine. Drumming muscles in both sexes (Fig. 1B, hatched area). Otoliths similar to other *Stellifer* species (Fig. 3C), with thick and broad sagitta, deep notch on antero-dorsal margin; sulcus with narrow ostium, deeply grooved L-shaped cauda, and marginal groove along dorsal margin; outer surface rough, with crest-like projections. Lapillus ovoid, with thin antero-ventral flange; inner surface smooth, outer surface with irregular grooves. Asteriscus triangular, with lanceolate groove near ventral margin of inner surface. Preopercular margin finely serrated with (6–9) slightly distinct spines at lower angle; upper spines often reduced to thin, flat, flexible points. Head smoothly arched, dorsal profile rather straight; interorbital broad, more than 2.8 times in HL; top of head cavernous but with rather strong frontal bone arches and ridges, not spongy to touch. Snout short, not projecting beyond upper lip, tip with three upper and five marginal pores; rostral fold slightly indented below marginal pores. Eye large, 3.8–4.7 in HL, orbit rounded. Mouth large, oblique, upper jaw 2.1–2.5 in HL; jaws subequal gape forming angle of about 45°. Anterior tip of upper lip, horizontally, passing through middle of orbit. Posterior end of maxilla reaching vertical between posterior borders of pupil and orbit. Underside of lower jaw with six pores, medial pair minute and separated by symphyseal ridge (Fig. 6D). Teeth in upper jaw subequal, in 2–3 narrow rows, outer row with slightly enlarged teeth, the longest not exceeding one quarter of pupil diameter. Teeth in lower jaw minute in 2–3 rows ridge; inner row teeth slightly enlarged. Gill-rakers long and slender, longest much longer than filament at angle of arch, shorter than eye diameter. Anal fin truncate, the second spine long and strong, 1.6 in HL and exceed about three-quarters of first ray length. Caudal fin rhomboid, slightly shorter than HL. Pectoral fin long, vertical from its tip passing much tip of pelvic fin. Tip of pelvic fin, exclusive of filamentous prolongation, reaching to vent. Scales large, thin, and strongly ctenoid everywhere on body, except for one or two rows of cycloid scales beneath opercular flap. Head squamation cycloid, except for patch of ctenoid scales on opercle; scales reduced and somewhat embedded on snout. Spinous dorsal with three or four rows of reduced cycloid scales at base, basal sheath not well-defined.

Interspinous membrane naked except for row of minute, elongated scales along posterior border of each spine. Soft dorsal and anal fins uniformly covered by small cycloid scales. Caudal, pectoral, and pelvic fins finely scaled. Lateral line pored scales ctenoid, indented in middle of posterior margin, and much smaller than scales of adjacent rows. Lateral line pored scale with arborescent canal.

Coloration. Fresh specimens with silvery color, becoming darker dorsally through dense stippling of chromatophores, dorsal fin dusky, pectoral fin and anal fin dusky with yellowish hue, pelvic fins slightly dusky. Caudal fins often darker. Inside gill cover pale to reddish yellow. Preserved specimens with body uniformly pale to brownish slightly darker above. Upper edge of opercle sprinkled with large chromatophores. Some concentration of chromatophores on snout and around orbit. Dorsal margin of anterior half of upper lip with conspicuous dark band, few chromatophores scattered posteriorly. Anterior part of lower lip sprinkled with chromatophores. Tongue and inside of mouth pale. Inside gill cover pale with scattered chromatophores, no distinctly darker area. Spinous dorsal covered with large chromatophores, concentrated distally, apex of fin dark; soft dorsal similar but less densely dusted. Upper half of pectoral fins sprinkled with chromatophores, anal fin punctuated, becoming dark toward trailing edge. Caudal fin evenly dusted with small chromatophores. Peritoneum silvery.

Distribution. Endemic to Brazil, south of Amazon River delta from Bragança, Pará, to Bahia.

Etymology. This species is named in honor of the late Dr. Jack A. Musick, formerly at the Virginia Institute of Marine Science, College of William and Mary. Jack was the major professor of N.L. Chao and many students, including several Brazilian ichthyologists.

Redescription of *Stellifer gomezi* (Cervigón, 2011) from Brazil

Ophioscion sp. in Valdez & Aguilera (1987)

Ophioscion sp. in Cervigón (1993)

Ophioscion gomezi Cervigón 2011, p. 96.

This species is recently found to be common in the littoral zone from the northeastern to southeastern Brazilian coast; we redescribe it to complement the original description of Cervigón (2011).

Diagnosis. *Stellifer gomezi* can be distinguished from all other Atlantic species of the genus with inferior mouth by the combination of ctenoid scales on top of head and five mental pores, except *S. punctatissimus* and *S. menezesi*, from which it differs by the elongated body and HL greater than body depth (both have a body depth greater or equal to HL); additionally, *S. gomezi* also differs from *S. menezesi* by having a longer pectoral fin, its tip posterior to the tip of pelvic fin, a long and thick second anal-fin spine, reaching beyond the tip of first anal ray, snout length less than 4.0 times in HL and nostrils rounded and almost the same height (anterior nostril slightly oval and forward directed, posterior nostril bean-shaped forming an angle between them in *S. menezesi*) (Fig. 18). *Stellifer punctatissimus* and *S. menezesi* have distinctly darker pectoral, pelvic, and anal fins than *S. gomezi*.

Description of Brazilian specimens. Dorsal-fin rays XI+I, 22–24; anal-fin rays II, 7; pectoral-fin rays 17–18; gill rakers 6–8 + 12–14 = 18–22; preopercular spines 9–11; pored lateral-line scales 48–51; 5–6 transverse scale rows from lateral line to dorsal fin origin and 8–10 rows to anal fin origin. Anterior chamber of gas bladder smooth without appendages; posterior tip of posterior chamber terminating anterior to base of first anal spine (Fig. 1A, left). Drumming muscles in males only (Fig. 1B, hatched area). Sagitta (Fig. 3B) thick with notch anterodorsally; sulcus with small ovoid ostium, deeply grooved L-shaped cauda, and shallow groove along the dorsal margin; outer surface with crest-like elevations. Lapillus ovoid, with thin anterior flange; inner surface smoothly convex, outer surface roughly concave. Asteriscus triangular, thin, with lanceolate groove near ventral margin of inner surface. Preopercular spines short, usually 10 or 11, more prominent at angle; upper spines progressively shorter and weaker, uppermost appearing as flat points, lower margin of preopercle weakly serrated. Head conical, interorbital region slightly convex, not cavernous in appearance. Snout conical, 3.2–3.8 in HL, projecting beyond upper lip, its tip with three upper and five marginal pores. Eye moderate, 4.2–5.9 in HL; orbit rounded, its diameter less than interorbital width. Mouth moderately large, inferior, upper jaw 3.2–4.0 in HL; jaws subequal with nearly horizontal gape. Anterior tip of upper lip, horizontally, passing much below ventral margin of orbit. Maxilla ends below anterior half of eye. Underside of lower jaw with six sensory pores, median pair set in common pit (Fig. 6C). Teeth thin and short on both jaws set in villiform bands, the longest not exceeding one quarter of pupil diameter. Tooth band on lower jaw slightly broader than upper jaw. Gill rakers moderately short and slender, longest at corner distinctly shorter than

filament at angle of arch, less than one third of eye diameter. Nostrils below middle of eye, both rounded and with almost same height, distance between them almost equal as posterior nostril height (Fig. 18B). Anal fin truncate; second spine long and strong, 1.5–1.9 in HL, distal end extending almost to tip of first anal ray. Caudal fin rhomboidal, much shorter than HL. Tip of pectoral fin vertically passing short or equal to pelvic fin tip when depressed. Pelvic fins lack filamentous elongation. Scales moderately large, strongly ctenoid on body and head, except for small cycloid scales patch on preorbital and embedded under skin on lachrymal bones. Spinous dorsal with three or four rows of reduced cycloid scales along base, basal sheath not well-defined. Interspinous membrane naked, soft dorsal and anal fins uniformly covered with small cycloid scales on membrane behind each soft ray and extending distally to half of fin height. Caudal, pectoral, and pelvic fins finely scaled. Lateral line pored scales ctenoid, indented in middle of posterior margin, and much smaller than scales of adjacent rows. Lateral line canal system appearing arborescent on scales.

Coloration. Fresh specimens with silvery color, becoming darker dorsally through dense stippling of chromatophores, and with silvery blue tinge on nape; dorsal, anal and pectoral fins dusky with yellowish to lemon hue; pelvic fins pale to yellowish, dusky on base, eventually greyish on central area and distally; caudal fin dark greyish. Opercle with dark patch above level of angle; inside gill cover light dusky, darker dorsally around pseudobranchiae. Preserved specimens with body pale brown, slightly darker dorsally through dense stippling of tiny chromatophores. Opercle with dark patch above level of angle sprinkled with large chromatophores. Some concentration of chromatophores on snout and around orbit. Dorsal margin of anterior half of upper lip with conspicuous dark band, few chromatophores scattered posteriorly. Tongue and inside of mouth pale. Inside gill cover black dorsally around pseudobranchiae, variably dusky elsewhere. Skin covering cleithrum heavily dusted with large chromatophores. Spinous dorsal fin covered with large chromatophores, concentrated distally at apex of fin appearing dark; soft dorsal similar but less densely dusted. Lower half of pectoral fins sprinkled with chromatophores. Pelvic fin generally pale at base but densely punctuated distally. Caudal fin evenly dusted with small chromatophores. Peritoneum membrane silvery.

Distribution. Widely distributed in the central western Atlantic from the Caribbean coast of Venezuela, including the Dominican Republic, to Santa Catarina, Brazil.

Specimens examined. Venezuela: MCZ 157234, 9 (40.8–108 mm SL), Playa Sauca, Estado Falcon, Venezuela, collected by O. Aguilera & J. Valdez, 6 June 1985; same as USNM 287532 and NMMP 20781. MCZ 157274, 3 (61.8–81.6 mm SL), collected with MCZ 157234. MCZ 157275, 6 (51.8–88.3 mm SL), Playa Sauca, Estado Falcon, Venezuela, collected by O. Aguilera & J. Valdez, 4 October 1984. NMMP 21569, 105 mm SL, same as USNM 287532, Playa Sauca, Estado Falcon, Venezuela. NMMP 21569, 105 mm SL, same as USNM 287532, Playa Sauca, Estado Falcon, Venezuela. NMMP 20733, 97.2 mm SL, (clear & stained), same as MCZ 157273. USNM 287532, 3 (95.2–97.8 mm SL), same locality as MCZ 157234 and NMMP 22354, Falcon, Venezuela. USNM 435341, 153 mm SL, Playa Sauca, Estado Falcon, Venezuela, collected by O. Aguilera and J. Valdez, 1 May 1985. NMMP 20781, 2 (89–103 mm SL), (clear & stained), same as MCZ 157234. NMMP 22354, 2 (99.3–107 mm SL), same as MCZ 157234. Dominican Republic: MCZ 157273, 3 (52.2–112 mm SL), Mouth of Suco river, San Pedro de Macoris, Dominican Republic, collected by L. Sang, 30 June 1985 (received by the first author). Brazil: AZUSC 5959, 2 (165–175 mm SL), Ilha dos Remédios, Balneário Barra Sul, Santa Catarina, Brazil, 26°27'50"S, 48°33'12"W, trawl, 31 m, collected by Faria, A.N, 01 November 2019. AZUSC 5937, 91 mm SL, Guarujá, São Paulo, Brazil, 24°00'26"S, 46°12'49"W, trap, 2.5 m, collected by Rotundo, M.M., 30 April 2018. MCZ 171854, 3 (80.0–117 mm SL), Fortaleza, Ceará, Brazil, collected by Cassiano Monteiro, 1991. USNM 435342, 2 (79.0–114 mm SL), same data of MCZ 171854. USNM 104297, 120 mm SL, Recife, Pernambuco, Brazil, collected by Von Ihering, 1932 (Comissão Técnica de Piscicultura do Nordeste, Brasil). USNM 435343, 2 (101–110 mm SL), Camburi Beach, Vitória, Espírito Santo, Brazil, collected by R. Teixeira, 24 August 1983. MZFS 17101, 132 mm SL, Porto de Trás, Itacaré, Bahia, Brazil. MZFS 17526, 106 mm SL, Praia de Ponta da Ilha, Ilha de Itaparica, Bahia, Brazil. MZFS 17678, 105 mm SL, Praia do Malhado, Ilhéus, Bahia, Brazil. MZUSP 13869, 2 (90–101.2 mm SL), Guarujá, São Paulo, Brazil, collected by P.E. Vanzolini. MZUSP 13875, 3 (62–77.1 mm SL), Praia da Avenida, Maceió, Alagoas, collected by J.G. Marques, 16 October 1978. MZUSP 70210, 5 (91–101.5), Enseada De Ubatuba, Ubatuba, São Paulo, Brazil, collected by Jorge de Abreu, 15 December 1973 to 29 January 1974. MZUSP 70213, 4 (3.9–5.7 mm SL), Praia de Itaguá, Ubatuba, São Paulo, Brazil, collected by J.L. Figueiredo, February 1971. MZUSP 70214, 101.6 mm SL, Guarujá, São Paulo, Brazil, collected by A. Carvalho-Filho, July 1984.

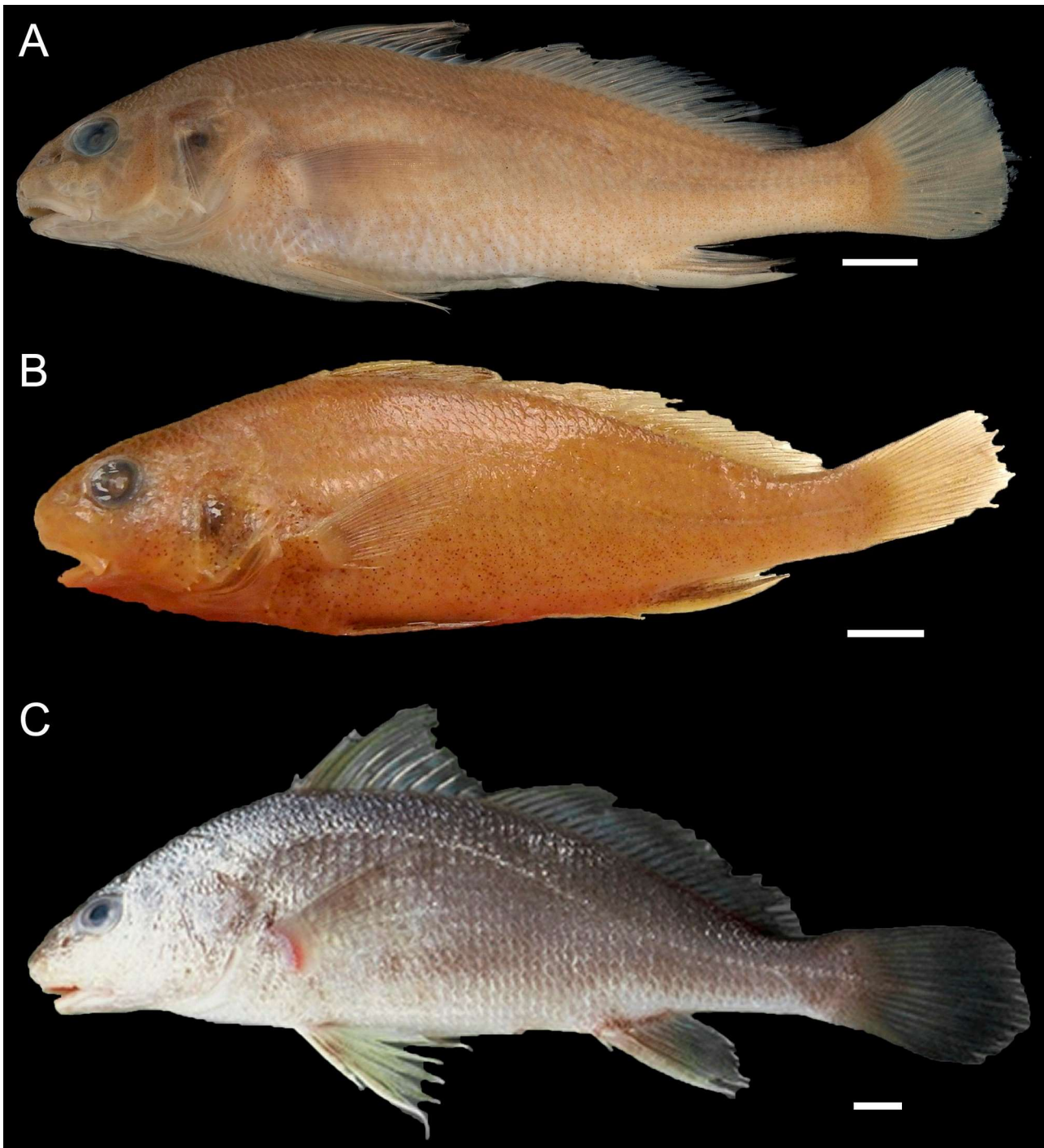


FIGURE 21. *Stellifer gomezi* from A. Dominican Republic. MCZ 157273 (one of five), 115 mm SL (photo by Andrew Williston, MCZ); B. Fortaleza, Brazil. MCZ 157284; C. Guarujá, São Paulo, Brazil, 170 mm SL, recently collected. Scale: 10 mm.

Key to the Atlantic species of *Stellifer*

- 1a. Mouth moderate to small, subterminal to inferior; position of anterior tip of upper jaw ventral to lower eye margin2
- 1b. Mouth large, terminal to strongly oblique; position of anterior tip of upper jaw horizontal to or dorsal to lower eye margin 11
- 2a. Scales on top of head cycloid, smooth to touch; underside of lower jaw with 6 mental pores3
- 2b. Scales on top of head ctenoid, rough to touch; underside of lower jaw with 5 mental pores.....6
- 3a. Spinous dorsal fin with XII or XIII spines; roof of mouth and underside of gill cover jet black; total gill rakers 37–40 (Table 2)*S. cervigoni* new species (Dominican Republica, Colômbia, Venezuela to Pará, Brasil)

- 3b. Spinous dorsal fin with X or XI spines (rarely XII); roof of mouth pale to dusky, never black; total gill rakers fewer than 32. 4
- 4a. Dorsal profile strongly arched; top of head firm to touch; total gill rakers 27–32, longest raker longer than gill filament; second anal-fin spine stout, about equal length to first soft ray, 1.9–2.4 in HL; anterior gas bladder with a pair of small knob-like appendages (Fig. 1B, right).....*S. colonensis* Meek & Hildebrand, 1925 (Panama, Puerto Rico, Haiti and Venezuela)
- 4b. Dorsal profile smoothly arched; top of head cavernous soft to touch; gill rakers fewer than 24, longest raker shorter than gill filament; second anal-fin spine 2.2–3.0 in HL; anterior gas bladder with digital-like tubes or U-shaped appendages5
- 5a. Second anal-fin spine strong, equal to length of the first ray, 2.2–2.5 times in HL; appendage on gas bladder in short digital-like tubes (Fig. 1B, left)*S. microps* (Steindachner, 1864) (Caribbean coast from Colombia to Northeastern Brazil)
- 5b. Second anal-fin spine shorter than first ray, 2.4–3.0 times in HL; a pair of U-shaped tubular appendages on gas bladder (Fig. 1C, left)*S. brasiliensis* (Schultz, 1945) (Endemic to Brazil from the Northeast region to the Southeast region)
- 6a. Pelvic fin short, 5.8 times or more in SL, its tip well anterior to tip of pectoral fin; anterior chamber of gas bladder with a pair of kidney-shaped appendages (Fig. 1A, right).....7
- 6b. Pelvic fin moderately long, 5.8 times or less in SL, its tip reaching posteriorly to that of pectoral fin; anterior chamber of gas bladder with or without appendages, but never kidney-shaped8
- 7a. Eye large, 3.5–4.2 in HL, equal to or slightly longer than snout length; pelvic fin 5.8–6.8 times in SL; total gill rakers 21–25*S. naso* (Jordan, 1889) (Venezuela to Northeastern Brazil)
- 7b. Eye moderate, 4.1–5.3 in HL, shorter than snout length; pelvic fin very short, 6.4–8.1 times in SL; total gill rakers 25–30*S. venezuelae* (Schultz, 1945) (Honduras, Colombia, Venezuela and Trinidad)
- 8a. Eye small, 6.3–6.4 in HL; a small fish, females mature at 60 mm SL; pelvic fin short, 5.2 to 5.8 times in SL, its filamentous tip ending posterior to vent; total gill rakers 25–29*S. magoi* Aguilera, 1983 (Known only from Gulf of Venezuela)
- 8b. Eye moderately large, 6.2 or less in HL; females mature greater than 100 mm SL; pelvic fin less than 5.2 in SL, its filamentous tip short ending anterior to vent; total gill rakers fewer than 23; no appendages on posterior margin of anterior chamber of gas bladder.....9
- 9a. Back strongly arched; body depth 2.7–2.9 in SL; interorbital wide, 3.5 or less in HL; pectoral and pelvic fins black.*S. punctatissimus* (Meek & Hildebrand, 1925) (From Panama and Porto Rico through Caribbean and Northern South America and along Atlantic coast to Southeastern Brazil, at least São Paulo)
- 9b. Body elongate; body depth more than 3.3 in SL; interorbital narrow, 3.6 or more in HL; pectoral and pelvic fins pale or black only distally.....10
- 10a. Body depth equal to or less than HL; eye 4.2–5.6 in HL, slightly shorter than snout length; nostrils rounded and almost the same height (Fig. 18B); tip of pectoral fin posterior to tip of pelvic fin; second anal spine slightly longer than first soft ray; all fins pale to dusky*S. gomezi* (Cervigón, 2011) (Caribbean coast from Colombia to Venezuela and along Atlantic coast to Southeastern Brazil, at least to São Paulo)
- 10b. Body depth slightly greater than HL; eye 3.6–4.6 in HL, equal to or slightly greater than snout length; anterior nostril slightly oval and forward-directed forming an angle with the bean-shaped posterior nostril (Fig. 18A); tip of pectoral fin reaching to or posterior to tip of pelvic fin; second anal spine slightly shorter than first soft ray; distal portion of pectoral, pelvic and anal fins blackish *S. menezesi* new species (From Paraíba to São Paulo state, uncommon south of Bahia, on the Brazilian coast)
- 11a. Preopercular margin with two or three prominent spines 12
- 11b. Preopercular margin with four or more prominent spines..... 14
- 12a. Preopercular margin with three prominent spines (occasionally four on one side); total gill rakers 33–39; dorsal-fin rays 18–20*S. stellifer* (Bloch, 1790) (Venezuela to Southern Brazil, one record from Puerto Rico)
- 12b. Preopercular margin with two prominent spines; total gill rakers 36 or more; dorsal-fin rays 20–24.....13
- 13a. Nape and pre-dorsal region with one to several median rows of ctenoid scales; total gill rakers 36–52; inside of gill cover jet black; anterior chamber of gas bladder with a pair of long tubular appendages (Fig. 1C, right).*S. rastrifer* (Jordan, 1889) (Venezuela to Rio Grande do Sul, Brazil)
- 13b. Scales on nape and pre-dorsal region cycloid; total gill rakers 52–59; inside of gill cover dusted with melanophores; anterior chamber of gas bladder with a pair of small knob-like appendages (Fig. 1B, right)*S. griseus* Cervigón, 1966 (Venezuela, Honduras, and Trinidad)
- 14a. Eye large, greater than snout length, 3.4–4.5 in HL; anal-fin rays 9 (rarely 8); total gill rakers 29–36*S. musicki* new species (Found in Brazil, from Pará to Bahia)
- 14b. Eye moderate to small, shorter than snout, 4.4 times or more in HL; anal-fin rays 8 (rarely 9); total gill rakers 28–48.....15
- 15a. Underside of lower jaw with four mental pores; eye small, 5.1–6.4 in HL..... 16
- 15b. Underside of lower jaw with six mental pores; eye moderately large, 4.4–5.5 in HL..... 17
- 16a. Head scales all cycloid, scales on body ctenoid; total gill rakers 41–48*S. chaoi* Aguilera, Solano & Valdez, 1983 (Colombia and Gulf of Venezuela)
- 16b. Head scales mostly ctenoid, cycloid in interorbital region; total gill rakers 28–37.*S. collettei* new species (Southeast Venezuela, Surinam, French Guyana to Southeastern Brazil)
- 17a. Top of head extremely cavernous, spongy to touch; total gill rakers 29–33, longest raker about equal to filament length at the angle; gas bladder appendage knob-like (Fig. 1B, right)*S. lanceolatus* (Holbrook, 1855) (Chesapeake Bay to Gulf of Mexico)
- 17b. Head not spongy to touch; total gill rakers 28–31, longest raker longer than filament length at the angle; gas bladder without appendages*S. macallisteri* new species (Caribbean sea from Canal zone Panama, Colombia to Gulf of Venezuela, also in Dominican Republic)

TABLE 2. Key morphological characters and total gill rakers of Western Atlantic *Stellifer* spp. with a subterminal or inferior mouth. N=Total samples, n=partial samples, Bold=diagnostic characters

Species	Characters				
	Eye in HL	Inteorbital in HL	Pelvic fin in SL	Mental pores	Inteorbital scales
<i>S. brasiliensis</i>	4.7–5.6	2.8–3.4	4.4–5.6	6	Cycloid
<i>S. cervigoni</i>	4.5–5.1	2.9–3.1	4.8–5.3	6	Cycloid
<i>S. colonensis</i>	5.5–6.2	2.9–3.1	4.3–5.2	6	Cycloid
<i>S. gomezi</i> *	4.2–5.6	3.8–4.7	4.6–5.5	5	Ctenoid
<i>S. magoi</i> **	6.3–6.4	2.7–3.0	5.1–5.8	5	Ctenoid
<i>S. menezesi</i>	3.6–4.6	3.6–4.7	4.3–5.0	5	Ctenoid
<i>S. microps</i>	4.7–5.5	3.0–3.4	4.3–5.3	6	Cycloid
<i>S. naso</i>	3.3–4.2	3.1–3.6	5.8–6.8	5	Ctenoid
<i>S. punctatissimus</i>	4.4–5.4	3.2–3.6	4.9–5.3	5	Ctenoid
<i>S. venezuelae</i>	4.1–5.3	2.9–3.4	6.4–8.1	5	Ctenoid

Continued.

Species	Gill-raker count																							Total (N)	
	16	17	18	19	20	21	22	23	24	25	26	27	28	29	30	31	32	33	34	35	36	37	38		
<i>S. brasiliensis</i>						3	2	4	6																15
<i>S. cervigoni</i>																					1	7	10	4	22
<i>S. colonensis</i>												3	13	23	13	9	3								64
<i>S. gomezi</i> *		1	2	2	5	9	1																		20
<i>S. magoi</i> **												1	1	2											6
<i>S. menezesi</i>	9	4	21	12	5																				51
<i>S. microps</i>				1		12	18	3																	34
<i>S. naso</i>							5	5	9	6															25
<i>S. punctatissimus</i>		1	6	6	15	4	2																		34
<i>S. venezuelae</i>										1	2	7	7	4						3					24

*including Cervigón (2011) (n=73) and current (n=16) **including Aguilera (1983) (n=5), current (n=1)

Conclusions on *Stellifer* and sciaenid taxonomy

The subfamily Stelliferinae is unique within Sciaenidae by having a two-chambered gas bladder and an enlarged pair of lapillus, about the same size as the sagitta. Both characters are also present in the Indo-West Pacific *Johnius* (tribe Johniini) which has a slightly enlarged lapillus but less than one-third the size of the sagitta, they also have an expanded anterior end of the gas bladder (Chao 1986; Chao *et al.* 2019). Thus, because they are distant in sciaenid phylogeny, their share a last common ancestor dating from the Late Oligocene to Early Miocene expansions (Lo *et al.* 2015), these characters are probably convergent.

In this study, we found that *Stellifer* species (e.g. *S. collettei*) can show significant geographic variation. Recent studies of Southwestern Atlantic sciaenids, such as *Bairdiella* (Marceniuk *et al.* 2019), *Macrodon* (Carvalho-Filho *et al.* 2010), *Menticirrhus* (Marceniuk *et al.* 2020), and *Isopisthus* (Guimarães-Costa *et al.* 2020) have shown that cryptic species are not uncommon. These studies demonstrated that the hidden diversity is often found in species caught as fisheries by-catch, reinforcing the need for detailed studies on taxonomy and zoogeography that can lead to better conservation management. We expect that *Stellifer* and widely distributed sciaenids (e.g. *Cynoscion* and *Micropogonias*) might have similar patterns, when samples become available for further molecular and morphological study.

Acknowledgements

We are indebted to many fish curators and collection managers at many museums and institutes, particularly ANSP, AZUSC, CMNFI, NMNH, MCZ, MZFS, MZUSP, NMMBA, NMRJ, UFS, USNM, VIMS, and ZUEC, for their assistance and hospitality during our visits in four decades. We especially want to mention Naércio A. Menezes and José Figueiredo at MZUSP, São Paulo, Brazil; Karsten Hartel, Ann Beverley and Andrew Williston of MCZ, Cambridge; Jeff Williams, Kris Murphy, Sandra Raredon, Lisa Palmer and Susan Jewett of USNM; Chi Wei Chang, Shao-I Wang and R. Chen at NMMBA, Taiwan; Paulo Roberto, Jailza Tavares and Kileyza Santos at MZFS and Marcelo Brito at UFS, Brazil. Also, we want to thank especially Matheus M. Rotundo, Thaiza M. R. Rocha Barreto and Gustavo S. Cardoso at AZUSC, Brazil, who devoted time and experience to check the institution fish collection with the artificial key herein and found vouchers that extended the range of *S. menezesi* and *S. gomezi*. Bruce Collette and staff at the Systematics Laboratory of National Marine Fisheries Service at the Smithsonian Institution have supported the research of the senior author since 1970s. Ms. Keiko made otolith drawings (NMFS, Systematics Lab); photo credits also go to Andrew Williston (MCZ) and Luciano Gomes Fischer (UFRJ). For comments on phylogeny and species delimitation we thank Tércia Silva and Simoni Santos. For collecting and making specimens and references available to us, we thank Ross Robertson (Panama), Orangel Aguilera (Venezuela), Arturo Acero (Colombia), I. Sang (Dominican Republic), Cassiano Monteiro, Paulo Buckup, Ricardo Rosa, Beatrice Padovani Ferreira, Rayssa Lima, Flávia Frédo, Mario Barletta, Rogério Teixeira, Verônica Fernandes, Leonardo Moraes, Marcelo Carvalho, Rafael Oliveira, Perimar Moura and Alexandre Clistenes (Brazil). We would like to thank to the Coordination for Higher Education Personnel Training (CAPES) for financial support to JAS (finance code 001). Funding for NLC was provided by CNPq in numerous research grants and opportunities for over three decades (1980-2012).

References

- Agassiz, L. (1829–31) s.n. In: *Spix, J.B. & Agassiz, L., Selecta genera et species piscium quos in itinere per Brasiliam peracto colleget et pingendo curavit Dr J.B. de Spix. Part 2.* Typis C. Wolf, Monachii, pp. 83–138, pls. 49–101.
- Aguilera, O. (1983) Una nueva especie de pez *Stellifer* del genero Perciformes, Sciaenidae del noroeste de Venezuela. *Memoria de la Sociedad de Ciencias Naturales La Salle*, 43 (120), 147–156.
- Aguilera, O., Solano, O.D. & Valdez, J. (1983) A new species of fish of the genus *Stellifer* (Perciformes: Sciaenidae) from the South Caribbean Sea. *Anales del Instituto de Investigaciones Marinas de Punta de Betin*, 13, 5–16. <https://doi.org/10.25268/bimc.invemar.1983.13.0.480>
- Barbosa, A.J.B., Sampaio, I., Schneider, H. & Santos, S. (2014) Molecular phylogeny of weakfish species of the *Stellifer* group (Sciaenidae, Perciformes) of the Western South Atlantic based on mitochondrial and nuclear data. *PLoS ONE*, 9 (7), e102250.

<https://doi.org/10.1371/journal.pone.0102250>.

- Bloch, M.E. (1790) *Naturgeschichte der ausländischen Fische. Vol. 4*. Auf Kosten des Verfassers, und in Commission in der Buchhandlung der Realschule, Berlin, xii + 128 pp., pls. 217–252. [also a French edition, *Ichthyologie, ou Histoire naturelle des Poissons*, v. 7, published 1797]
- Boulenger, G.A. (1899) Viaggio del Dr. Enrico Festa nell'Écuador e regioni vicine. Poissons de l'Équateur. [Deuxième Partie] (1). *Bollettino dei Musei di Zoologia ed Anatomia Comparata della R. Università di Torino*, 14 (335), 1–8.
<https://doi.org/10.5962/bhl.part.7275>
- Caldwell, D.K. (1958) A new fish of the genus *Ophioscion*, family Sciaenidae, from Caribbean Costa Rica. *Quarterly Journal of the Florida Academy of Sciences*, 21 (2), 117–124.
- Carvalho-Filho, A., Santos, S. & Sampaio, I. (2010) *Macrodon atricauda* (Günther, 1880) (Perciformes: Sciaenidae), a valid species from the southwestern Atlantic, with comments on its conservation. *Zootaxa*, 2519 (1), 48–58.
<https://doi.org/10.11646/zootaxa.2519.1.3>
- Casatti, L. & Menezes, N.A. (2003) Família Sciaenidae. In: Menezes, N.A., Buckup, P.A., de Figueiredo, J.L. & de Moura, R.L. (Eds.), *Catálogo das espécies de peixes marinhos do Brasil*. Museu de Zoologia de Universidade de São Paulo, São Paulo, pp. 86–89.
- Cervigón, F. (1966) Una nueva especie de *Stellifer* de las costas de Venezuela (Pisces: Sciaenidae). *Novedades Científicas, Contribuciones Ocasionales del Museo de Historia Natural La Salle, Serie Zoológica*, 34, 1–4.
- Cervigón, F. (1966) *Los peces marinos de Venezuela. 2 Vols. Monografía No. 11–12*. Estación de Investigaciones Marinas de Margarita, Fundación La Salle de Ciencias Naturales, Caracas, 951 pp.
- Cervigón, F. (1993) *Los peces marinos de Venezuela. Vol. 2*. Fundación Científica Los Roques, Caracas, 497 pp.
<https://doi.org/10.2307/1446324>
- Cervigón, F. (2011) *Los Peces de Venezuela. Vol. VI*. Edit. Ex Libris, Caracas. pp. 96–98.
- Chao, L.N. (1978) A basis for classifying western Atlantic Sciaenidae (Pisces: Perciformes). *NOAA (National Oceanic and Atmospheric Administration) Technical Report NMFS (National Marine Fisheries Service)*, Circular No. 415, 1–64.
- Chao, L.N. (1981) Sciaenidae. In: Fischer, W., Bianchi, G. & Scott, W.B. (Eds.), *Identification sheets of Central East Atlantic, Fishing area 34 and 74. Vol. 1–7*. In part. FAO, Rome, 41 sheets.
- Chao, N.L. (1986) A synopsis on zoogeography of Sciaenidae. In: *Indo-Pacific Fish Biology. Proceedings of the Second Indo-Pacific Fish Conference*, 28 July 28–3 August 1985, Tokyo, pp. 570–589.
- Chao, N.L. (1995) Sciaenidae. In: Fischer, W., Krupp, F., Schneider, W., Sommer, C., Carpenter, K.E. & Niem, V.H. (Eds.), *Guía FAO para la identificación de especies para los fines de la pesca. Pacífico-centro Oriental. Vol. III. Vertebrados. Parte II*. FAO, Rome, pp. 1392–1481.
- Chao, N.L. (2001) Two new species of *Stellifer* from inshore waters of the eastern Pacific with a redescription of *S. ephelis* (Perciformes, Sciaenidae). *Revista de Biología Tropical*, 49 (Supplement 1), Systematics of Tropical Eastern Pacific fishes, 67–80.
- Chao, N.L. (2002) Sciaenidae. In: Carpenter, K.E. (Ed.), *The living marine resources of the Western Central Atlantic. FAO Species Identification Guide for Fishery Purposes and American Society of Ichthyologists and Herpetologists. Special Publication No. 5*. FAO, Rome, pp. 1583–1653.
- Chao, N.L., Frdou, F.L., Haimovici, M., Peres, M.B., Polidoro, B., Raseira, M., Subir, R. & Carpenter, K. (2015) A popular and potentially sustainable fishery resource under pressure – extinction risk and conservation of Brazilian Sciaenidae (Teleostei: Perciformes). *Global Ecology and Conservation*, 4, 117–126.
<https://doi.org/10.1016/j.gecco.2015.06.002>
- Chao, L.N., Chang, C.W., Chen, M.H., Guo, C.C., Lin, B.A., Liou, Y.Y., Shen, K.N. & Liu, M. (2019) *Johnius taiwanensis*, a new species of Sciaenidae from the Taiwan Strait, with a key to *Johnius* species from Chinese waters. *Zootaxa*, 4651 (2), 259–270.
<https://doi.org/10.11646/zootaxa.4651.2.3>
- Desmarest, A.G. (1823) Première Décade Ichthyologique, ou, Description complète de dix espèces de poissons nouvelles, ou imparfaitement connues, habitant la mer qui baigne les côtes de l'île de Cuba. *Mémoires de la Société linnéenne de Paris*, 2, 163–210.
- Devincenzi, G.J. (1925) El primer ensayo sobre Ictiología del Uruguay. La clase “Peces” de la zoología de don Dámaso A. Larrañaga. *Anales del Museo Nacional de Historia Natural de Montevideo*, Serie 2, 1 (pt. 6), 295–323.
- Fowler, H.W. (1937) A collection of Haitian fishes obtained by Mr. Stanley Woodward. *Proceedings of the Academy of Natural Sciences of Philadelphia*, 89, 309–315.
- Fricke, R., Eschmeyer, W.N. & Fong, J.D. (2021) Eschmeyer's catalog of fishes: Genera/Species by Family/Subfamily. Available from: <http://researcharchive.calacademy.org/research/ichthyology/catalog/SpeciesByFamily.asp> (accessed 29 April 2021)
- Frizzell, D.L. & Dante, J.H. (1965) Otoliths of some early Cenozoic fishes of the Gulf Coast. *Journal of Paleontology*, 39 (4), 687–718
- Gilbert, C.H. (1897) Descriptions of twenty-two new species of fishes collected by the steamer Albatross, of the United States Fish Commission. *Proceedings of the United States National Museum*, 19 (1115), 437–457.
<https://doi.org/10.5479/si.00963801.19-1115.437>
- Gill, T.N. (1863) Descriptive enumeration of a collection of fishes from the western coast of Central America, presented to the

- Smithsonian Institution by Captain John M. Dow. *Proceedings of the Academy of Natural Sciences of Philadelphia*, 15, 162–174.
- Guimarães-Costa, A., Machado, F.S., Reis-Filho, J.A., Andrade, M.C., Araújo, R.G., Miranda, E., Sampaio, I. & Giarrizzo, T. (2020) DNA Barcoding for the assessment of the taxonomy and conservation status of the fish bycatch of the northern Brazilian shrimp trawl fishery. *Frontiers in Marine Science*, 7, 566021.
<https://doi.org/10.3389/fmars.2020.566021>
- Günther, A. (1867) On the fishes of the states of Central America, founded upon specimens collected in fresh and marine waters of various parts of that country by Messrs. Salvin and Godman and Capt. J.M. Dow. *Proceedings of the Zoological Society of London*, 1866 (Pt. 3), 600–604.
- Günther, A. (1868) An account of the fishes of the states of Central America, based on collections made by Capt. J.M. Dow, F. Godman, Esq., and O. Salvin, Esq. *Transactions of the Zoological Society of London*, 6 (14), 377–494.
<https://doi.org/10.1111/j.1096-3642.1868.tb00582.x>
- Hildebrand, S.F. (1946) A descriptive catalog of the shore fishes of Peru. *Bulletin of the United States National Museum*, 189, 1–530.
<https://doi.org/10.5479/si.03629236.189.1>
- Holbrook, J.E. (1855) *Ichthyology of South Carolina*. John Russell, Charleston, South Carolina, 182 pp.
<https://doi.org/10.5962/bhl.title.6911>
- Hubbs, C.L. & Lagler, K.F. (2004) *Fishes of the Great Lakes region. Rev. Edition of 1964 by G.R. Smith*. University of Michigan Press, Ann Arbor, Michigan, 332 pp.
<https://doi.org/10.3998/mpub.17658>
- Jordan, D.S. & Eigenmann, C.H. (1889) A review of the Sciaenidae of America and Europe. *United States Commission of Fish and Fisheries. Report of the Commissioner*, 14, 343–451.
- Jordan, D.S. & Evermann, B.W. (1898) The fishes of North and Middle America, a descriptive catalogue of the species of fish-like vertebrates found in the waters of North America, north of the Isthmus of Panama. Part II. *Bulletin of the United States National Museum*, 47, i–xxx + 1241–2183.
<https://doi.org/10.5962/bhl.title.39717>
- Jordan, D.S. & Gilbert, C.H. (1882) Descriptions of nineteen new species of fishes from the Bay of Panama. *Bulletin of the United States Fish Commission*, 1, 306–335.
- Jordan, D.S. & Gilbert, C.H. (1884–85) Description of *Sciaena sciera*, a new species of *Sciaena* from Mazatlan and Panama. *Proceedings of the United States National Museum*, 7 (452), 480–482. [pp. 480 with new taxon name and part of diagnosis published on 23 October 1884, pp. 481–482 on 25 February 1885]
<https://doi.org/10.5479/si.00963801.7-452.480>
- Larrañaga, D.A. (1923) *Escritos de Don Dámaso Antonio Larrañaga. Los Publica el Instituto Histórico y Geográfico del Uruguay. Vol. 2. Edición Nacional*. Impr. Nacional, Montevideo, 512 pp.
<https://doi.org/10.5962/bhl.title.116606>
- Lo, P.C., Liu, S.H., Chao, N.L., Nunoo, F.K.E., Mok, H.K. & Chen, W.J. (2015) A multi-gene dataset reveals a New World origin and Oligocene diversification of croakers (Perciformes: Sciaenidae). *Molecular Phylogenetics and Evolution*, 88, 132–143.
<https://doi.org/10.1016/j.ympev.2015.03.025>
- Marceniuk, A.P., Molina, E.G., Caires, R.A., Rotundo, M.M., Wosiacki, W.B. & Oliveira, C. (2019) Revision of *Bairdiella* (Sciaenidae: Perciformes) from the western South Atlantic, with insights into its diversity and biogeography. *Neotropical Ichthyology*, 17 (1), 1–18.
<https://doi.org/10.1590/1982-0224-20180024>
- Marceniuk, A.P., Caires, R.A., Rotundo, M.M., Cerqueira, N.N.C.D., Siccha-Ramirez, R., Wosiacki, W.B. & Oliveira, C. (2020) Taxonomic revision of the *Menticirrhus americanus* (Linnaeus, 1758) and *M. littoralis* (Holbrook, 1847) (Perciformes: Sciaenidae) species complexes from the western Atlantic. *Zootaxa*, 4822 (3), 301–333.
<https://doi.org/10.11646/zootaxa.4822.3.1>
- Meek, S.E. & Hildebrand, S.F. (1925) s.n. In: *The marine fishes of Panama. Part II. Field Museum of Natural History Publications 226. Zoological Series 15*. Field Museum of Natural History, Chicago, Illinois, pp. i–xix + 331–707, pls. 25–71.
- Menezes, N.A. & Figueiredo, J. (1980). *Manual de Peixes Marinhos do Brasil. 3 (2). Sciaenidae*. MZUSP, So Paulo, 96 pp.
- Parenti, P. (2020) An annotated checklist of fishes of the family Sciaenidae. *Journal of Animal Diversity*, 2 (1), 1–92.
<https://doi.org/10.29252/JAD.2020.2.1.1>
- Sabaj, M.H. (2020) Codes for natural history collections in ichthyology and herpetology. *Copeia*, 108 (3), 593–669.
<https://doi.org/10.1643/ASIHCODONS2020>
- Santos, S., Gomes, M.F., Ferreira, A.R.S., Sampaio, I. & Schneider, H. (2013) Molecular phylogeny of the western South Atlantic Sciaenidae based on mitochondrial and nuclear data. *Molecular Phylogenetics and Evolution*, 66, 423–428.
<https://doi.org/10.1016/j.ympev.2012.09.020>
- Sasaki, K. (1989) Phylogeny of the family Sciaenidae, with notes on its zoogeography (Teleostei, Perciformes). *Memoirs of the Faculty of Fisheries Sciences*, 36 (1/2), 1–137.
<https://doi.org/10.1007/BF02905681>
- Schultz, L.P. (1945) Three new sciaenid fishes of the genus *Ophioscion* from the Atlantic coasts of Central and South America.

Proceedings of the United States National Museum, 96 (3192), 123–137.

<https://doi.org/10.5479/si.00963801.96-3192.123>

Silva, T.F., Schneider, H., Sampaio, I., Angulo, A., Brito, M.F.G., Santos, A.C.A., Santos, J.A., Carvalho-Filho, A. & Santos, S. (2018) Phylogeny of the subfamily Stelliferinae suggests speciation in *Ophioscion* Gill, 1863 (Sciaenidae: Perciformes) in the western South Atlantic. *Molecular Phylogenetics and Evolution*, 125, 51–61.

<https://doi.org/10.1016/j.ympev.2018.03.025>

Steindachner, F. (1864) Ichthyologische Notizen. *Sitzungsberichte der Kaiserlichen Akademie der Wissenschaften. Mathematisch-Naturwissenschaftliche Classe. Abt. 1, Mineralogie, Botanik, Zoologie, Anatomie, Geologie und Paläontologie*, 49, 200–214.

Steindachner, F. (1867) Ichthyologische Notizen VI. vii. Über einige neue order seltene Fisharten von Westindien und Surinam. *Sitzungsber. Akademie der Wissenschaften*, 56, 347–357.

Valdez, J. & Aguilera, O. (1987) *Los peces del Golfo de Venezuela*. Conicit, Caracas, 215 pp.

Vinson, C., Gomes, G., Schneider, H. & Sampaio, I. (2004) Sciaenidae fish of the Caet river estuary, northern Brazil: mitochondrial DNA suggests explosive radiation for the western Atlantic assemblage. *Genetics and Molecular Biology*, 27, 174–180.

<https://doi.org/10.1590/S1415-47572004000200008>